Aalto University
School of Chemical
Technology

School of Chemical Technology
Degree Programme of Forest Products Technology

Joonas Hokka

STRENGTH AND DRAINAGE POLYMER CHEMISTRY FOR LINER AND FLUTING

Master's thesis for the degree of Master of Science in Technology submitted for inspection, Espoo, 23rd September, 2013.

Supervisor **Professor Jouni Paltakari**

Instructor **M.Sc. Matti Hietaniemi**

Aalto University
School of Chemical
Technology

Aalto University, P.O. BOX 11000, 00076 AALTO
www.aalto.fi

Abstract of master's thesis

Author	Joonas Hokka
Title of thesis	Strength and drainage polymer chemistry for liner and fluting
Department	Forest Products Technology
Professorship	Paper and Printing Technology
Code of professorship	P3003
Thesis supervisor	Professor Jouni Paltakari
Thesis advisor(s) / Thesis examiner(s)	M.Sc Matti Hietaniemi
Date	23.09.2013
Number of pages	113+8
Language	English

Abstract

The aim of this thesis was to study the effect of the polymer nature in regard to wet-end conditions within OCC furnishes to achieve both dry strength and drainage improved properties for liner and fluting. At first, the literature review introduces the relevant theories of polymer adsorption and underlines factors participating in the development of dry-strength and drainage. The experimental part emphasizes on the influences of molecular weight and charge density of the polymer on the improvements of strength and drainage with liner and fluting.

Comprehensive scientific knowledge on fiber adsorption and filtrate fixation of the polymers was obtained by turbidity, charge and zeta potential –measurements. The performance of drainage and retention was measured using Dynamic Drainage Analyzer (DDA). Strength tests involving short span compression test (SCT) and burst strength were determined from liner and fluting sheets made by pilot paper machine and hand sheets.

A high molecular weight and low charged polymer seemed to have an obvious effect on the drainage improvement with OCC furnish as a function of increasing polymer dosage. Similarly high retention with this additive was achieved. A successful performance of the polymers in conjunction with A-PAM and with C-PAM and bentonite appeared efficiency in drainage.

The evidence from the strength results suggested that favourable development between SCT and burst strengths required divergent polymer attributes. The finding supported by formation measurement revealed that the high dosages of the polymers caused poor formation that is consistent with the deteriorated strength properties of hand sheets at those chemical dosages. The applicability of the high molecular weight and low charged polymer was concluded to be suitable to achieve additional SCT strength and drainage improvements with liner and fluting OCC furnish.

Keywords Drainage; dry strength; liner; fluting

Tekijä Joonas Hokka

Työn nimi Lujuuden ja vedenpoiston polymeerikemia lainerilla ja aallotuskartongilla

Laitos Puunjalostustekniikka

Professuuri Paperi- ja painatustekniikka **Professuurikoodi** P3003

Työn valvoja Professori Jouni Paltakari

Työn ohjaaja(t)/Työn tarkastaja(t) DI Matti Hietaniemi

Päivämäärä 23.09.2013 **Sivumäärä** 113+8 **Kieli** englanti

Tiivistelmä

Tässä työssä tutkittiin polymeeriominaisuuksien ja paperikoneen märkäpään olosuhteiden vaikutuksia kuivalujuuteen ja vedenpoistoon käyttäen lainerilla ja aallotuskartongilla tyypillistä kiertokuitukartonkimassaa (OCC). Kirjallisuuskatsauksessa syvennytään polymeeriadsorption teoriaan ja perehdytään lujuuden ja vedenpoiston muodostumistekijöihin. Kokeellisen osan pääpaino on tutkia polymeerin molekyylimassan ja varaustiheyden vaikutuksia lujuuden ja vedenpoiston parantamiseksi.

Tulokset polymeerin kuituadsorptiosta ja suodoksen fiksauksesta osoitettiin sameus, varaus ja zeta-potentiaali -mittauksilla. Polymeerin vedenpoisto- ja retentiokykyä testattiin dynaamisella vedenpoistoanalysaattorilla (DDA). Lujuusmittaukset määritettiin pilotti paperikoneen koeajoarkeista ja käsiarkeista käyttäen lyhyen välin puristuslujuus- (SCT) ja puhkaisulujuustestejä.

Ominaisuuksiltaan korkea molekyylimassa ja matala varaus polymeerissä osoittivat ilmeisen vaikutuksen vedenpoistoon polymeeriannoksen funktiona. Samoin korkea retentiokyky saavutettiin samoilla polymeeriominaisuuksilla. Lisäksi, polymeerit toimivat menestyksekkäästi A-PAM:n kanssa sekä yhdessä C-PAM:n ja bentoniitin kanssa tehostaen vedenpoistoa.

Lujuustulokset viittasivat siihen, että erilaiset polymeeriominaisuudet vaikuttivat puristuslujuuden ja puhkaisulujuuden muodostumiseen. Formaatiotuloksista kävi ilmi, että suurilla polymeeriannoksilla formaatio huonontui, mikä näin selittää käsiarkkien heikentyneitä lujuusominaisuuksia korkeilla kemikaaliannoksilla. Johtopäätöksenä todetaan, että korkea molekyylimassa ja matala varaustiheys polymeerissä soveltuvat parantamaan sekä puristuslujuutta että vedenpoistoa lainerin ja aallotuskartongin kiertokuitukartonkimassalla.

Avainsanat Vedenpoisto; kuivalujuus; laineri; aallotuskartonki

PREFACE

This study was performed at Kemira's Research and Development Center in Espoo during the period of January – August 2013.

I am very thankful to my thesis supervisor Professor Jouni Paltakari for the interest and priceless advice.

I would like to express my warmest thanks to my instructor Matti Hietaniemi for the interest and helpful advice for my thesis. The guidance and all discussions during thesis work were very valuable. Moreover, I would like to thank the all Kemira's specialists for their kind help and there especially Kimmo Strengell, Mikko Virtanen, Asko Karppi and Sacha Legrand for supporting suggestions during my thesis work.

My sincerest thanks go to all technicians of Wet-end Process Chemistry team for their kind help. I am grateful to Kirsi Terävä, Maarit Latvanen and Marja-Liisa Montonen for your assistance with the laboratory devices and Lea Rintala and Salla Timperi for your priceless work in the preparation of the polymers.

I wish to express my sincere thanks to my parents and brothers for all the help and support they have always given me. Great thanks go also to Ida-Maaria, and to all my friends and relatives for their support during thesis work.

Espoo, 23rd September 2013

Joonas Hokka

Table of Contents

LITERATURE REVIEW

LIST OF ABBREVIATIONS

A-PAM	Anionic polyacrylamide
COD	Chemical oxygen demand
C-PAM	Cationic polyacrylamide
DCS	Dissolved and colloidal substances
DDA	Dynamic drainage analyzer
DDJ	Dynamic drainage jar
DS	Degree of substitution
EDL	Electrical double layer
ESCA	Electron spectroscopy for chemical analysis
FTIR	Fourier transform infrared spectroscopy
G-PAM	Glyoxylated polyacrylamide
Mw	Molecular weight
OCC	Old corrugated container
PNVF	Poly(N-vinylformamide)
PVAm	Polyvinyl amine
QCM	Quartz crystal microbalance
RBA	Relative bonded area
SCT	Short span compression test
SPAR	Stagnation point adsorption reflectometry

LITERATURE REVIEW

INTRODUCTION

One of the major trends in the manufacturing of packaging paper grades is cost efficiency obtained by the reduction of basis weight, the increase of filler content, the exploiting of renewable material and developing production output. This course of actions has caused challenging requirements for the strength and retention properties of paper and board grades. To meet these demands, variations of chemical additives have been introduced to maintain important properties of the final product. The topic of this study concerns the liner and fluting of the corrugated box board produced from the recycled pulp consisting of old corrugated containers (OCC).

The manufacturing of cellulosic fiber sheet involves depositing of furnish on a moving wire and a fabric by forming paper web from the solid components of the suspension by draining the web. To obtain a fast consolidation with the sufficient retaining of solid materials in the web formation denotes a successful drainage of the web. In paper machine, this brings faster runnability with reduced energy consumptions in the press and dryer sections due to the higher dry content of the papermaking furnish. The strength property of the paper web is originated from the interaction of fibers due to the attractive entanglement of fibrils and bonding by hydrogen bonds.

In the last decades, polymer chemistry has been a hot topic in the field of paper chemistry. The additions of synthetic polymers in the wet end of the paper machine are daily events in the papermaking process to advance desired features of paper or to facilitate the operation of the process. The trend has been towards an increased use of polymeric additives to contribute to the dry strength improvement of paper and the dewatering process. The behavior of

polymeric enhancement depends highly on the characteristics of polymer, such as the molecular weight and the charge density, and the process conditions of the wet end, including pH and conductivity. However, much uncertainty still exists in the practical applications related to these issues. The aim of this thesis is to find out the molecular weight and the charge density of the polymer with regard to process conditions within OCC furnish, influencing polymer functionality to increase dry strength of liner and fluting -grades with improved drainage properties in the papermaking.

The purpose of the literature part is to review coherent phenomena and to underline factors participating in the development of dry-strength and drainage with liner and fluting. The literature review begins with an introduction to the adsorption of polymer additives on fibers. It will then address the measuring techniques of polymer adsorption and the development of the drainage and strength in papermaking. The last two chapters emphasize on assessing the polymer characteristics and the wet-end conditions influencing on strength and drainage.

1. ADSORPTION OF POLYMERS ON FIBERS

Electrical aspects of surface chemistry are intrinsic for researching phenomena and consequences relative to papermaking processes. By understanding the regularities of the fundamentals including the influence of electrical charges at an interface and the nature of potential will vouch for the comprehending of practical applications and implications.

In this paper, we deal with the colloidal systems related to the papermaking. Speaking about the most of present particles (fibers, fillers, polymers and other dissolved substances) in the process are in the colloidal range (≈1nm-1µm). Considering more precisely, for example, dewatering process in the wet end of a paper machine where small colloids, such as filler and binder particles, percolate through the porous structure of web matrix and the holes in the wire without attaching to it. /1, p.175-179/.

Polymer adsorption at the solid-liquid interface has been widely studied in many experimental and theoretical investigations. The adsorption behavior of polyelectrolytes is unique at interfaces and therefore their applications are related to differing phenomenon of processes including retention, flocculation and as a strength-enhancing additives. In this chapter, we discuss briefly theoretical aspects for the basis of phenomenon, turning to conformational issues of a polymer layer and to the measurement techniques of adsorption. Our emphasis on introducing the adsorption phenomenon at the interface solid-liquid is to consider polymer adsorption onto wood pulp fibers.

A simple definition of the adsorption conception can be explained as a tendency of a soluble polymer to concentrate at the interface and is said to adsorb on the surface on the fiber. This tendency is mainly due to electrostatic effects when the charge of the polymer contributes to the interaction of the oppositely charged fiber.

1.1 Adsorption of ions and the electrical double layer

In papermaking, the interaction of a solid surface in contact with a solution of an electrolyte is usually denoted the interplay of cellulose fiber and polyelectrolyte in cellulose pulp stock. Both parties carry electric charges either positive or negative, determining adsorption to a substrate to do occur or not. This simple approach is based on *Helmholtz model*, dealing with the oppositely charges ions from the distribution of ions absorb on the solid surface and are supposed to be balanced by neutralizing the charge of the solid surface by an equal number of excess charges. Hereby, the electrical potential between ions of the solid surface and solution falls to zero and the system becomes electrically neutral. Considering the Helmholtz model, the solid surface is equally charged having a uniform charge density and assuming that the thermal motion of the ions and solvent molecules will not occur. Straightforwardly, the concept of the electrical double layer signifies the chemical interaction of oppositely charged ions due to the ion adsorption on the substrate, in which one is localized on the surface of the plane and another originated from the distribution of ions. /2, p. 266-273, 3/.

The *Gouy-Chapman model* developed the occurrence by introducing a diffuse model of electrical layer. A diffuse layer exhibits an extended ion region of solution, in which the ions are distributed depending on the local potential through a *Boltzmann distribution*. The electric potential decreases exponentially as a function of increasing distance from the charged layer on the solid surface. /3/

The current view of the electrical double layer theory was first suggested by Stern. He revised the theory by considering the sizes of ions. The aim of the proposition was to establish a competence for conditions of high ionic strength and high electrical potential whom the previous theories did not perceived. Thus, the sizes of adsorbed ions near the solid surface delineate the thickness of the first layer (the *Stern Layer* or *inner Helmholtz plane (IHP))*, whereas the *Diffuse*

Layer (or *outer Helmholtz plane* (*OHP*)) defined by Gouy-Chapman is formed by the ion distribution of the outer layer.

As a whole, the core of matter of the electrical double layer is presented in Figure 1. Due to the negative charged solid surface, the positive charged counter ions are adsorbed on the surface by Coulomb forces inducing a drop in potential. The interplay between charged particles is dominated by overlapping diffuse layer which dictates a relevant potential distinction with the Stern layer. This potential difference of the layers is called the zeta (ζ)-potential /4/.

The electrical potential and net charge density decrease linearly in the stern layer and exponentially in the diffuse layer as a function of distance, until obtaining corresponding value such as a solution has away from surface plane.

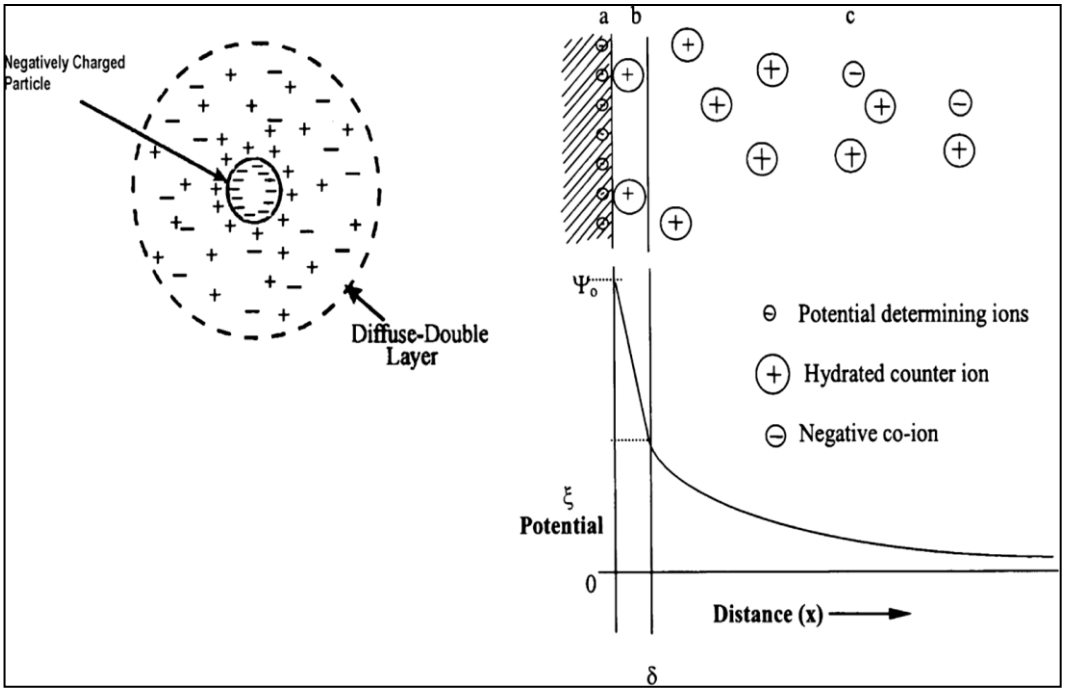

Figure 1. Illustration of the Double Layer structure and potential curve across the layers: (a) surface charge, (b) Stern layer and (c) Diffuse layer. /4/

More mathematically theory founded on the Gouy-Chapman-Stern model was introduced by the differential equation 1 of *Poisson-Boltzmann*, which induces the mathematical context of the theory.

$$\Delta^2\psi = \frac{8\pi n_0 ze}{\epsilon}\sinh\frac{ze\psi}{kT} \qquad (1),$$

where	ψ	is	electrical potential (J)
	n_0	¨	concentration at zero altitude (mol/m^3)
	z	¨	the valence of ion
	e	¨	electrostatic charge (Coulombs, C)
	ϵ	¨	permittivity (C^{2}J^{-1}m^{-1})
	k	¨	Boltzmann constant (J/K)
	T	¨	temperature (K)

Later on, Debye-Hückel developed the equation by linearization that $ze\psi/kT \ll 1$, so the following equation 2 was formed:

$$\Delta^2\psi = \frac{8\pi n_0 z^2 e^2\psi}{\epsilon kT} = \kappa^2\psi \qquad (2),$$

where κ^{-1} is a unit of Debye length, describing the thickness of the diffuse layer, which is dependent on ionic strength as the equation 3 points out.

$$\kappa = \left(\frac{2e^2 N_A}{\varepsilon kT}\right) I \qquad (3)$$

The equation reveals as I (ionic strength) increases Debye length κ^{-1} decreases and the potential as well. In consequence, the thickness of the electrical double

layer has a significant impact on colloid stability and for that matter on flocculation /4/. Moreover, the equations are revealed substantive dependencies influencing on the stability of colloids by the changes of the parameters including the concentration of electrolyte, a value of valence and the thickness of the diffuse layer.

Figure 2 shows the effects of variables on the electrical potential (ψ) and surface charge density (σ). An increase of the electrolyte concentration (Fig. 2b) decreases the curve more steeply by meaning that the potential is minor even at small distance from the surface plane. Accordingly, the highest values of the surface charge density are achieved with the increasing concentration of electrolyte (Fig. 2d). Considering Figure 2 relative to polymer chemistry, low electrolyte concentration reveals that internal repulsion between polymer segments is higher and thus more extended conformation of the polymer is achieved. This enables more effective flocculation due to longer distance of electrostatic forces between particles.

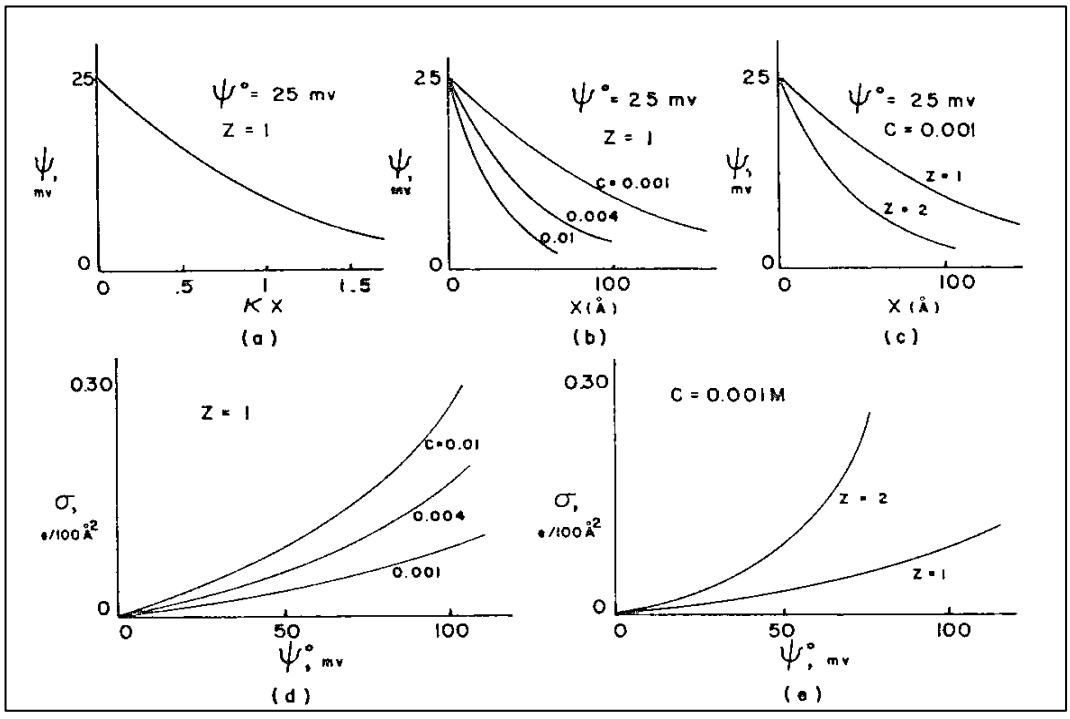

Figure 2. Above (a,b&c) is represented the change of the potential as a function of distance (X) due to the concentration change of an electrolyte (b) and the valence of ion (c). Graphs (d&e) illustrate the relationship between surface charge density and surface potential. /3/

1.2 Theoretical explanation of polymer adsorption behavior

A major theoretical issue that has been dominated the field for many years, is termed as a self-consistent-field (SCF) model provided by Scheutjens and Fleer. The theory describes statistically the thermodynamic equilibrium distribution of polymer at the solid-liquid interface based on the postulate of the lattice model /5/. This theory is accurate in concerning polyelectrolyte adsorption, despite it has several drawbacks related to the parameters of the chain length, the solvency, the solution concentration etc.

Böhmer et al. /6/ and van de Steeg et al. /7/ developed the theory by introducing the influences of pure electrosorption, chemical affinity and counterions in their experiments. They concluded that by a non-electrostatic contribution and by a specific interaction of counterions could be explained the adsorption behavior between the polyelectrolyte and the cellulose fiber.

Fleer et al. /8, p. 339-371/ summarized the theoretical background of polyelectrolyte adsorption based on the Scheutjens-Fleer (SF) -theory as presented in Figure 3. The curves 1, 2 and 2’ are not focused because they refer to the situations where the surfaces are uncharged or have the same sign. Curve 3 indicates a characteristic of opposite charged surfaces in which *pure electrosorption* is domineering. This behavior is predictable for cationic polyelectrolytes with a high charge density where the interplay is charge balanced between the polymer segments and the surface of the cellulose as a result of opposite charges. The adsorption decreases by cause of increasing ionic strength because the interaction between the segments and the surface is decreased. /9/.

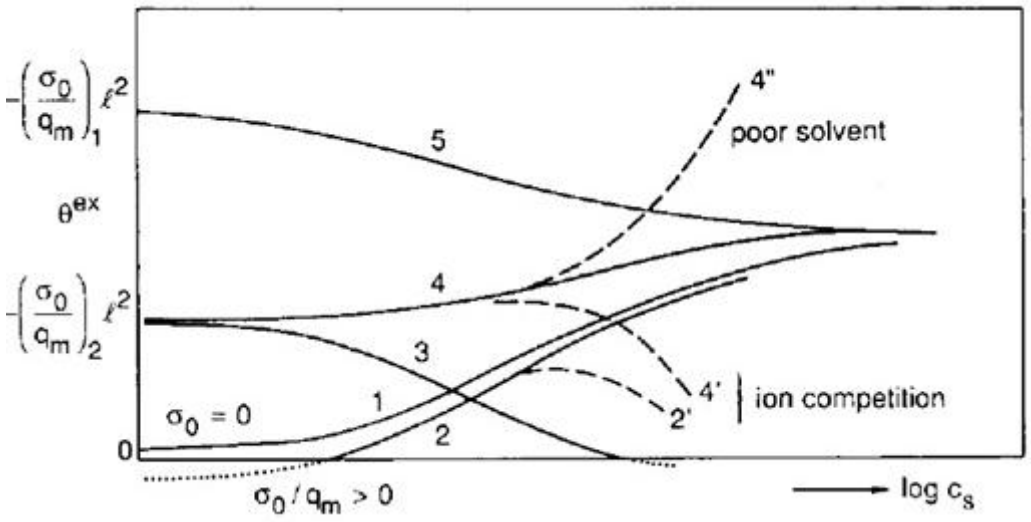

Figure 3. Schmatic representation overviews the adsorption behavior of polyelectrolyte. The vertical axis indicates the adsorbed amount θ^{EX} of polymer on the surface, whereas the horizontal describes logarithmic salt concentration c_S (i.e. the ionic strength). $-(\sigma_0/q_m)_1 l^2$ – equation corresponds to a low charge density and $-(\sigma_0/q_m)_2 l^2$ refers to a high charge density. /9/

The curves 4 and 5 depict the influence of both electrosorption and non-electrostatic contributions on the adsorption of polymer. It can be stated from the graph that *the non-electrostatic interactions* either increase the adsorption or decrease it with growing electrolyte concentration. Here, a role of the charge density becomes a crucial parameter. In case of curve 4 (high charge density), due to increasing salt concentration the repulsion between the polymer segments and the substrate decreases and the adsorption of the polymer onto the surface increases. A typical situation as shown in the figure (4'') where the solvency of polyelectrolyte is poor reveals a drastic enhancement in polymer adsorption at high salt concentration. The behavior of the curve 4' can be explained similarly as the curve 3 because the counterions compete with the polymer segments. Finally, the curve 5 represents polyelectrolyte with a low charge density that adsorbs to similar level as highly charged polyelectrolytes with increasing salt concentration. /8, 9/.

The preceding description is a vital theoretical background to review polymer adsorption onto cellulose fibers. The examination of polymer adsorption in regards to electrolyte concentration and charge density is explained by the SF theory. The most striking observation to recognize from the theory is the effect of increasing electrolyte concentration on the polymer adsorption to fibers.

1.3 Polymeric stabilization of colloids

Colloidal particles (≈<1µm) tend to collide with each other due to *Brownian motion*. Particle collisions result in the stability of colloids. The term colloidal stability has generally come to be used to refer to the chemical balance of attractive and repulsive interactions at the interface. This balance governs the overall stability of colloidal dispersions. Colloidal stability deviates substantially from flocculation phenomenon. It reveals an irreversible equilibrium state which has a tendency to a long-lived stability. Colloidal stability in suspension shows as a slow settling with dense and strong adhering between particles, whereas the flocculation can be formed at large particle distances and appearing a flat and easily reversible aggregate. /2, 4/.

Hence, the theory of colloidal stability explains a fixation effect in papermaking, where polymers tend to attach hydrophobic compounds on fibers surfaces. In practice, this may lead to disadvantageous action relative to strength agents because they can go to fixation, which impedes the development of strength.

During the 1940s, a theoretical demonstration of colloidal stability was developed by Derjaguin, Landau, Verwey and Overbeek, as later called DLVO-theory. It suggests that the stability of colloids depends upon the overall potential energy of interaction (V_T), which is the sum of attractive (V_A) and repulsive potentials (V_R).

$$V_T = V_A + V_R \quad (4)$$

Acting as attractive forces, *Van der Waals* forces are the primary source for generating attraction between colloids because of its long-range bonding ability. In contrast, repulsive forces are electrostatic interactions originated from interaction of similarly charged electrical double layers. Based on the DLVO theory, the interaction between colloids can explicitly be characterized by analyzing Figure 4. The summation of the repulsive and attractive forces may result in an energy barrier. This prevents colloids adhering to each other because of the repulsive forces. However, if the particles collide with sufficient energy to overcome this barrier, the attractive forces will dominate by pulling into a contact between colloids. As a conclusion can be noted, the sufficiently high repulsion forces promote colloidal stability by forming a higher energy barrier. /1, 2, 11/.

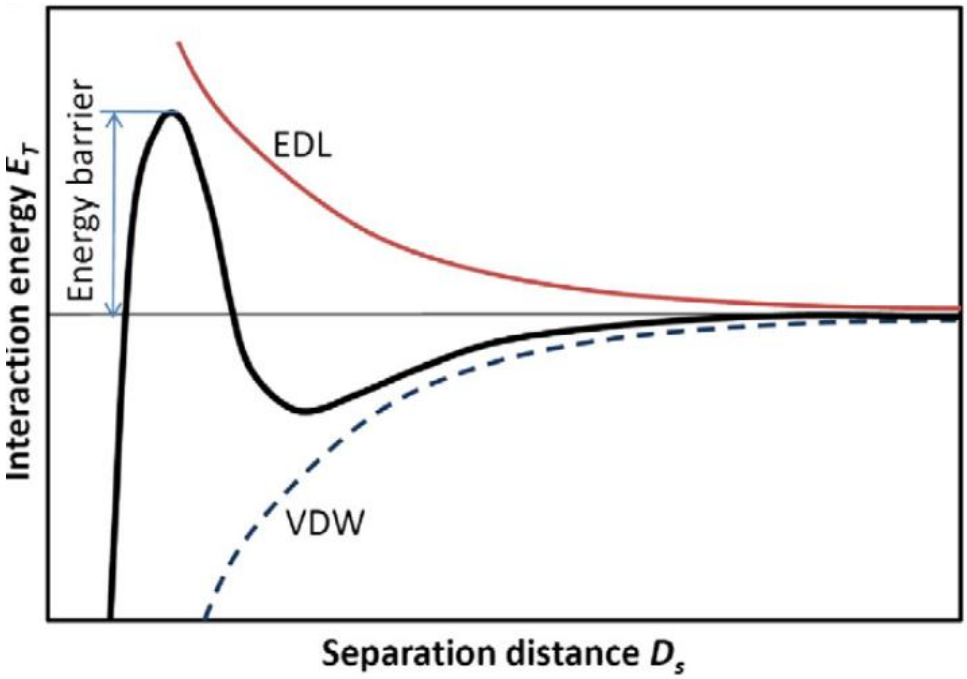

Figure 4. The interaction energy E_T as a function of separation distance D_S. The bold black curve indicates the overall potential energy (V_T), electrical double layer EDL (V_R) and van der Waals VDW (V_A).

The overall energy potential of the interaction is strongly dependent on various physicochemical factors, such as the size of particle, zeta potential, ionic strength and surface roughness. The influence of ionic strength can be exemplified by adding electrolyte concentration when EDL of the particles compress near each other, weakening the repulsion and diminishing the energy barrier. This follows that the aggregation of colloids is destabilized. In contrast, an increase of surface potential (zeta potential) leads to better stability by raising the repulsion. /2, 11/.

Colloidal stability achieved by polymer adsorption onto the surface of the colloid particles is called steric stabilization. Basically, it appears when polymers are strongly adsorbed onto the surface, the colloidal particles are fully covered by the polymer layer and the adsorbed polymer layer forms loops and tails with protruding chains into the solution. The part of the polymer that extends from the surface must be completely soluble. Thus, steric stabilization occurs due to repulsion between the colloids of the fully adsorbed polymer layers.

The thickness of the adsorbed layer on the colloidal particle plays a significant role for the interaction energy of two steric stabilized colloids. Steric repulsion is a highly dependent upon the distance between the colloids. Therefore, a thin adsorbed polymer layer may lead to an occasion where van der Waals forces are still domineering, in consequence a poorly flocculated dispersion is formed. On the contrary, a thick polymer layer quells the attraction of the van der Waals forces to negligible. /12/.

This reveals the fact that steric stabilization governs when low charged and high molecular weight polymers are fully adsorbed onto colloids forming an outwards directed structure of the polymer layer. It is important to note that steric stabilization requires high polymer surface coverage to occur. Otherwise, partly adsorbed polymers on the surface interact with non-adsorbed areas of the

particle surface due to the bridging, charge neutralization and patch formation interactions of polymers /13/.

According to van Duijneveldt /14/, steric stabilization can be preferable achieved by employing copolymers in place of homopolymers. Then one head of the copolymer is adsorbed strongly on the surface of a colloid, whereas the other is stick out into solution and provide steric stabilization. In addition, the architectures of copolymers have an influence on the efficiency of steric stabilization. For example, the copolymers consisted of blocks and grafted structures promote the stability due to the steric mechanism.

1.4 Conformation of adsorbed polymer

An addition of a polymer into solution leads to the change of the polymer behavior. In solution, polymer acts like a random coil by changing its conformation mostly due to thermal motions. There are some restrictions in regards to randomly formed polymer conformation. Depending on the mobility of the monomer units by actual chain structure and intramolecular interactions, the conformation of the polymer in solution is determined. The bonding angels between the atoms restrict fairly the motion of the polymer backbone, whereas the repetitive monomer units are able to rotate around the bonds. The intramolecular restrictions are based on the internal electrostatic interactions, such as adjacent hydrogen bonds, the excluded volume effect between polymer segments and crosslinking and branching. /1, 14, 15/.

Furthermore, the conformation of polymer is highly dependent on time and the solvency of medium. A polymer configuration fluctuates always in the course of time. This is an essential consideration in practical applications, such as in polymer adsorption on the porous structure of fiber. A longer interaction time between polymer and porous substrate facilitates the penetration of the polymer segment into the voids of the fiber surface. Figure 5 illustrates polymer

adsorption onto porous fiber surface. As a result of time the polymer coil tends to penetrate into fibrous pores of the substrate.

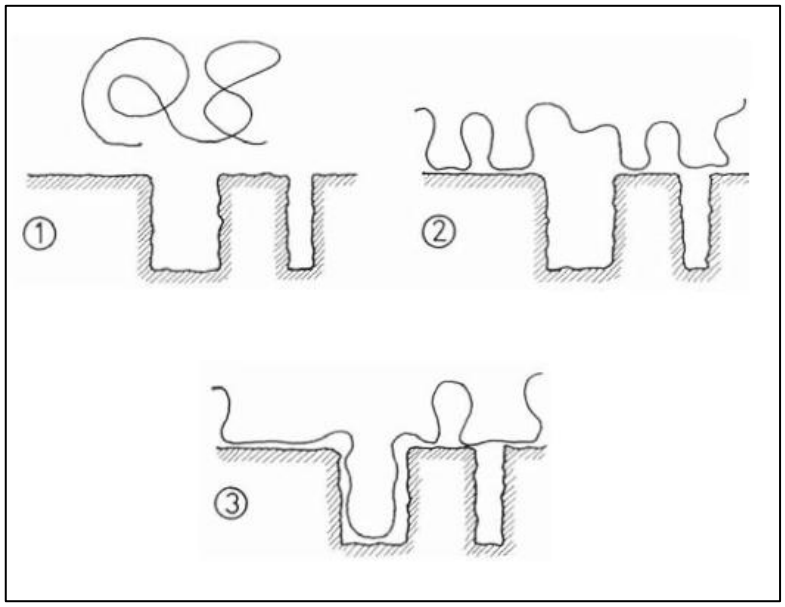

Figure 5. Schematic representation of the polymer adsorption on the surface of the porous fiber. /15/

A presence of a good solvency of medium dictates that the polymer coils are osmotically swollen and their size gains the maximum radius of gyration. A decrease in the solvency denotes the collapsing of the chain loops which cause finally precipitation in poor solvent. /1, 14, 15/.

As a rule of thumb, it is obvious to characterize the conformation of a polymer by describing a size of a polymer coil. The dimensions of a linear polymer coil can be depicted by the mean distance between the ends of the polymer chain (R_m). When the polymer segments are closed to each other forming globular structure, the conformation of the polymer is theoretically described:

$$R_m \propto r^{1/3} \qquad (5)$$

Furthermore, the radius of gyration (R_g) is commonly used to elucidate the average distance of polymer segments from the point of gravity of the coil. More precisely, tangled tails and loops of unequal lengths are oriented outwards from the center of mass of the molecule forming a curling thread that is explained by the following equation:

$$R_g^2 = \frac{1}{m}\sum_{i=1}^{r} m_i a_i^2 \qquad (6)$$

Polymer adsorption on the surface of a substrate is schematically illustrated in Figure 6. At the local scale, trains adsorb through classical specific or non-specific interactions: acid-base, hydrophobic or hydrogen bonding, including the displacement of solvent molecules from the surface /14/. This denotes that the small fractions of polymer segments anchor to the surface by forming a loopy structure.

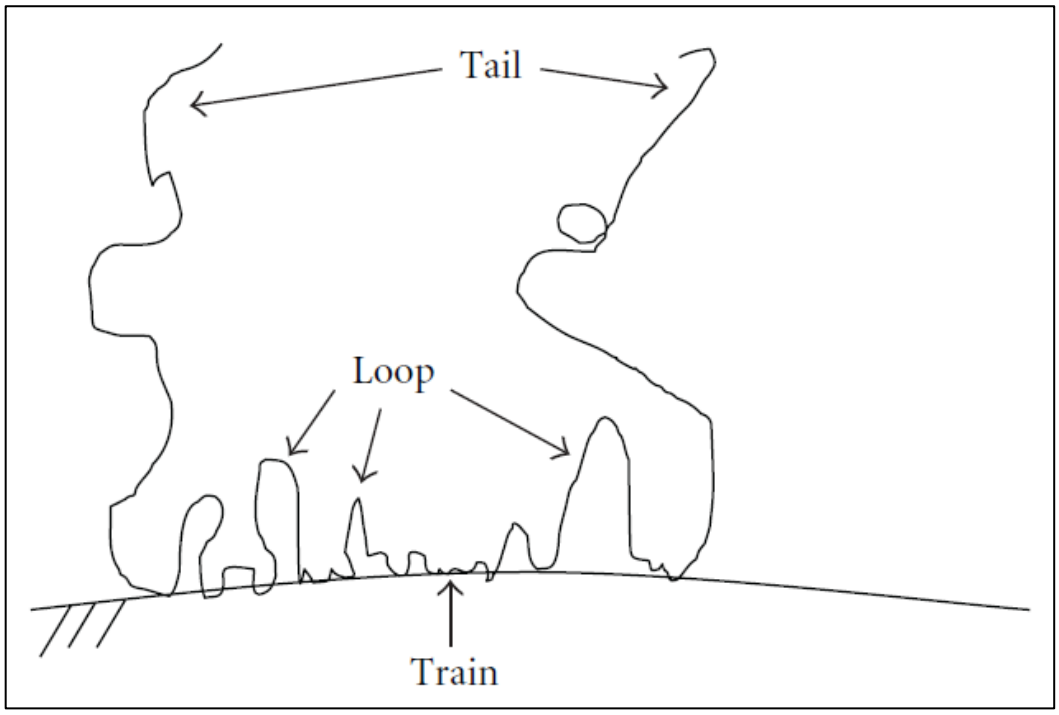

Figure 6. Schematic presentation of polyelectrolyte adsorption on the surface. /16/

The charge density of polyelectrolyte is one of a major factor affecting the conformation of the adsorbed layer. Highly charged polyelectrolyte has a tendency to constitute a flatter structure on the surface because of strong electrostatic repulsion within the polymer chain. In contrast, the polymer chains with lower charge densities are less rigid and are able to form larger loops, trains and loose composition as presented in Figure 5. This means that lateral electrostatic repulsion decreases between the surface and adsorbed polyelectrolyte.

Evaluating the effect of the charge density on the polymer conformation, it is worthwhile to define the concepts of the degree of substitution (DS) and the degree of ionization (α). DS reveals an amount of modified monomers by substitution in a polymer chain. While the degree of ionization exposes the fraction of ionizable groups within the polymer chain and therefore rests upon pH. By selecting polymer based on the degree of substitution and ionization can be influenced on the configuration of the polymer. When both parameters increase, the polymer coil tends to form an expanded shape. In other words, an increase in pH induces the polymer adsorption in more extended conformation. /1/.

Respectively, the ionic strength of the medium is a driving force for the conformation of the adsorbed polymer layer as well. By increasing the ionic strength of the medium, can be promoted the flexibility of the polymer conformation forming a more outward and released composition. This sort of polymer behavior is illustrated in Figure 7. Hydrodynamic diameter is a measure of molecular size of polymers. The diameters decrease as a result of adding salt concentration to the suspension. Polymer coil strives to extend because the charges within the coil become screened by the electrolyte, and thus bring the polymer segments closer together. /17/.

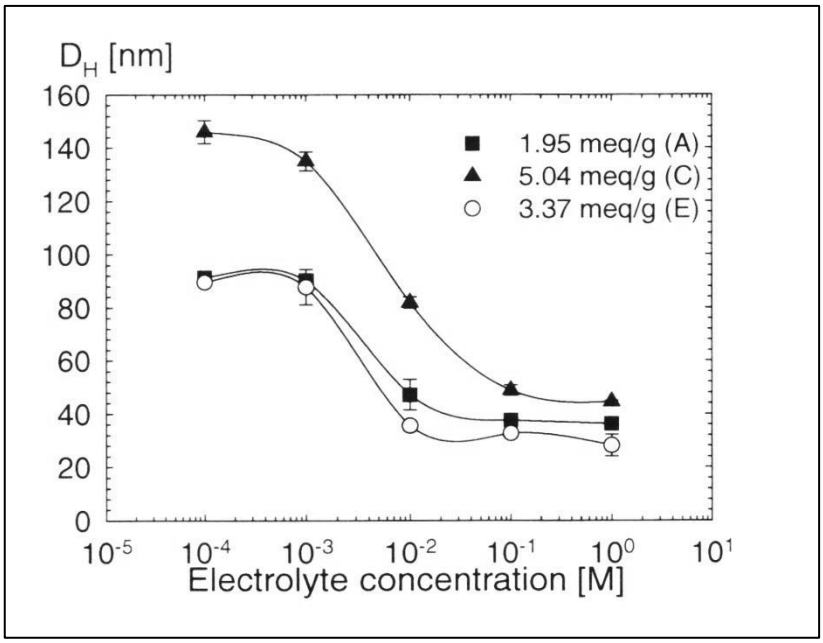

Figure 7. Hydrodynamic diameter (D_H) of different copolymers A, C & E as a function of electrolyte concentration. /17/

Accordingly, the growing ionic strength in polymer solution expands the polymer coil itself but at the interface of the polymer segment and surface the enlargement of polymer decreases. The swelling of polyelectrolytes in the presence of water occurs as a result of the osmotic pressure. Thus, an increase in the salt concentration weakens the intramolecular repulsion within the polymer segments that in consequence the swelling of the polymer deteriorates similarly with the viscosity of the polymer solution. /1, 8, 14/

Equally, a molecular weight of polyelectrolyte influences on the extended configuration of the adsorbed layer in conjunction with the charge density of polymer. In case of the low charge density, a high molecular weight polymer forms a loose structure on the surface with long tails and loops. On the contrary, a low molecular weight polymer with the higher charge density adsorbs in a flat conformation on the surface. In consequence of the polyelectrolyte having low molecular mass is able to penetrate into the fiber cell wall by adsorbing with larger amount on the surface. Despite a low molecular mass of the

polyelectrolyte does not only denote that it adsorbs to a greater amount, the charge density of the polyelectrolyte intervenes in the adsorption as well. /17/.

1.5 Measuring polymer adsorption

Generally, the measuring methods of polymer adsorption are divided into indirect and direct methods. In the indirect method, the adsorption is determined by analyzing the supernatant after physical separation between the surface and continuous phase. The supernatant is typically analyzed by spectroscopic methods, such as UV, FTIR or NMR, in order to measure concentration and to distinguish the chemical composition /8/. Infrared methods give information on the fraction of macromolecules segments attached to the surface. Instead, nuclear magnetic resonance (NMR) can determine the segments of the adsorbed layer in trains and in tails and loops /18/. Some drawbacks regarding to small particle sizes, high polymer solution concentration or volatile solvents and low surface area may lead to disturbed measurements by using the indirect method /8/.

By contrast, the direct method is based on measuring the adsorbed amount of polymer in contact with the surface either in situ or after separation. The results of that enable a more accurate quantity of the adsorbed amount compared with the indirect measuring technique. To investigate the adsorption of a dilute polymer solution on a relative thick surface layer can be done by varying methods, such as *evanescent wave methods, neutron* and *optical reflectometries, ellipsometry, surface plasmon resonance, surface-enhanced Raman scattering and the quartz crystal microbalance.* /8, 18/

As an optical method, the ellipsometry allows to investigate the average thickness of the adsorption layer and the average mass of the adsorbed polymer by measuring the change in polarization of elliptically polarized light when it is reflected to the surface of the sample /19/. Instead, the evanescent wave

method determines the segment density profile of adsorbed polymer layer /18/. Although several analytical techniques exist for obtaining the polymer adsorption, this study concentrates on the few most commonly used methods in measuring the thickness of adsorbed polymer layer and the bound fraction of polymer chain. Firstly, the widely employed applications to explore polymer adsorption are discussed.

1.5.1 Zeta potential

Zeta potential measurement is a common used indirect method to investigate the adsorption characteristics of cationic polyelectrolytes onto negatively charged fiber surface. Measuring zeta potential in the wet-end of the paper machine reveals the performing effect of the drainage- and strength-aids within papermaking stock. The zeta potential is widely used as a controlling parameter in the papermaking process to optimize the dosages of the wet-end chemicals. An addition of a cationic polymer into the stock means a neutralization of the negative surface charge by reaching the zeta potential to zero. The closer to zero is the zeta potential the more polymers are adsorbed on the surfaces of the fibers.

Figure 8 indicates the change of the zeta potential when a cationic polymer is added into the stock. As can be noted, the increase of the zeta potential is nearly identical to the adsorption curve. Because the zeta potential deals with the adsorption behavior of polymer, the performing effect of the wet-end additive can be deduced.

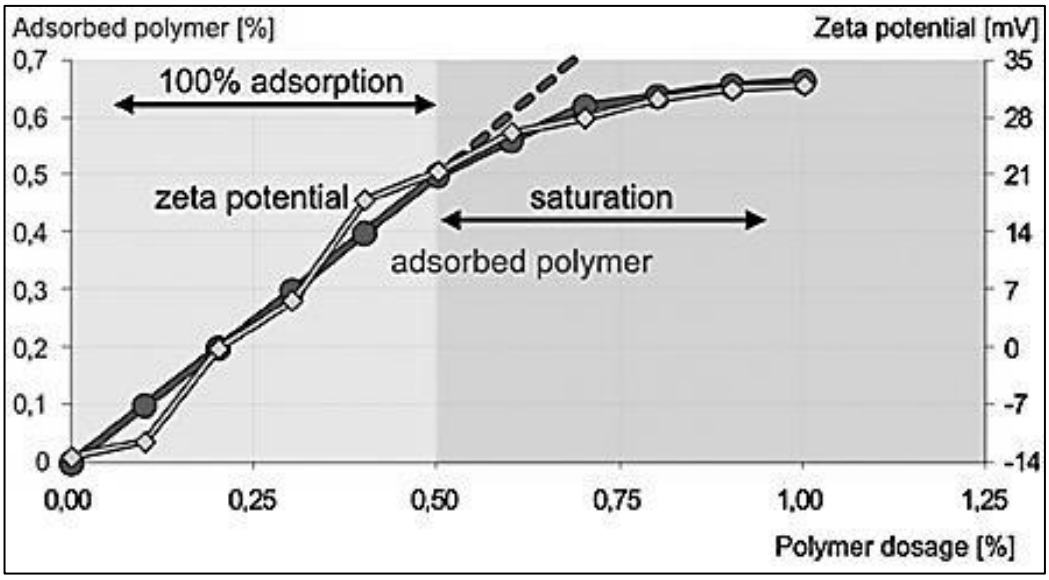

Figure 8. Zeta potential as a function of polymer dosages. /20/

It has been perceived that a thin layer of fluid adheres to the charged surface of particle due to tangential liquid flow as expressed in the chapter 1.1. This layer is called *slip plane*, which is hydrodynamically stagnant layer, where hydrodynamic forces do not exist. Slip plane is placed at distance d^{ek} from the particle surface as shown in Figure 9. The charge density at this level is denoted σ^{ek}. The potential at the slip plane where the particle tend to slip from hydrodynamically immobile layer to bulk solution is called *zeta-potential* (ζ). /21/.

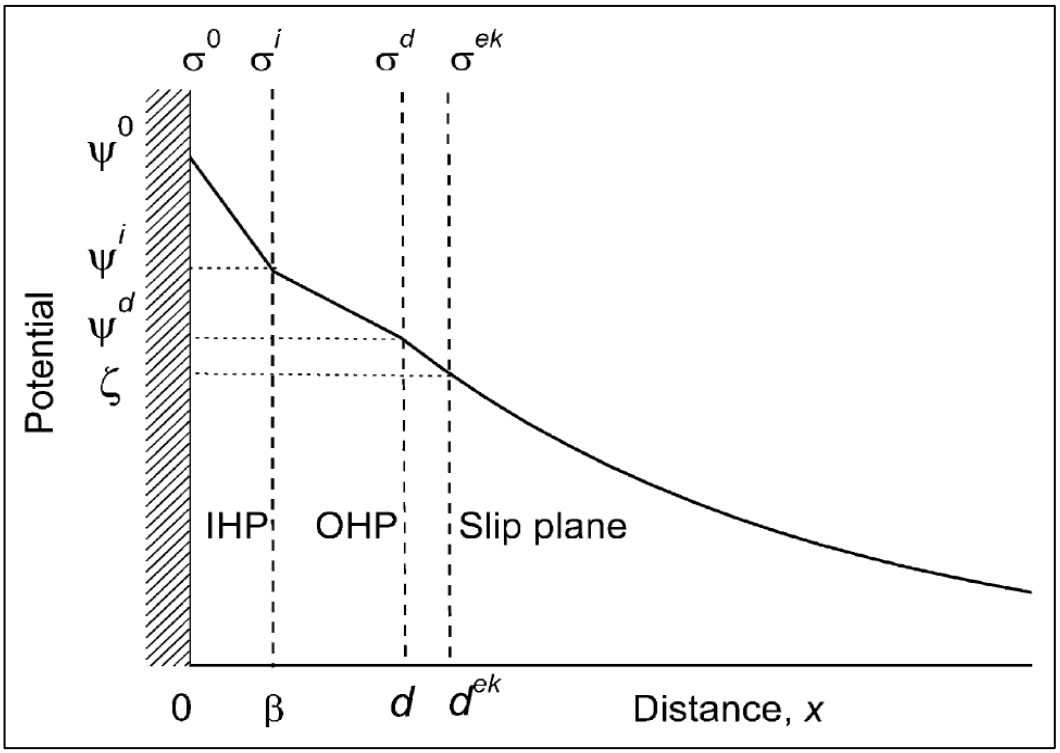

Figure 9. Representation of the charges and potentials at a positively charged interface, where is described the electric potential of the surface Ψ^0, Ψ^i, Ψ^d and charge density as symbols of σ^0, σ^i, σ^d and σ^{ek} as a function of distance x. IHP (inner Helmholtz plane) is at distance $\beta(0 \leq \beta \leq d)$ and OHP (outer Helmholtz plane) determines the beginning of the diffuse layer (at distance d from the surface). /21/

The magnitude of the zeta potential defines the electric static interaction of colloid particles and surfaces in terms of colloidal stability and aggregation. Furthermore, it is stated that the magnitude and sign of the zeta potential are affected by the nature of the surface, its charge, and the electrolyte concentration and nature of the solvent /21/. By changing pH can be affected to the zeta potential. At the certain pH value the zeta potential is zero, this is called the *isoelectric point* (*iep*) of the material, whereas the *point of zero charge* (*pzc*) signifies the pH-value in which the net charge of the surface is zero. /1, p. 252-256/.

1.5.2 Polyelectrolyte titration – PET

Polyelectrolyte adsorption onto cellulosic fiber surface is commonly determined by measuring with the polyelectrolyte titration method. The idea of the direct polyelectrolyte titration technique is to bring an excess of anionic charged polyelectrolytes (A) to solution in order to complex a cationic polyelectrolyte (C) in the presence of a cationic indicator (I). The complexing of the cationic polyelectrolyte by titration can be expressed as:

$$A + C \overset{K_1}{\leftrightarrow} AC \tag{7}$$

$$A + I \overset{K_2}{\leftrightarrow} AI \tag{8}$$

In case when above reaction occur faster in comparison with below ($K_1 >> K_2$), the complex formation can be achieved. Dependencies of the molecular mass and charge density of polyelectrolyte are less important with this method. /17/.

Alternatively, the indirect method of the polyelectrolyte titration is based on an assumption of 1:1 stoichiometric relationship between the charges of polyelectrolyte and fiber surface where the accessibility of the surface charge depends on the molecular mass of the adsorbing polymer. The usual procedure by the indirect technique determines the concentration difference in the solution before and after the adsorption process. Afterwards the amount of the adsorption can be analyzed by constructing adsorption isotherm, which illustrates the adsorbed amount of polyelectrolyte as a function of equilibrium concentration of polyelectrolyte as shown in Figure 10. The quantity of adsorbed polyelectrolyte charges adsorbed can be then evaluated by extrapolating the

adsorption isotherm plateau back to an equilibrium concentration of zero. /17, 22/.

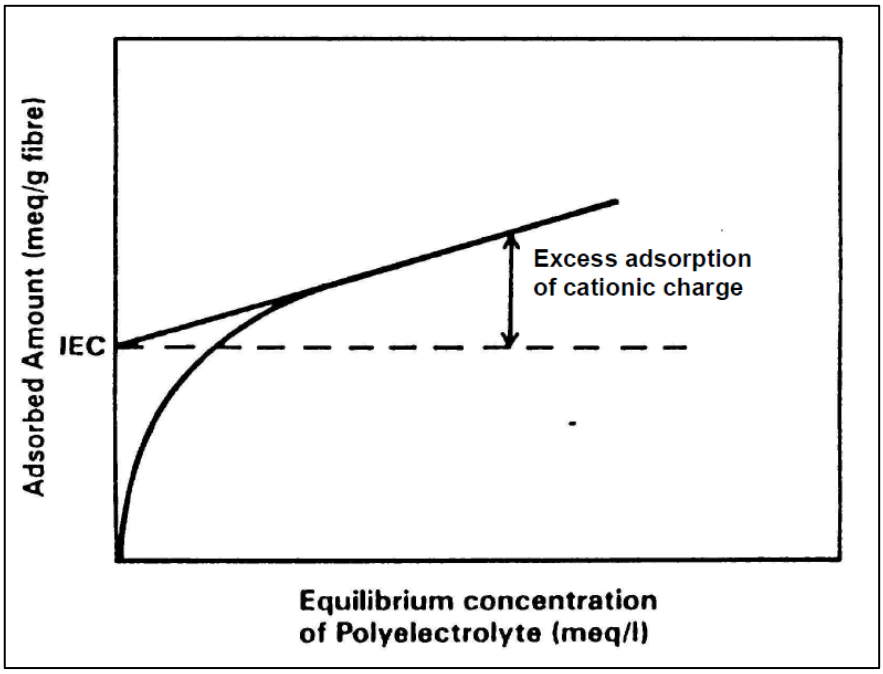

Figure 10. An adsorption isotherm with Ion Exchange Capacity (IEC) in order to compensate for the polyelectrolyte expansion mechanism. /17/

1.5.3 Quartz Crystal Microbalance – QCM

Quartz crystal microbalance (QCM) is a practical researching tool for in-situ adsorption studies for inspecting the adsorption of polymer on the surface. The viscoelastic properties of adsorbed layer can be further studied with an additional dissipation measurement (QCM-D), which determines damping of the amplitude of the oscillation with a decay rate. Furthermore, the adsorbed polymer conformation dependent upon solution conditions may also be evaluated based on the gathered data. Usage of QCM is founded on the capability to analyze mass changes on rigid surface.

In the literature several studies /23, 24, 25/ by using the QCM technique to explore surface interactions between cellulose and polyelectrolytes can be found. The principle of QCM is that the quartz crystal of the instrument oscillates at a specific frequency due to a voltage being applied to the quartz crystal. As the mass on the quartz crystal changes, the frequency of the resonator will change. In other words, the frequency of the oscillating sensor changes as a function of time due to the mass of adsorbed polymer on a sensor. Depending on the mass of material adsorbed on the crystal sensor reduces the resonance frequency.

More theoretically, this can be described by using the Sauerbrey relationship, characterizing that the adsorbed layer to be rigid, evenly distributed and thin and water-free /24, 25/. Although some water will be remained within the adsorbed layer, QCM cannot measure a fully dry mass of adsorbed amount, only a sensed mass including the presence of water. According to Sauerbrey equation (9), the adsorbed mass per surface unit can be calculated on the basis of the resonance frequency shift (Δf), the constant indicating sensitivity of the device (C) and the overtone number of the resonance frequency (n).

$$\Delta m = \frac{-C\Delta f}{n} \tag{9}$$

The frequency shift can be determined by the calculus of differences as shown below.

$$\Delta f = f - f_0 \tag{10}$$

A sign of f denotes a resonant frequency value when material adsorbs on the crystal, while f_0 relates to oscillating without adsorbate.

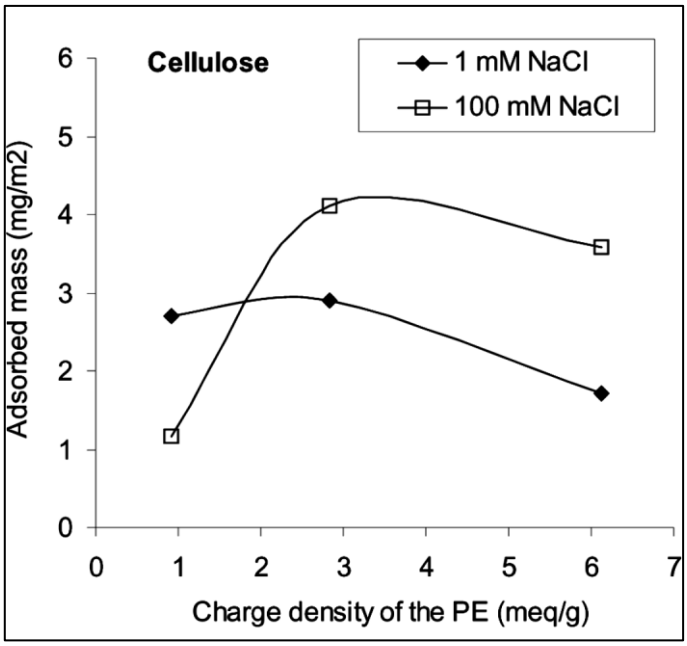

Figure 11. Representation of adsorbed mass of polyelectrolyte (PE) dependent on charge density. Adsorbed mass on cellulose surface determined by using the Sauerbrey equation with QCM-D. The polyelectrolytes used were C-PAM$_{LC-LMW}$, C-PAM$_{MC-LMW}$ and PDADMAC$_{HC-LMW}$. /23/

By QCM can be achieved interesting knowledge on the amount of adsorded mass of polyelectrolytes as shown in Figure 11. Thus, the performance of the polyelectrolytes can be considered by the parameters of the charge density and the molecular weight.

1.5.4 Electron Spectroscopy for Chemical Analysis – ESCA

ESCA, also referred as XPS (X-ray photoelectron spectroscopy) enables to determine the chemical composition of a solid's outer surface (within the first 10 nm) by a spectroscopic technique. With ESCA, the adsorption of material on the fiber surface can be directly determined. It reveals information on the relative amount of different elements adsorbed on the surface. In addition to ESCA measurement, further analysis related to morphology of fiber surfaces is usually examined by atomic force microscopy (AFM). /26, 27/.

In principle, ESCA method detects the emissions of photoelectrons which are derived from irradiation of the detected sample with X-rays. By measuring the kinetic energy of the emitted photoelectrons in the detector of the ESCA permits the calculation of the binding energy /26/. This can be theoretically obtained by the equation of the kinetic energy:

$$E_k = hv + E_b + \theta \qquad (11)$$

where

E_k	is	kinetic energy
hv	¨	the energy of the X-ray
E_b	¨	the binding energy of the photoelectron
θ	¨	work function (the minimum energy required to remove an electron from a solid surface)

The emitted photoelectrons losing no energy as a result of X-ray penetration in to surface give only responses to the series of photoelectron peaks that reflect the binding energy of the electrons. The presence of adsorbed layer on the solid surface achieves discrete signals compared to the bare surface due to diverse escaping photoelectrons, as illustrated in Figure 12. Thus, by comparing spectra of the pure and adsorbed surfaces the relative amounts and coverage of the adsorbent can be determined. More detailed description of the principle of the ESCA technique is presented in literature /27, 28/.

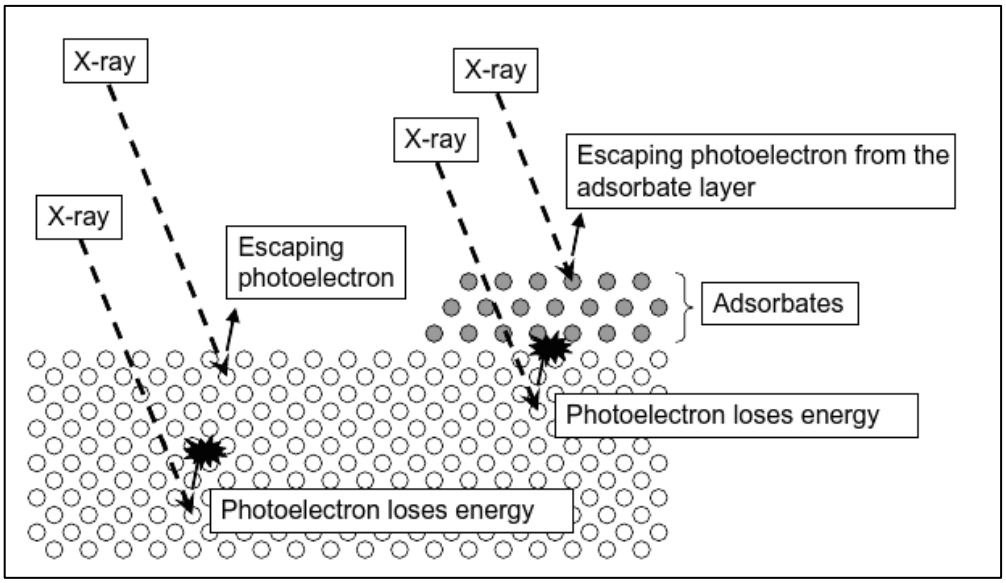

Figure 12. Schematic illustration of the emissions of photoelectrons with X-ray radiation on the solid surface and on the adsorbed surface. /27/

Generally, the usage of the ESCA technique for examining the chemistry of solid surface has gained popularity due to its attributes. The advantages of ESCA are its elemental identification and quantification of any element, high sensitivity in elemental analysis and ease of analysis and interpretation of spectra /27, 28/.

1.5.5 Stagnation Point Adsorption Reflectometry (SPAR)

Optical reflectometry is a tool for examining directly and quantitatively the adsorbed amount of per unit area on a solid surface. The method uses a linearly polarized light beam, which is aimed towards surface substrate and is reflected from the adsorbed surface in the stagnation point. The reflected beam is guided into the detector, where it splits into parallel and perpendicular components of polarized light by using a polarizing beam splitter. A pair of photodiodes measures continuously the intensities of the parallel and perpendicular components. With the ratio of these intensities the output signal S of the

reflectometer is determined. The adsorbed amount can be calculated by the equation:

$$\Gamma = \frac{1}{A_S}\frac{\Delta S}{S_0} \qquad (12),$$

where $A_s$is the sensitivity factor and $\Delta S/S_0$ reveals the reflectometer signal as S_0 describes the conditions of the bare surface prior to adsorption. Benefits for reflectometry are its simplicity and cheapness in comparison with another optical method of ellipsometry. Moreover, reflectometry offer an opportunity for the measurement of adsorption kinetics. /29, 30/.

2. DRY STRENGTH DEVELOPMENT OF WEB

After the characterization of the polyelectrolyte adsorption on fiber surface, it is natural to turn to concentrate on the effect of chemical dry strength agent in the formation of paper web. In this chapter, the mechanisms of dry strength, the influence of chemical strength additives on the enhancement of dry strength and the adhesion between the surfaces of fibers and polymers are discussed.

The key factor to controlling the strength of paper web is in the rate of contacts between the fibers in the web matrix. This rate of fiber contacts can be increased by beating which increases the ability to form stronger web. Respectively, the strength property of paper web can be improved by adding chemical additives which enhance the adhesion of existing contact zones between fibers and polymers. /29/.

Dry strength property of a paper web is primarily generated due to the development of fiber-fiber bonds influenced by the consolidation and drying of the fiber network in papermaking. Due to removing of water from the interface of fibers, the balance of colloidal and capillary forces (Campbell forces) is sufficient strong to bring facing surfaces of fibers into contact /35/. There are several factors affecting the strength of a paper sheet in terms of fiber-fiber bonds /32/:

- strength of inter-fiber bonds, i.e. joint strength between fibers
- fiber strength
- number of bonds per unit volume of the sheet
- distribution of fibers, i.e. the macroscopic formation of the fiber network

In consequence of the carboxylic groups on the hemicelluloses engender an anionic charged of wood fibers. For that reason repulsive electrostatic forces and attractive van der Waals forces are present in the papermaking furnish affecting the final molecular adhesion between individual fibers.

2.1 Entanglement of fibrils

Figure 13 depicts schematically, how cellulose fibrils may arrange in the paper making process generating dry-strengthening effect of paper web. In the presence of water, very small diametric micro-fibril bundles of a cellulosic fiber start to expand. This is due to water eddies in the free spaces inside of the micro-fibrils to break it, causing a flexible and loose structure. These relatively long hairy and flexible fibrils tend to entangle with each other forming a coherent structure resulting in wet strength of the fiber network. The entanglement of the fibrils matrix is enhanced by the pressing of papermaking where the fibrils are sufficiently brought to each other. The consolidation of the fiber network occurs at the drying section where water is removed, resulting in the dried entangled web of the cellulose fibers. /33/.

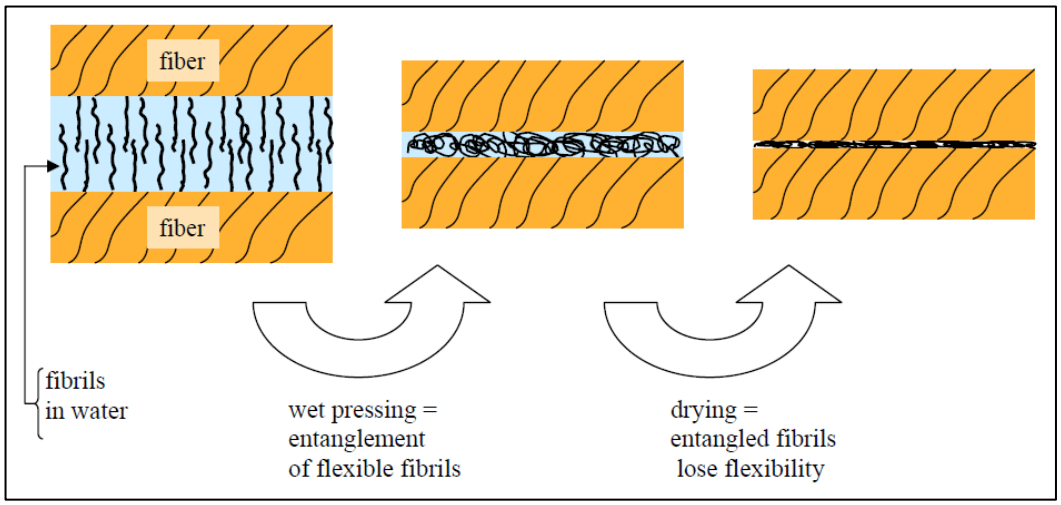

Figure 13. Illustration of cellulose fibril arrangement in papermaking. /33/

This sort of mechanical surfaces linking is highly dependent on the kinks and curl of fibers and fibrillated fiber surfaces. Thus, the entanglement of such fibers may occur inherently with the recovered fibers whose external structure is more protruded due to the repulping procedures.

The addition of dry strength additives into furnish prior to paper formation promotes paper strength. Thus, these synthetic and water-soluble polymers adsorb on the surfaces of the micro-fibrils of fibers and bond them together. Physical improvement as a result of dry strength polymers is affected by the increased stiffness of fibrils, in consequence of decreasing the number of fibril ruptures. /33/.

2.2 Strength in paper web

In the literature /34, 35/ can be found a large number of books and journals dealing with molecular adhesion. Briefly, the phenomenon of adhesion refers to the ability of diverse materials to stick together. Work of adhesion describes the energy needed to overcome adhesion in the unit area of contact between surfaces 1 and 2. From the molecular adhesion of papermaking perspective, work of adhesion between two surfaces in contact can be determined by the following equation /36/:

$$W_{12} = W_{12}^{d} + W_{12}^{p} = 2\sqrt{\gamma_1^{d} \times \gamma_2^{d}} + 2\left(\sqrt{\gamma_1^{+} \times \gamma_2^{-}} + \sqrt{\gamma_1^{+} \times \gamma_2^{-}}\right) \qquad (13),$$

where

W_{12}	is	work of adhesion between surfaces 1 and 2
W_{12}^{d}	¨	van der Waals contribution
W_{12}^{p}	¨	polar contribution

γ^d	¨	dispersive part of the surface energy of a material
γ^+	¨	acid part of the polar part of the surface energy of a material
γ^-	¨	base part of the polar of the surface energy of a material

A concept of the molecular adhesion refers to the force experienced when bodies make contact at the molecular level. In this study, the term of adhesion denotes the molecular adhesion. According to Kendall et al. /34, p. 3-24/, the adhesion is difficult to examine as phenomenon in a fiber level due to the surface roughness of fibers and unavoidable contamination of the surfaces.

The effect of adhesion phenomenon in a paper sheet can be illustrated in three levels: macroscopic, microscopic and molecular. Immersing more detailed to the microscopic (10µm-1mm) and the molecular (0,1-100nm) levels promotes understanding of strength development within fiber network. The porous and heterogeneous surface of the cellulose fiber makes it challenging to apply adhesion theories directly to inter-fiber bonds.

Based on the earlier studies, the joint strengths between individual fibers can be simply explained by Page's adhesion theory indicating that the interfiber bond strength is crucial for weakly bonded paper, whereas the strength of well bonded paper is dependent on the fiber strength. Based on this approach, it is a common practice in papermaking to influence on paper properties by improving interfiber bond strength (B) through such as beating and chemical additives. This can be simplified by the following equation /35/:

$$\frac{1}{T} = \frac{1}{F} + \frac{1}{B} = \frac{9}{8Z} + \frac{12g \times C}{P \times l \times b \times RBA} \quad (14),$$

where

T	is	tensile breaking length
F	¨	fiber strength

B	¨	interfiber bond
Z	¨	zero span of fibers
C	¨	fiber coarseness
P	¨	fiber perimeter
l	¨	fiber length
b	¨	fibre-fibre bond strength
RBA	¨	relative bonded area

Generally, it has been demonstrated /37/ that an addition of polyelectrolytes enhances the adhesion between the fibers by growing the molecular contact area and/or the amount of fiber-fiber bonds. Furthermore, it has shown /38/ that the strength of the joint between fibers is stronger with increasing charge of surfaces, denoting an increase in the molecular contact area. The high surface charge of the fibers influences on the swelling of the fiber surface and hence the transverse elastic modulus of surface, resulting in a larger molecular contact area. The molecular contact area is often referred to the relative bonded area (RBA) determined by use of the light scattering of paper sheet, as defined by equation 15:

$$RBA = \frac{s - s_0}{s_0} \qquad (15)$$

S is the light-scattering coefficient of a sheet and S_0 describes the total scattering coefficient for a completely unbonded sheet /39/. Figure 14 describes schematically fiber-fiber contact, where light scattering measurements are used to detect the areas in molecular contact in a paper /36/.

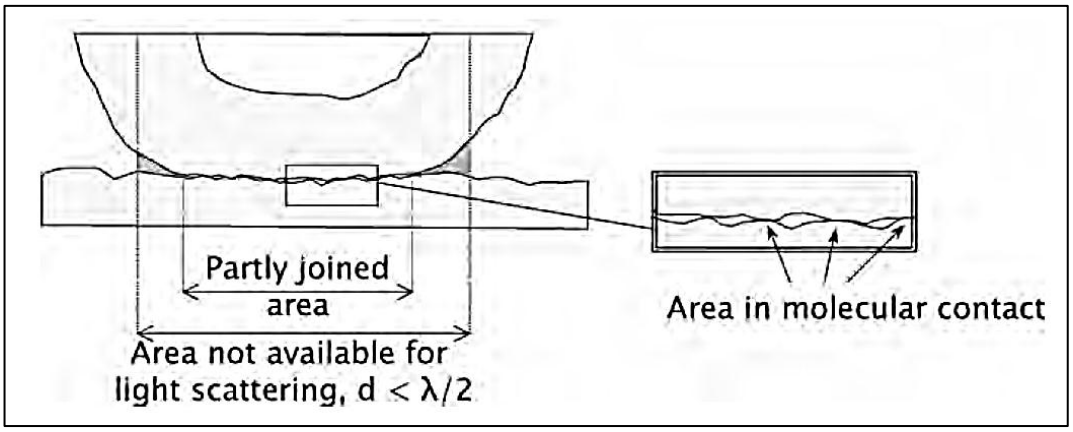

Figure 14. Depiction of the areas between the fiber-fiber joint to detect the relative bonded area by light scattering. /36/

Even though there is a broad set of articles in literature related to the polymer adhesion and measuring the adhesion, the fundamental understanding of adhesion between fiber-fiber joints is not yet fully found. Essentially, difficulties to measure and to verify the mechanisms regarding the molecular adhesion in paper have been limited. In terms of work of adhesion presented by the equation 13, the contributions of the polar and the van der Waals forces to the adhesion cannot be absolutely determined. Lindström et al. /36/ and Eriksson /37/ summarized three major mechanisms of adhesion based on the earlier researches:

1) *Mechanical interlocking* – greatly rough and fibrillated surfaces of fibers are linked together by contributing adhesion between fibers. The effect of this mechanism increases with a greater number of fibrils to entangle with each other.

2) *Molecular interdiffusion* – molecules at the interface of fiber surface are able to diffuse into each other during pressing and drying. According to the interdiffusion theory suggested by McKenzie /40/, polymer segments adsorbed onto fiber surfaces adhere with each other as the fibers are forced into contact with each other during sheet

formation. In this connection, the fibers orient themselves in order to form hydrogen bonds. It is accurate as well with polymer chain contacts when they dissolve in each other.

3) *Chemical interactions/attractions* – a close molecular contact between fibers give reason to consider van der Waals forces as a possible bonding force for the fiber-fiber joint. However, most of theoretical models consider that the role of hydroxyl groups on the cellulose are domineering and forming attracted bond between surfaces as water is removed. Furthermore, the electrostatic interactions may contribute to molecular adhesion in the contact zone between fibers.

2.3 Strength parameters of liner and fluting

Short span compression test (SCT), also known as STFI, is a common industrial used measuring method for determining the compression strength property of linerboard and fluting. The compressive strength is one of the major requirements for the corrugated container and as a performance metric, it informs substantially about stacking capabilities of the corrugated containers. The SCT denotes a pure loading at the fiber length scale (0,7 mm), implying the actual intrinsic compression of fibers. Thus, it will not fail due to buckling or large scale voids created by delamination join. Nevertheless, the micro-scale non-uniformities in the substrate may increase sources of uncertainty within the measurement. The SCT method is also strongly affected by unevenness at the structural level of the material. The primary strength considerations for the SCT are CD (cross direction) stiffness, ZD (Z-direction) stiffness and fiber orientation. Density of the fiber network is a critical factor controlling the compression strength of linerboard and fluting because the SCT increases with higher densities of sheets. However, density is less remarkable factor to SCT in comparison with ring crush test (RCT). /41, 42, 43/.

Burst strength describes an ability of liner sheet to withstand a thrusting force against a facing of the sheet until the facing bursts. The burst strength is a common test method for the quality control of liner because it is the uppermost of the corrugated container.

Characteristic of stiffness is a major property for the corrugating medium that has been assessed by measuring flat crush of corrugating medium (CMT test). The CMT is described in ISO 7263. The aim of this method is to anticipate crushing of the fluting before it is fabricated into combined board. Traditionally, the corrugated medium test is measured either immediately (CMT_0) after fluting or 30 minutes (CMT_{30}) after pre-conditioning at 23°C and 50% RH. The latter is more used practice in the industry giving more reliable values due to the longer time span after corrugating. /44/.

3. DRAINAGE DEVELOPMENT OF WEB

Retention and dewatering are key issues in papermaking. Retention term denotes the extent to which the pulp fibers and other additives which are added to furnish are retained in the finished paper. The manufacturing of cellulosic fiber sheet involves: producing aqueous slurry of cellulosic fiber containing inorganic material, depositing of this slurry on a moving wire or fabric and forming a sheet from the solid components of the slurry by draining the web. Hence, a filtration property of pulp fiber suspension during the sheet formation is a primary phenomenon in the drainage of the paper web. The retention aid chemicals are used to improve retention and drainage in consequence assists the attachment of solid materials. The advantage of their usage achieves faster runnability in paper machines and drier sheets in the press and dryer sections, resulting in reduced energy consumption. In case of the recycling stock, the fines retention plays a significant role in papermaking because of high level of fines. Inadequate retaining of fines will lead defectives in the final product as well as increasing costs. /45, 46/.

3.1 Dewatering

In practice, the performance of dewatering of paper web can be characterized by the filtration process. Thus, the filtration of water through the porous paper web describes dewatering time of pulp suspension in the sheet formation stage. Briefly, a principal approach regarding the flow resistance of the filtration process through packed beds of granular material was first introduced by Kozeny and later modified by Carman /47/. An equation of the Kozeny-Carman is given below:

$$k = \left(\frac{\gamma}{\mu}\right) \times \left(\frac{2}{C_{K-C}}\right) \times \left(\frac{1}{S_0^2}\right) \times \left[\frac{e^3}{(1+e)}\right] \quad (16),$$

where

k	is	permeability (length/time)
γ	¨	unit mass of fluid
μ	¨	viscosity of fluid
C_{K-C}	¨	the Kozeny-Carman coefficient
S_0	¨	specific surface area
e	¨	fractional void volume

This conception is commonly established and further adapted by several researchers to specific situations including heterogeneous and fibrous material of papermaking. Zhu et al. /48/ submitted that the theory can be applied in modeling of flow through the pulp fiber mat. In addition, it has been demonstrated based on the Kozeny-Carman concept in the previous studies /49, 50/ that fine material having the smallest size and highest specific surface area tends to have the greatest detrimental effect on dewatering.

These conclusions support the concept of the choke-point mechanism by which unattached fiber fines can move freely through the network of paper web and may block the fiber channels within the web by restraining the flowing water /47/. By adding a cationic polymer into pulp suspension, fines start to agglomerate to larger flocs and adhere on the fiber surface. The choke-point mechanism is illustrated in Figure 15.

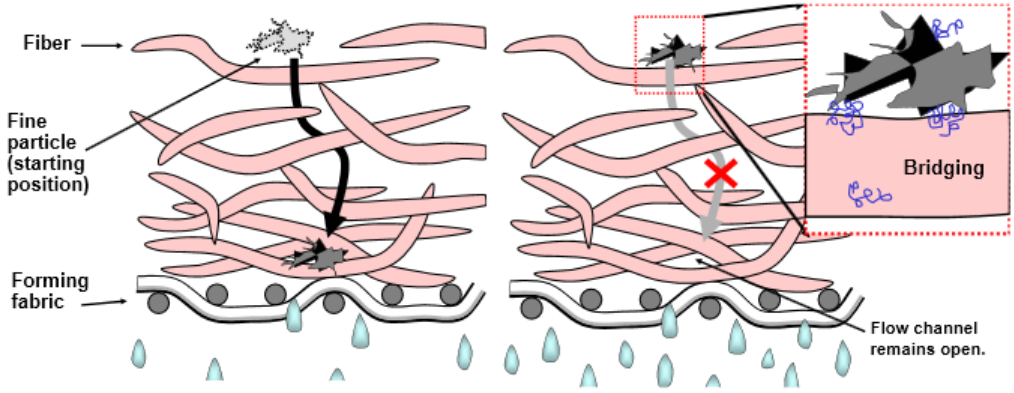

Figure 15. Schematic representation of the filtration process during sheet formation. Unattached fine particle migrates to position where it tends to block the water flow (left). HMW polymer adheres by bridging on the fiber surface promoting the release of water. /47/

Hubbe et al. /51/ validated the hypothesis of the choke-point mechanism that then the agglomerates of fines have less effective surface area, flocculated fiber mat is less uniform to assist the drainage and adhering fines are not acting as blockers of the released water. Furthermore, another fundamental approach concerning the dewatering process is described as a sealing mechanism. A contribution of this mechanism is that more rigid fibers can be forced together as a result of applied vacuum or wet-pressing, so that water flows easily through paper web. By contrast, flexible fibers tend to slide past each other forming a dense network and thereby the channels between fibers are blocked. /47/.

Generally, the function of cationic polyelectrolytes as drainage-enhancing aids is based on their mechanisms to form flocs. High molecular weight and water soluble polymers with cationic or anionic charged have been typically used as retention and drainage aids. When adding a high molecular weight polymer, its extended configuration adsorbed onto surface promotes the flocculation by bridging. Alternatively, a high charge density of polymer achieves coagulation of particles by charge neutralization effect. The drainage efficiency of the polymers or copolymers depends on the type of monomers but also the arrangement of the monomers in the polymer matrix. Antunes et al. /52/ proposed that the

branched polymers enhance dewatering in comparison with linear polymers because they tend to form smaller flocs.

3.2 Flocculation

Flocculation is usually a necessary phenomenon to recognize in evaluating the dewatering system of papermaking, containing significant quantities of auspicious particles sizes to aggregate. The relationship between flocculation of pulp fiber complexes and drainage capability has been studied by authors /51, 52, 53, 54/. Based on their results, it is concluded that an increasing flocculation rate of the fibers can make more porous structure of the fiber network, enabling faster water removal through fiber channels.

Generally, three types of mechanisms for the polyelectrolyte flocculation of charged particles are widely discussed in the literature /54, 55/. These mechanisms are also known as retention mechanisms. First, a *bridging* mechanism is presumed to occur with high molecular weight and low charged polymers. Extending loops and tails of the polymer reinforce the adsorption onto the negative surface of a second particle. Alternatively, the mechanisms of *charge neutralization* and *patch flocculation* prevail with the low/moderate molecular weights and high charged polymers. Since the polymer is adsorbed, collisions of oppositely charged patches on another particle lead to coagulation. Depending on the type of polymer, their molecular weight, charge density, configuration and environment can be determined that which of the above mechanisms may participate in the action of additions of polymer additives with pulp stock.

4. FACTORS OF OCC FURNISH INFLUENCING ON STRENGTH AND DRAINAGE OF LINER AND FLUTING

This chapter deals with the parameters affecting strength and drainage properties of liner and fluting OCC pulp. The characteristics of OCC pulp influencing on the strength and drainage development of the paper web and on the performance of dry-strength and drainage aids are discussed. Moreover, the common challenges that need to be considered in processing of recycled fiber are introduced.

4.1 Effect of recycled fiber

The use of inexpensive fiber sources in papermaking has been increased over the past decades. Particularly, old corrugated container (OCC) pulp as an environmental friendly recycling material in the manufacturing of liner and fluting grades are generally used in Central Europe, China and the North America. Nevertheless, virgin pulp is commonly used raw material in the Nordic countries and in the North America in the producing of the corrugated boxboard.

Recycling of OCC pulp requires a right type of waste. In many cases liner and fluting producers use mixed waste recycled paper grades in conjunction with OCC as raw material. This causes deterioration of fiber properties. Consequently, closed loop recycling ensures that only old corrugated containers and cardboard boxes are recycled into OCC pulp. OCC is mainly made up of used unbleached or bleached kraft pulps, hardwood semi-chemical pulp and grass pulp /56/. Previous researches /57,58/ have shown that the strength properties of finished paper deteriorates due to the number of cycles in the fiber recycling. This is mainly because of the decreasing of fiber bonding ability through the hornification phenomenon and a loss of flexibility /59,60/.

Refining is a common operation for the secondary fibers. Even though recovered fibers have already refined, they need to refine again to achieve good bonding properties. Generally, the fiber length of OCC is shorter compared with the virgin pulp and thus the refining is done with gently refining intensity to obtain the fibrillated surface structure of fibers, avoiding further degradation of the fibers. In particular, due to the right refining the burst and tensile strength properties of OCC furnish can be improved /61/.

To clarify differences between recycled fiber and virgin fiber, the following list is summarized to describe the major points in which secondary fibers deviate from virgin fibers /61/:

- Lower freeness
- Shorter fiber length and more fines
- Increased density
- Lower strength properties (e.g. burst and tensile)
- Less fiber swelling
- Less fiber flexibility
- Reduced fibrillation
- Deteriorated bonding ability
- Lower water retention

4.2 Quality requirements of OCC furnish

A challenging issue in the future that will be encountered in the global world is a quality of recovered pulp. By meaning that fiber sources of recycled pulps are diverse depending on geographical locations and the growing global streams of goods mix the fiber sources with each other. Particularly, the compositions of recycled pulp are variable in the largest market areas, such as in the North America, Europe and Asia. American OCC furnish contains typically longer fibers and less contaminants compared with European and Asian OCC pulps, where the

characteristics of stickies and waxes are hindered their separation from the process /62/. In consequence of the characteristic differences of recovered pulp the quality requirements for the finished product are challenging to meet. Furthermore, variety of the incoming material can be expected to cause large fluctuations in the charge demand remaining in the pulp as a result of instability of operations. For instance, some of undesired substances, like palmitic acid salts, cationic starch and other dissolved and colloidal substances are present in the process, even though they are re-pulped several times. /63/.

A common method to improve the quality of the raw material is fiber fractionation. This mechanical process has been used mainly in packaging materials lines. Typically higher-grade fractions including long and short fibers and lower-grade fractions including fines and ash are separated into each storage chests. Thereafter, the long and short fibers are further fractionated or remixed in order to exploit their specific properties. Long-fibered fractions are used for the linerboard to give strength, whereas short-fibered fractions are applied to the fluting board to achieve a bulky medium. Generally speaking, the idea of the fiber fractionation is to produce two furnishes in order to obtain more desirable fiber properties relative to the original pulp. Respectively, the economic advantages support the use of the fractionation because of the reduced energy and chemical costs. /62, 64, 65/.

A general conception related to the use of long fibers is that they contribute to good strength and drainage properties of the forming paper. Long-fiber fractions contain mainly softwood fibers. A high length-to-width ratio of long fiber explicates a role of fiber dimensions influencing on the contacts with the neighboring fibers. The larger amounts of hydrogen bonds within fibers the higher is tensile and tear strength of the sheet network. /60/.

Short-fiber fractions and fines are considered being of lower papermaking value due to their characteristics. Presence of fine fractions raises a volume of impurities because small dirt and ink particles are easily concentrated on fines.

Moreover, the ash content of the short fraction is higher in comparison with the longer fiber fractions. It has been demonstrated that fines have a negative effect on the drainage and strength properties of the resulting paper. However, the surface area of fines is three to five times larger per unit mass than the long fibers have. For that reason the drainage of the forming sheet is more complex. The fines are eddied to positions by blocking the flow of water through the fiber channels in the web. The rest of unretained fines pass through into the white water. Consequently, the dewatering is decelerated and the unevenness of fines in z-direction increases. /60/.

A term of hornification is essential to define due to its relation to the properties of recovered fiber. Briefly, it denotes the structural change in the bonds of the cell wall derived from rewetting after drying. In water suspension fibers tend to fibrillate externally by opening pores between the lamella and fibrils and spreading out fibrils from the surface, in which case fibers swell. During drying, the pores close and the appearance of the external fibrillation flattens due to water removal. On rewetting, the fiber does not adsorb water similarly because drying causes an irreversible physical contraction of the fiber cell wall. Thus, irreversible hornification implies the loss of fiber flexibility resulting in a stiff fiber because of the reduced internal fiber swelling. Previous studies have been demonstrated that the fiber flexibility decreases mostly during the first two recycles. /66, 67/.

4.3 Conductivity

Conductivity is one of the major properties influencing on the characteristics of the OCC pulp. Generally, a term of conductivity in papermaking refers to salt concentration in furnish. Salt is dissociated into ions and they are measured through solution conductivity. The importance of the parameter is highly related to the adsorption of polyelectrolytes due to electrostatic forces affecting to the

conformation of polymer coils and fibrils at the surface of the fiber. The conductivity of the recycled pulp is typically high because increased recirculation of white water back to the process accumulates the levels of salt. The recycling of process water causes the amount of unwanted ionic trash (polyelectrolytic and ionic surfactant-type material) and COD consuming organic material to cycle up in the process system. /60, 69/.

Salts are small ions which are not retained in the paper web. Because of the high stability of the salt ions in water solution they tend to stay in the process water. For instance, the high stability of the sodium atom is based on its ionized form with a single plus charge in water that the stable set of eight outer-most electrons surrounding the nucleus is completed.

According to the literature /60/, the conductivity rises as increased recirculation of water back to the headbox increases. Excessively high conductivity (>4000 µS/cm) worsens the usage of the most commercial wet-end additives. Salt ions interfere with phenomena within processes that depend on electrical charges. At the certain high salt level the adsorption of polyelectrolytes is decreased. Thus, the conformation of polyelectrolyte molecule is flatter because of decreased internal repulsion within the polymer segments. Increasing the concentration of salt shortens the effective distance of electrostatic forces between particles as explained in the chapters of 1.1 and 1.4. This is expected to prevent the formation of molecular bridges between particles. Reduced intra-molecular repulsion denotes that less swelling and flexibility of fiber is occurred. Moreover, the fibrils on the fiber surface tend to stay lying position by impairing flocculation.

4.4 pH

Besides the conductivity, the change of pH has an extent impact on the actual charge on the fibers. Previous studies /68, 69/ have been revealed that an

increase of pH raises fibre surface charge that is consistent with the expected dissociation of carboxyl groups. The carboxyl functional groups of cellulose fiber are deprotonated due to an increase of pH.

Furthermore, it has been suggested /70/ that the pH during drying process affects the extent of hornification. Furnish having low pH value contains larger number of the carboxyl groups exposing more effectively to hornification of cellulosic fibers. On the contrary, the higher pH-level (<8) transfers the carboxyl groups to their Na^+-form, making them independent on the changes of pH.

Swelling of fibers increases with an increasing pH-value due to dissociation of the carboxyl and phenolic groups. Additions of electrolyte into solution lead to decreases in swelling over the pH-range. The swelling behavior is highly dependent upon the type of pulp because the amounts of acid groups present in the cell wall and their pK_a-values vary. In the manufacturing of pulp is striven to achieve the swelling maxima of fibers by adjusting appropriate pH-level. /70/.

As it is well known, micro-organisms derived from waste paper have a major effect on the recycled pulp quality, particularly when the waste paper is stored for days or months. Thus, the activity of the micro-organisms grows by degrading starch from cellulosic material during storage time. It has been discovered that treating of pulp with a sufficient amount of a suitable biocide, can hinder degradation of starch affected by the microbiological activity. The degradation of starch results in a decrease of pH value of the aqueous cellulosic material causing acidic process condition. Such as acid process water harm the quality of pulp by reducing filler content in pulp. /71/.

4.5 Dissolved and colloidal substances (DCS)

Due to several recycling processes, the surfaces of secondary fibers are primarily covered by fine material, such as cell wall fragments and other fine material

including fatty acid salts, hemicellulose and extractives. Such substances released during pulping are called dissolved and colloidal substances (DCS). Chemical oxygen demand (COD) refers to the amount of organic pollutants in waste water that must be considered in the use of recycled water to improve water quality of the process. It has been concluded /63/ that a high COD loading may correlate with the cationic demand.

A general concept is that the dissolved and colloidal substances have an adverse effect on the performance of the wet-end additives. If the retention aid polymer interacts with these substances, then their ability to adsorb effectively on the interfaces of fibers deteriorates and the polymer loses its functionality. Furthermore, it has shown that DCS can have similar influences on dewatering like as fines. Intrinsically, dissolved and colloidal substances move mainly through the fiber mat but the flocculating DCS agglomerates may plug up the drainage channels within a web of paper by impairing the dewatering time on the wire. /63/.

Bhardwaj et al. /66/ validated that the electrical potential of secondary fiber is not the same in comparison with the virgin pulp. In other words, the zeta-potential value of the recycled pulp is normally closer to zero, whereas the virgin pulp gains more negative electrical potential. The less negative zeta-potential of secondary fibers relates the fact that those fibers are already being adsorbed with other material. This indicates that recycled pulp is not uniform because of containing various pulp types, various fillers, cationic and anionic polymers, sizes etc., resulting in detrimental agglomerates of anionic trash. Due to overcrowding on the surfaces of secondary fibers, the adsorption capability of cationic polyelectrolytes tends to be diminished. It may be predictable that an addition of highly cationic polymer increases the drainage up to the point until zeta-potential of the furnish solids approaches zero /60/.

4.6 Ash content in OCC pulp

Generally, the ash content of OCC furnish varies depending on the geographical area of a mill and its used raw material. For instance, the Asian OCC furnish contains larger filler content than the North American OCC mainly due to rice straw as a medium material. Straws are known to contain high silica content /72/. As is well known, the increasing ash content does not form hydrogen bonds and thus does not contribute to strength properties of the fiber network.

The common trend has been developed by reason of the economic pressure that the high ash content of recycled fiber -furnish replaces a high quality OCC. Such a trend is presented in Figure 16. Moreover, it can be noted that the high ash level also denotes higher freeness value which is known to be a deteriorating effect on the drainage of furnish /73/.

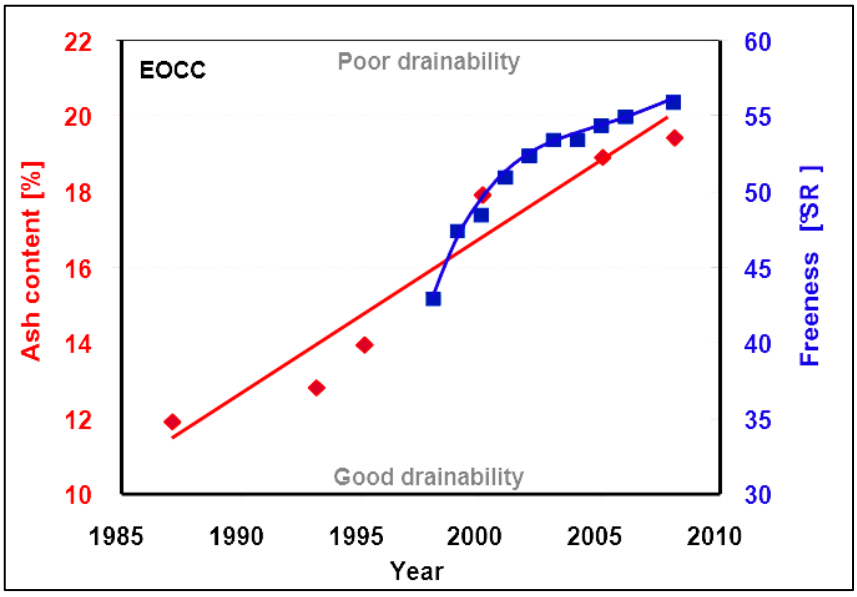

Figure 16. A historic increase of ash content with European OCC. /73/

5. EFFECT OF POLYVINYL AMINE ON STRENGTH AND DRAINAGE

Generally, the strength and drainage enhancing polymers are added in the wet end of paper machine, where they adsorb on the fibers and fines before the formation of web. In this chapter is emphasized on the parameters of polymer chemistry, and particularly on the properties of polyvinyl amine influencing on the strength and drainage properties of OCC furnish.

5.1 Characteristics of polyvinyl amine

Polyvinyl amine (PVAm) as a homopolymer is a linear hydrocarbon chain bearing primary amine groups on alternating carbons. Due to the primary amine groups in their chemical composition, makes them highly reactive. Moreover, the cationic nature of polyvinyl amine in appropriate pH region advances their usage because the high cationic charge density tends to react with anionically charged surfaces. Polyvinyl amine is widely used in numerous applications because of its high charge density, the reactivity of primary amine groups and water solubility. The polyvinyl polymer can be a copolymer of poly(N-vinylformamide), PNVF and polyvinylamine as well. In the present study, the term of PVAm refers to a linear homopolymer of PVAm and the copolymer of PNVF and PVAm. /74, 75/.

Polyvinyl amine resins have increased their popularity within papermaking industry because of their improvements for the paper in terms of the increased dry strength, retention and drainage. In consequence of the increasing use of recycled pulp, the dissolved and colloidal substances can be treated with the vinylamine containing polymer as a fixing agent /76, 77/. Moreover, the effect of PVAm on the fixation can be tuned by altering its molecular weight, cationic charge density and hydrophopic groups. However, polyvinylamine can have a negative effect due to overflocculation with excessively increasing dosages.

Overflocculation is a result of the heavy cationic charge of polyvinylamine. This causes a poorly formed and weak finished product. /75/.

5.2 Preparation of polyvinyl amine

Polyvinyl amine is typically produced by hydrolysis of poly(N-vinyl formamide) by the presence of basic, such as sodium hydroxide. The basic hydrolysis occurs fairly easily compared to acidic conditions because of the attack of strong nucleophile (OH^-) on the amide group in basic solution, whereas the electrostatic forces between cationic amine groups and proton hydrates with acid hydrolysis deteriorates the conversion. /76-79/.

In Figure 17, the chemical mechanisms of acid and base hydrolysis of poly(N-vinyl formamide) is presented. N-vinyl formamide (NVF) is generally used as a precursor for the polymerization of PNVF due to its simplicity and economically aspects. Furthermore, N-vinyl formamide has an ability to form high molecular weight amide and amine functional polymers /77/. Witek et al. /80/ suggested that the homopolymers of polyvinyl amine cannot be obtained via basic hydrolysis of PNVF. Their experiments demonstrated that the PNVF as a highly stereoregular polymer will render beside a primary amine group always one hydroxyl group.

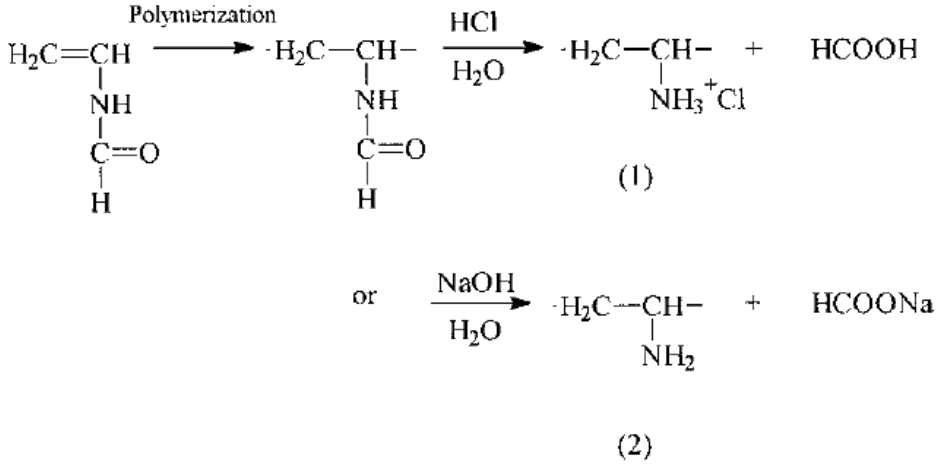

Figure 17. The chemical scheme of poly(N-vinyl formamide) acidic with HCl (1) and basic with NaOH (2) hydrolysis to form polyvinyl amine and copolymers. /77/

5.3 Molecular weight

Molecular weight is one of primary structural parameters affecting to the functionality of polymers. Largely, molecular weight is linked to the mechanical properties of polymers. In the case of linear polymer, molecular weight provides the chain length of polymer. The larger is molecular weight, the longer is the length of polymer chain. Similarly, the viscosity of most polymer increases as a function of molecular weight. /81/

As illustrated in Figure 18, it can be noted that an increasing size of polymer coil with the higher molecular weight leads to a thicker layer of the adsorbed amount. Hence, the adsorbed polymer forming extended structure with tails and loops is more appropriate for the rough and porous structure of cellulose fibers. According to suggestion by Tiberg et al. /82/, it can be deduced that polymers bearing high molecular weight does not penetrate into the micropores at that extent as low molecular weight polymer tends to diffuse into them. Here, it is substantive to take account of time, which has been proven to affect the

anchoring of polymers on porous substrate. However, Wågberg et al. /83/ proposed that an extended conformation of adsorbed high molecular weight polymer tend to form back on the fiber surface with time, while polymers of low molecular weight begin to diffuse into pores of fibers without the reconformation of the structure. /82, 84/

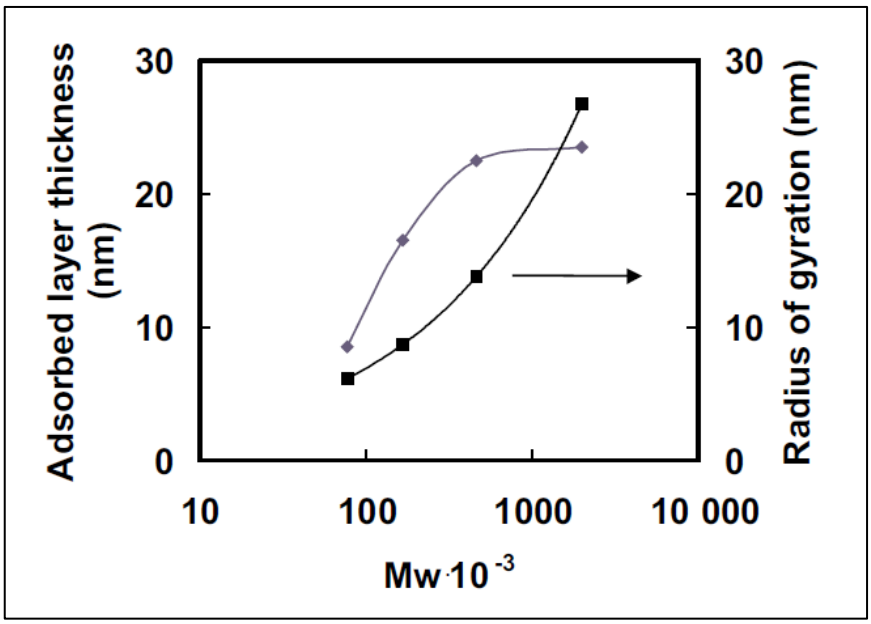

Figure 18. Effect of molecular weight (M_W) on adsorbed layer thickness and radius of gyration. /81/

Even though molecular weight related to the strength enhancing property is widely studied, there is not a simple explicable relationship between them. Previous study /85/ found that a very high molecular weight of polymer may form excessive fiber flocculation, causing poorer formation of the fiber mat. Based on the results by Pelton et al. /84/, the role of the growing molecular weight with the carbohydrate polymers, such as starch, is used to increase the strength properties of paper. Similarly, Zhang et al. /81/ demonstrated that high molecular weight polymers are more effective for strength-enhancing because they tend to adsorb onto exterior surfaces of fibers promoting the inter-fiber

bonding strength. Moreover, they concluded that linear cationic polymers with low molecular weight can adsorb at the larger amount on cellulosic fibers, reflecting that the ability of low molecular weight polymer to penetrate the fiber wall.

The effect of the molecular weight on the adsorption of PVAm shows a typical performance such as other polyelectrolytes on cellulose surface. Oulanti et al. /86/ compared the adsorption of PVAm polymers having similar rates of hydrolysis with distinctive molecular weights in their experiments by observing the adsorption isotherms. The adsorption isotherm of the 90 % hydrolyzed PVAm with both low and high molecular weight is presented in Figure 19.

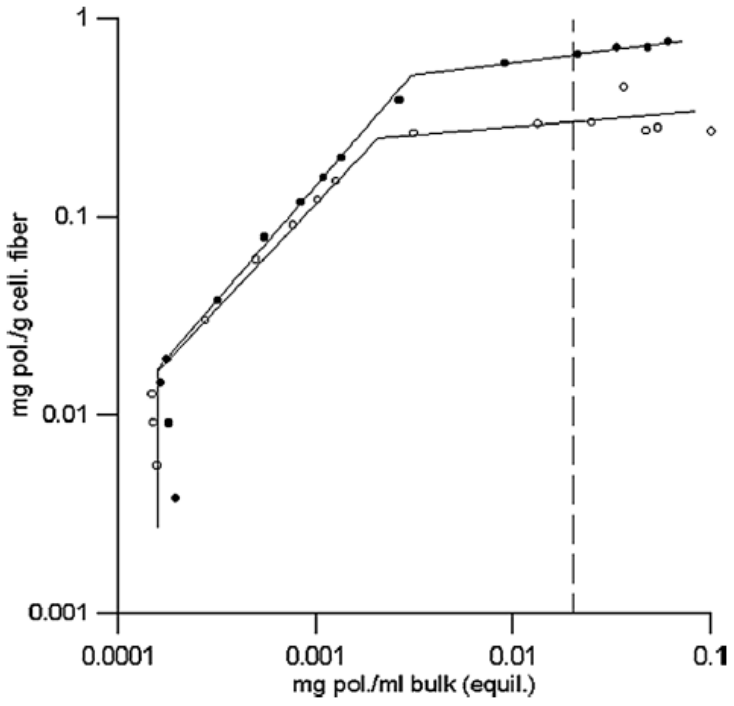

Figure 19. The adsorption isotherm of the 90% hydrolyzed PVAm with low M_w (●) and high M_w (○). /86/

Furthermore, they concluded that the low molecular weight PVAm with the half-hydrolyzed (54%) achieved almost an equal total amount of adsorption on

cellulose surface in comparison with the fully hydrolyzed PVAm with the high molecular weight. This is a remarkable observation in the consideration of PVAm performance in papermaking. /86/

Brungardt et al. /87/ suggested based on their results that the vinylamine-containing polymer is most effective when its molecular weight is from 75 000 to 750 000 g/mol. There was not observed any enhancement in dry strength and drainage performances with the molecular weight of below 75 000 g/mol. Furthermore, they concluded that a polymer having the molecular weight above 750 000 g/mol can generally negatively affect formation at dosages required for dry strength enhancement because of the tendency to overflocculate the sheet, resulting in lower strength. Besides, an aqueous solution of the polymer with the molecular weight above 750 000 g/mol is typically made at such high viscosities as to render product handling extremely difficult. In contrast to the results by Brungart, Lai et al. /88/ proposed that the very high molecular weight of 7 million g/mol denotes an effective burst strength improvement compared to the low molecular weight of 80 000 g/mol. Respectively, the high molecular weight polymer appeared better filler retention characteristics of PVAm in papermaking.

In conclusion, the molecular weight of the vinylamine-containing polymers can be varied at the large range from several ten thousands to several millions. However, the prospect of the overflocculation with the very high molecular weights must be considered in relation to the formation of the paper. Otherwise, it may cause undesired strength issues in papermaking. The optimum molecular weight is dependent on fiber characteristics (chemical vs. mechanical pulp, refining, recycling etc.), process variables (time, conductivity, pH, temperature), structure of polymer (linearity vs. branched).

Moreover, considering drainage-enhancing capability of polymer it must examine the impact of molecular weight of polymer. The lowest dewatering times are typically obtained with increasing degree of flocculation. Thus, the high molecular weight of polymer with a certain charge density and branched

structure corresponds to maximum flocculation /52/. Similarly to floc size, the increased strength of floc promotes drainage because then the resistance of flocs improves against external loads, contributing the flocculation phenomenon and the drainage during sheet formation /53/.

5.4 Charge density

Charge density of polyelectrolyte is a major factor in conjunction with the molecular mass to affect the properties of strength and drainage through the polyelectrolyte adsorption. As the electrolyte concentration of pulp suspension is adjusted at constant level, the conformation of a polyelectrolyte depends primarily on its charge density. Thus, a highly charged polyelectrolyte forms an extended configuration with flatter structure, whereas more coiled conformation with tails and loops is obtained with a low charged polyelectrolyte. These aspects comprehend the degree of the polyelectrolyte adsorption on the fiber surface. Figure 20 depicts typical adsorption performances of polyelectrolyte having same molecular weight. The polyelectrolyte having the lowest charge density results in a higher adsorbed mass on fiber.

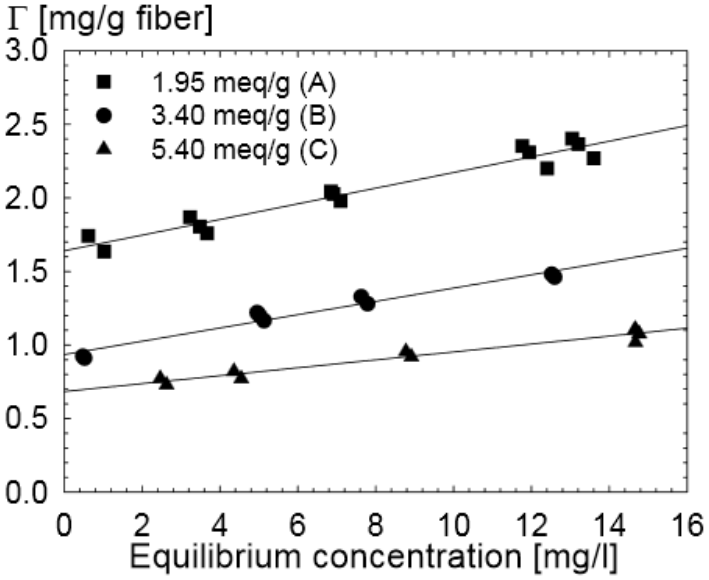

Figure 20. Adsorption isotherm for poly(AM-co-DADMAC) vary with similar molecular weight as a result of charge densities. /23/

Concerning polyvinyl amine, the degree of PNVF hydrolysis reveals the number of formamide groups and primary amino groups in the polymer chain of PVAm and therefore the positive charge density. The charge density increases directly as a function of the amount of primary amino groups in the polymer chain. The charge density of PVAm can be varied over the wide range due to the ability of PVAm to act as both a donor and a receptor for hydrogen bonding. /37/.

The influence of the charge density on strength and drainage is not straightforward because an increasing charge density affects the adsorption amount of polymer and the thickness of adsorbed layer. Hugel et al. /95/ investigated the elasticity and desorption of PVAm based on *atomic force microscopy* (AFM) experiments. They attached amino functions of PVAm on the substrate surface by several loops and strands. Their results demonstrated that an increase in the charge density of PVAm increases the adsorbed layer thickness of PVAm. In addition to changing electrolyte concentration was found to affect its adsorbed thickness. An increase in salt concentration results in a thicker layer of adsorbed amount with the low charge density of PVAm. However, the effect of pH change in the range of 5 to 9 was stated to be unimportant.

Voigt et al. /96/ published similar results that the high degree of hydrolysis increases the adsorbed amount of the polymer onto the substrate. The higher number of amino groups increases the number of positively charged ammonium groups in the PVFA-co-PVAm chain by meaning the polyelectrolyte to be more reactive to interact with the oppositely charged surface centers of the substrate. Thus, such a polyelectrolyte chain having an excessive amount of the interacting spots has more readiness to adhere to surface with train conformations. Strictly speaking, the higher degree of hydrolysis of PVAm indicates the larger amount of amine groups in the polymer chain and a dense and tight deposition on the substrate surface.

From the perspectives of strength and dewatering properties in papermaking, it is a common observation that low charged cationic polyelectrolytes may act effectively for retention and drainage improvement by bridging with the protruding parts of the polyelectrolyte. /47,54/ The flat conformation of high charged polyelectrolyte leads to slower water removal from the compact formed flocs on the fiber surfaces /52/. Hubbe et al. /35/ proposed that a flat adsorbed polyelectrolyte covers more effectively the fiber surface. Considering polymer charge density affecting strength properties of paper, the conductivity level of the process must be taken into account. With increasing salt concentration, high charged strength polymers may act to best advantage. Thus, the polymer charge density plays a significant role in evaluating how they tend to attach to the cellulosic material.

5.5 Hydrophilicity

Polyvinylamine is a water-soluble, or hydrophilic polymer due to its charged functional groups. On the basis of the results by Eriksson /14/, the hydrophilic polyelectrolytes tend to enhance strength properties due to their ability to retain more coupled water by adsorbing on the fiber surface. The results were based

on the QCM-D measurements by indicating the visco-elastic properties of the fiber and polyelectrolyte surfaces, which demonstrates the amount of coupled water. The molecular weight and charge density of the polyelectrolytes were kept constant in order to estimate the influence of the hydrophilicity degree of different polyelectrolytes. The results showed that the more water is retained the stronger are fiber-fiber joints due to the amount of coupled water resulting in the larger contact area between fiber surfaces.

EXPERIMENTAL PART

6. OBJECTIVES OF THE EXPERIMENTAL PART

The aim of the experimental part is to study the influence of polymer characteristics on liner and fluting strength properties and the drainage in the paper machine. To find out empirical evidences reinforced by theoretical regularities is the purpose of this section. Emphasis of the molecular weight and the charge density of polyvinyl amines were considered in the experimental design.

In order to comprehend the performance of polymer in the wet-end of the paper machine, the factors affecting the features of furnish were reviewed. Considering such as conductivity, pH, charge in the wet-end are essential to recognize. Moreover, an application of the polymers with the recovered pulp was targeted. Hence, European Old Corrugated Container (OCC) pulp was employed in this study. The consumption of recycled pulp as a raw material of corrugated board has been grown in pursuance of some drawbacks such as weaker fiber strength and deteriorated bonding ability have been become solvable.

The tested cationic polyvinyl amines were intended to improve the dewatering of furnish in the wet-end of the paper machine to obtain higher increase in production. Moreover, dry strength of liner and fluting was determined by measuring short span compression test (SCT) and burst strength which are the most common used test methods for dry strength properties of liner and fluting. As already reviewed in the literature part, the desired features of polymer are varied depending on its application. Therefore, the experiments to figure out the optimum characteristics of polymer regarding the targets for development would be auspicious.

7. MATERIALS AND METHODS

7.1 Furnishes and test chemicals

Characterization of the furnishes

The study was performed by using the Central-European OCC as furnish for testing. The test stocks had been separated into long fiber and short fiber furnishes according to the fractionation process of the mill. The both furnishes were characterized and tested separately. In addition, the white water and the clear filtrate -water were included in the experiments in order to simulate the process environment at the mill.

The laboratory experiments related the drainage of furnish and strength tests of laboratory sheets were carried out separately with the stock derived from the same mill A. Therefore, the different furnishes from mill A are characterized singly. Alternatively, the trial with the pilot paper machine was performed similarly by using the Central-European OCC furnish but originated from the different mill B. Moreover, flocculation measurements were done with the stock from mill C. All characteristics of different furnishes are listed in tables 1-4.

Table 1. Characteristics of OCC furnish used in the drainage tests.

Mill A - OCC furnish	Long fiber	Short fiber	Thin stock	Clear filtrate
pH	6,2	6,3	6,8	6,7
Turbidity, NTU	2760	2478	866	491
Conductivity, mS/cm	4,0	4,0	2,9	2,7
Charge, µekv/l	-105,5	-89,8	-71,1	-90,9
Zeta potential, mV	-1,5	-1,4	-	-
Consistency, g/l	38,6	38,5	14,0	-
Ash content, %	14,5	16,3	25,1	-
Fines content (125P wire), %	20	24	-	-

Table 2. Characteristics of OCC furnish used in the laboratory sheets preparation.

Mill A - OCC furnish	Long fiber	Short fiber	Thin stock	Clear filtrate
pH	6,3	6,2	6,9	6,3
Turbidity, NTU	2477	2280	1236	517
Conductivity, mS/cm	3,8	3,7	2,3	2,3
Charge, µekv/l	-195,3	-122,7	-94,7	-103,1
Zeta potential, mV	-6,8	-6,2	-	-
Consistency, g/l	46,6	41,2	17,1	-
Ash content, %	14,9	16,4	23,3	-
Ca-content, mg/l	1144	1090	519	521

Table 3. Characteristics of OCC furnish used in the pilot papermachine trial.

Mill B - OCC furnish	Disintegrated stock	Mill water 25.6	Mill water 26.6
pH	-	7,95	7,46
Conductivity, mS/cm	1,9	2,3	2,5
Charge, µekv/l	-262,5	-149,0	-283,0
Zeta potential, mV	-8,7	-	-
Consistency, g/l	23,0	-	-
Ash content, %	-	-	-
Ca-content, mg/l	-	571	643
Alkanity, mmol/l	-	1,8	2,2
COD, mg/l	1013	-	630

Table 4. Characteristics of OCC furnish used in the flocculation tests.

Mill C - OCC furnish	Stock	White water
pH	7,0	6,9
Turbidity, NTU	1843	120
Conductivity, mS/cm	2,3	2,1
Charge, µekv/l	-148,2	-74,51
Zeta potential, mV	-10,9	-
Consistency, g/l	27,4	1,0
Ash content, %	15,0	4,7

Additionally, some tests were performed with the stock made by wet disintegrating dry testliner and fluting –sheets as listed in table 5. Wet disintegration of the stock was performed according to standard ISO 5263:1995. The pulp was prepared with Lorentzen & Wettre Pulp Disintegrator. The dry testliner and fluting –sheets were cutted pieces of $2{,}5 \times 2{,}5\ cm$ and weighted according to oven-dry mass of 60 g. Testliner and fluting –sheets with the ratio of 50:50 were dissolved in the white water of 50 degree for 10 minutes. The volume of the disintegration was 2700 ml and the rotation of the propeller was adjusted to 50 000 rotations.

Table 5. Wet disintegrated stock from dry testliner and fluting –sheets originated from Mill A.

Mill A - Testliner/fluting -sheets	Wet disintegrated furnish
pH	6,8
Turbidity, NTU	1950
Conductivity, mS/cm	2,9
Charge, µekv/l	-145,1
Zeta potential, mV	-5,1
Consistency, g/l	16,6

The stocks and the process waters employed within the study were characterized with the measuring equipments and according to standards as listed in Table 6.

Table 6. Devices and standards used in the characterizations.

Measurement	Device/standard
pH	Knick Portamess
Turbidity	WTW Turb 555IR
Conductivity	Knick Portamess 911
Charge	Mütek PCD 03
Zeta potential	Mütek SZP-06
Consistency	ISO 4119
Ca-content	ISO 777
Alkalinity	ISO 9963
COD	ISO 6060

The fines content of the furnish (Mill A) was measured according to standard SCAN-CM 66:05. In briefly, the procedure for determining the fines content was performed with DDJ (Dynamic Drainage Jar). A wire screen having aperture size 76±4 µm (125P) and a stirrer with the mixing speed of 750±50 rpm were used. Filter paper (Schleicher & Schuell No. 589/1) was employed for fines filtration during screening. The weighed test portion of wet mass was calculated according to oven-dry mass of test portion (0,5±0,1 g) and known consistency of the mass. Thus, total volume of water used for screening was 2500 ml.

Drainage and dry strength chemicals

In some of the testpoints were employed anionic polyacrylamides (APAM) with the tested cationic polymer. These anionic polyacrylamides were commercial products and were used as retention aids and anionic strength aids. In addition, some of commercial drainage and strength aids were used as references for the tested cationic polymers such as glyoxylated PAMs. Retention aids used within

the study were a cationic polyacrylamide Fennopol K3500R and a micropolymer of Fennosil EO –series. Likewise, an anionic strength polymer of solution PAM was included in the tests acting as a strength aid.

Characteristics of the employed chemical additives within the study are presented in table 7.

Table 7. Chemical additives used in this study.

Composition	Name	Molecular weight
Polyvinyl amine	PVAm 1H	high
Polyvinyl amine	PVAm 2H	high
Polyvinyl amine	PVAm 3H	high
Polyvinyl amine	PVAm 4H	high
Polyvinyl amine	PVAm 5H	high
Polyvinyl amine	PVAm 6H	high
Polyvinyl amine	PVAm 1L	very low
Polyvinyl amine	PVAm 2L	low
Polyvinyl amine	PVAm 3L	low
Polyvinyl amine	PVAm 4L	low
Cationic polyacrylamide	Ref. C-PAM 1	very high
Cationic polyacrylamide	Ref. C-PAM 2	very high
Anionic polyacrylamide	A-PAM 1	high
Anionic polyacrylamide	A-PAM 2	low
Polyepiamine	Fixative 1	low
Bentonite	Bent.	---

7.2 Flocculation measurements

The effect of tested polymers on flocculation was studied with Lasentec D600VL particle size analyzer (ISO 9001). The measuring method is based on Focused Beam Reflectance Measurement (FBRM), probing particles in concentrated suspensions without the need for sample extraction and sample preparation. It

enables an interpretation of the results over quantitative particle size and shapes.

Flocculation measurements were tested with the stock originated from mill C. The test pulp was diluted with the white water to the consistency of 8 g/l. A volume of 500 ml the test pulp was measured into a mixing mug. The mixing was started with the speed of 1000 rpm and after 30 seconds chemical dosages were added into the pulp. After 1 minute mixing, the speed of the propeller was adjusted to 1500 rpm. The measurement was stopped after 2 minutes of mixing. Software of the device collected data over measurements and drew the flocculation curves as function of time.

7.3 Fixation tests

A scope of the fixation test was to measure an ability of tested polymers to act as a fixation agent aiming to fix hydrophobic compounds onto fibers. Fixation test was carried out with the wet disintegration stock which was diluted to the consistency of 2 %. The test pulp was heated to 45°C for 1h during mixing. A volume of 100 ml the test pulp was poured into a plastic box of 200ml together with two magnetic stir bars. Chemicals were added according to the dosing table, so that the total volume was 10 ml. After the chemical additions, the plastic box was closed and well shaken by hand for 15 seconds.

The fixed pulp was diluted in the ratio of 1:4 with the deionized water. The diluted sample was mixed in a beaker with a spoon and then 1 ml of the sample was measured with a Pasteur pipette through a 30 M wire sock into a test tube. This sort of the sample preparation was performed for the analysis of Kemira Flyto^{TM}, which is based on a flow cytometry technique. Briefly, the principle of Kemira Flyto^{TM} is to research particles in a fluid sample giving knowledge on particle sizes, counts, particle size distribution etc. The rest of the undiluted fixed

pulp was filtered through a black-ribbon filter paper. The filtrate was analyzed by turbidity and charge.

7.4 Drainage measurements

A Dynamic Drainage Analyzer (DDA, AB Akribi Kemikonsulter) was used to evaluate retention and drainage effects of tested polymers. The DDA simulates the hydrodynamic conditions prevailing in a modern paper machine. The equipment measures drainage time elapsed by vacuum filtration. The principle of the DDA is that the mass is flocculated in a reaction jar after agitation (1500 rpm) and filtrated on the wire (0,25 mm) by vacuum filtration (300 mbar) when the water eddies through the fiber mat into a vacuum vessel. A change of the vacuum indicates the time of wet sheet permeability as illustrated in Figure 22. The DDA equipment is connected with a computer which draws the drainage curve as a function of time.

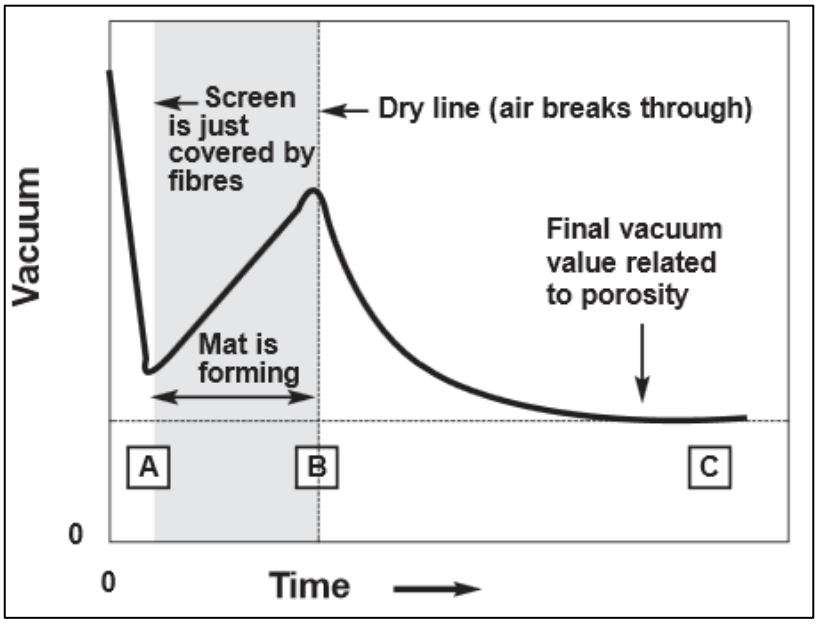

Figure 21. A typical drainage curve obtained with the DDA. /52/

In the beginning of the experiments, the drainage of the pulp was tested to find out suitable consistency (1%) of the test mass on the grounds of drainage time (6-10 s). Before a proper test procedure, the vacuum and the stirrer were calibrated and requisites for settings adjusted. In each measurement, 500 ml of the diluted test mass was poured into the reaction jar and the test program was started on the computer. The stirrer started to agitate at a speed of 1500 rpm for 30 seconds. The chemicals were added into the reaction jar in the following order: cationic polymer, 10 seconds and anionic polymer, 5 seconds prior to the ending time of the stirring. After the agitation, the piston was lowered and the water flows through the fiber mat into the vacuum vessel. The formed sheets on the wire were weighted, wet compressed (1 min, 4 bar) and dried in a drying cabinet on press plates overnight.

The DDA measurements within study involved the drainage consideration by using circulated filtrate as dilution water with the test pulp. The polymer dosage of 0,8kg/t as dry was added in each DDA measurement and the circulation of the filtrate was repeated seven times. The charge was analyzed from the every other DDA filtrate.

7.5 Preparation of laboratory sheets

Laboratory sheets were prepared by using Rapid Köthen sheet former in accordance with ISO 5269-2:2012. The principle of the sheet former is to remove water by suction pressure and to dry a sheet in a specific way to prevent shrinkage during drying. The preparation of the sheets was performed with the circulation water in order to simulate the process conditions. The circulation water was prepared in a separate container, where conductivity and hardness were adjusted similar with the white water. The hardness was adjusted with

$CaCl_2$ by determining the amount and the conductivity was adjusted with NaCl by measuring it with Knick Portamess 911.

In the beginning of the experiments, the pulp was diluted with clear filtrate to the consistency of 1 %. The basis weight of the sheets was adjusted by the volume of the white water and the amount of mass portion (240 ml) was kept constant. The targeted basis weight of the sheets was 120 g/m^2. The chemicals were added in sequence of cationic polymer (2 minutes reaction time) and anionic polymer (1 minute reaction time) into a mixing jar of the mass portion during the agitation of 700 rpm. After two minutes mixing, the measured volume of the white water was poured into the jar and mixed with 1500 rpm for 30 seconds until the suspension is ready for the sheeting. The sheets were dried in vacuum dryers for 6 minutes at 92 degrees and at 1000 mbar.

7.6 Pilot paper machine trial

The trial run was performed with a pilot paper machine (VPM3) owned by Kemira and Blankophor, which is located in Leverkusen, Germany. Running parameters of the pilot paper machine are listed in table 6.

Table 8. Running parameters of the pilot PM

Grammage	100 g/m²
Running speed	2 m/min
Rotation speed of holey roll	120 rpm
Width of the web	0,32 m
Dimensions of machine	L 4,99m x B 1,1m x H 1,7m
Press section	2 nips
Drying section	8 pre-drying cylinders, baby cylinder, 5 drying cylinder (after size press)
Size press	not in use
Machine calander	not in use

The furnish was deflaked using Andritz laboratory refiner for 35 minutes with open fillings. The dry bales from mill B were deflaked and diluted with the mill water to achieve the consistency of 2,3 % for the test pulp suspension. Fresh mill water from mill B was used as process water which was fed into a mixing tank. Chemical dosages, thick stock and the mill water were agitated in the mixing tank where the suspension was fed to the headbox of the paper machine. From every trial points, the sample of the suspension before headbox and the sample of wire water were collected. Zeta potential, charge, conductivity and turbidity were measured from these samples.

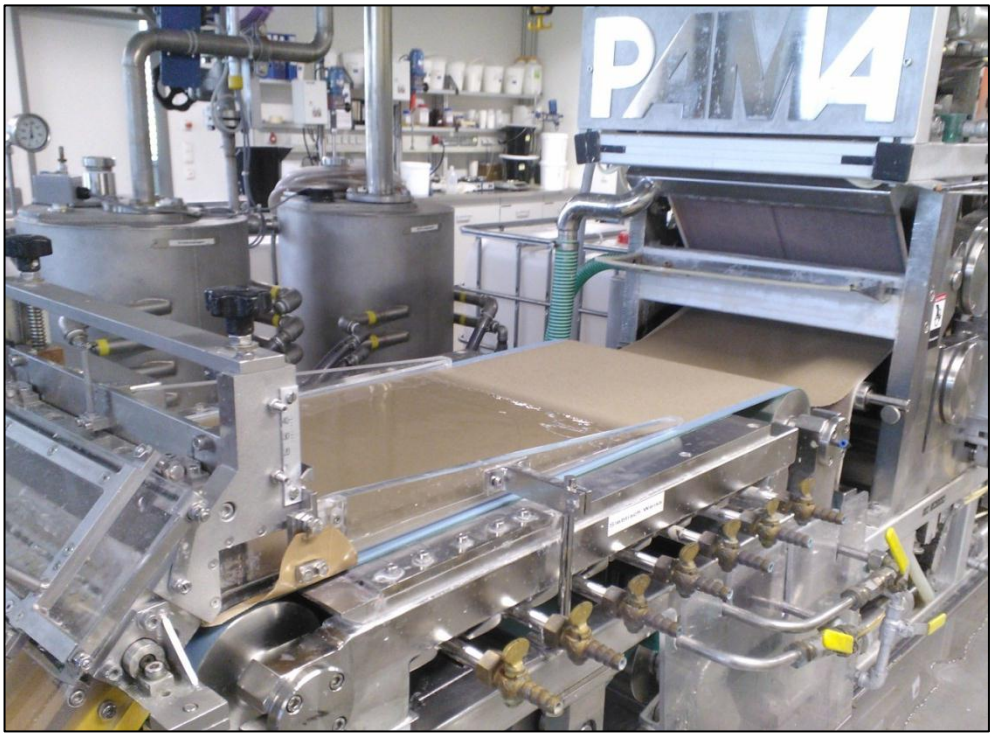

Figure 22. The wire section of the pilot paper machine (VPM3).

7.7 Paper testing

Before every paper testing measurements, the sheets were pre-conditioned for 24 h at 23°C in 50% relative humidity in accordance with ISO 187. The measurements for researching properties of the paper sheets were performed using the following devices and standards as listed in Table 9.

Table 9. Paper testing devices and standards.

Measurement	Device	Standard
Basis weight	Mettler Toledo	ISO 536
Thickness	Lorentzen & Wettre Micrometer	ISO 534
Formation	AMBERTEC Beta Formation tester	SCAN-P 92:09
Density	Lorentzen & Wettre Micrometer	ISO 534
Bulk	Lorentzen & Wettre Micrometer	ISO 534
Burst strength	Lorentzen & Wettre Bursting Strength tester	ISO 2758
SCT (Short Span test)	Lorentzen & Wettre Compression Strength tester	ISO 9895
Ash content	Precisa PrepAsh 229	ISO 1762

8. RESULTS AND DISCUSSION

In this chapter the all measurement results involved within study are presented and discussed. The results are divided into subtitles according to the used method. First, emphasizing on flocculation and fixation regarding charge, turbidity and zeta potential –determinations introduce understanding of the phenomena occurring due to the polymer additions. Then turning to the drainage and strength results demonstrate the effect resulting from the polymer additions into the liner and fluting OCC furnish. Finally, the correlation analysis is used for the statistical inspection to investigate linear statistical relationships between the variables related to the properties of sheets.

8.1 Flocculation results

To review a rate of flocculation with polymer additions can be found the relationship between polymer flocculation, drainage and retention, as has been discussed in the literature review. Figure 23 introduces how the mean floc size changes as a function of time with shearing forces. The multiplied floc sizes are highly dependent upon the characteristics of the added polymer into pulp slurry. Based on the prior studies in the literature /51, 91, p. 145-191/, the results of C-PAM1 are not surprising because as very high molecular weight polymer, it forms the flocs having the largest sizes and the most resistant to shear. Similarly, high molecular weight PVAm 4H increases the floc size by comparison low molecular weight polyvinyl amines.

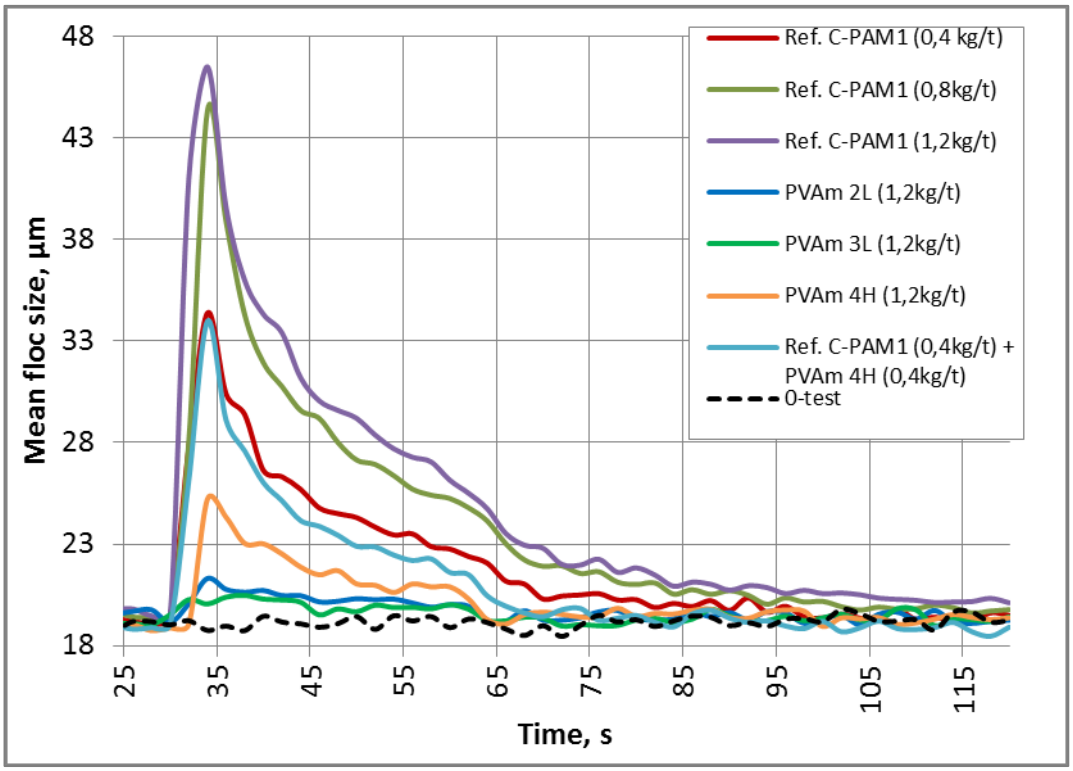

Figure 23. Mean floc size as a function of time determined by Lasentec D600VL. Polymer additions were made at the moment of 30 seconds.

Interestingly, the data from Figure 23 correlates with ash retention. Thus, by adding C-PAM1 can be improved significantly the ash retention by forming flocs with the filler particles and fines and restraining them in paper web. These results are consistent with those of other studies and suggest that the floc size increases with the molecular weight, revealing that bridging flocculation is required. Moreover, there is no significant impact of PVAm 4H in conjunction with C-PAM1 detected as compared to the bare C-PAM1.

8.2 Fixation results

8.2.1 Charge and turbidity

An ability of polymer to attach hydrophobic particles, such as contaminants, pitch particles, stickies etc. onto the surface of fiber is known as fixation.

Determining turbidity and charge as a function of polymer dosage are appropriate parameters to demonstrate the influence of the fixation. Figure 24 illustrates a decrease of the turbidity in pursuance of increase of the charge density when a cationic additive is introduced. Turbidity of the sample decreases because the addition of cationic polymer promotes adhering of hydrophobic compounds onto fibers. Therefore, it can be stated that greater turbidity reduction equals with a greater fixation effect. Respectively, an increase of the charge denotes that the additions of cationic polymer dosages remove the amount of anionic compounds by reducing cationic demand.

By comparing PVAm 4H with a commercial used fixation agent Fixative 1, they perform similarly with turbidity and charge. Turbidity of PVAm 4H decreases in same relation to Fixative 1, whereas the charge curves increase demonstrating the effect of the fixation. As can be noted, PVAm 4H deviates from low molecular weight of PVAms 2L and 3L by lowering turbidity more steep. PVAm 3L with higher charge density achieves the same charge level with the dosage of 600 g/t. Nevertheless, the reduction of turbidity is much lower with PVAm 3L and so the impact on the fixation is deteriorated.

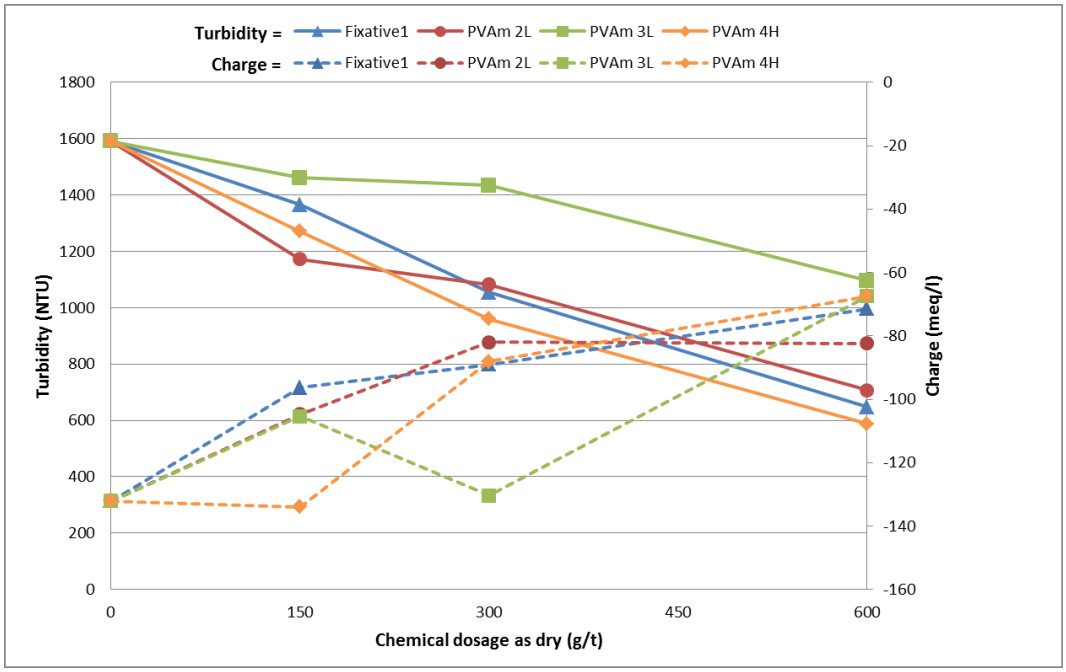

Figure 24. Development of turbidity (solid line) and charge (dash line) as a function of polymer additions.

Generally, polyvinyl amines have a positive impact on the fixation indicating that both high and low molecular weight PVAms control hydrophobic particles by attaching them onto fibers. These findings are in agreement with the literature review /92/, which defines a common fixing agent with relatively low molecular weight and high cationic charge density. Concluding that high molecular weight with relatively high charge density PVAm 4H treats effectively DCS on the surface of fibers. Additionally, low molecular weight PVAms perform as a fixation agent with such as OCC furnish.

8.2.2 Zeta potential

As already mentioned in reference to Chapter 1.5.1, the zeta potential describes the density of charges on the surface of a particle. The nature of cellulose fibers is anionic and therefore adding of a cationic polymer leads to adsorbing onto the surface of fiber by increasing a negative value of the zeta potential. Naturally, the zeta potential is closer to zero with the recycled fibers due to the adsorbed

contaminants and other anionic trash. These interfering substances cover the fiber surface so that there is less space for the adsorption of cationic polymers. The same appearance of wet disintegrated testliner and fluting stock can be observed in Figure 25, where the surface density of charges on the pulp fibers is poor.

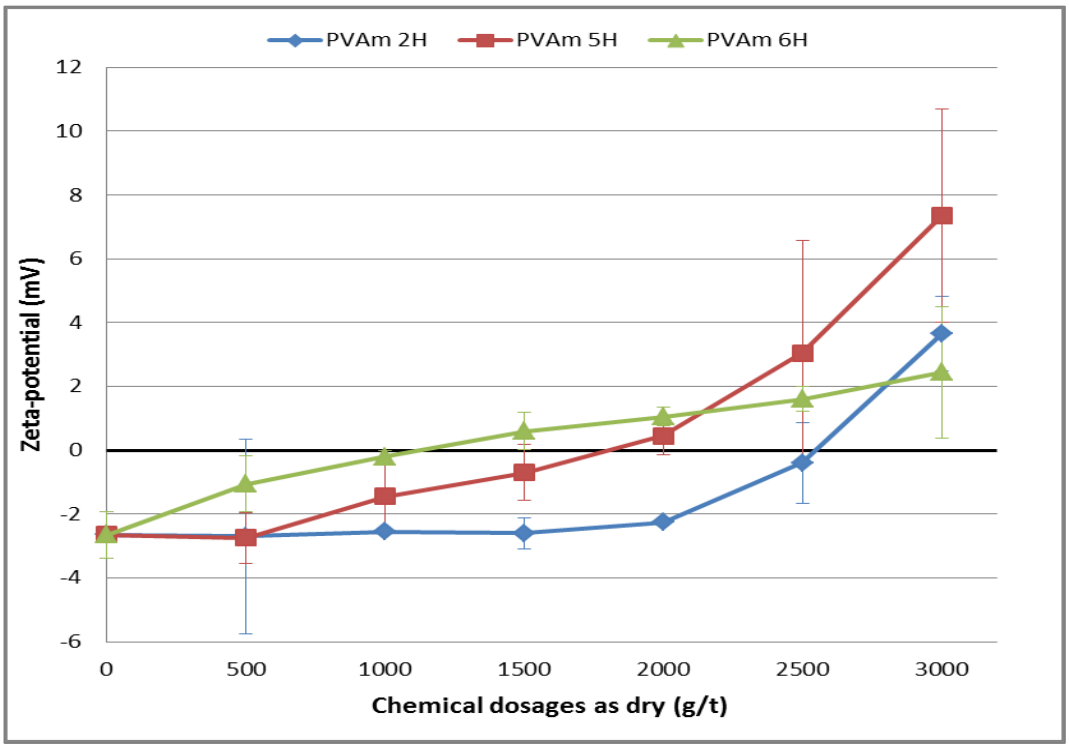

Figure 25. Zeta potential of wet disintegrated testliner and fluting stock approaches positive as a result of high molecular weight poluvinyl amine additions.

As expected, the zeta potential increases when cationic high molecular weight polyvinyl amines are added into the pulp as presented in Figure 25. The decrease in negativity of the zeta potential reveals that PVAms adsorb on the fiber surfaces of the pulp. Hence, the effect of the polymer properties prevails by bringing additional drainage and dry strength value for the end product.

PVAm 6H having the highest charge density adsorbs most efficient onto fibers with lower polymer additions. Considering PVAm 2H, which requires over twice as large polymer dosage as PVAm 6H to reach zero value of the zeta potential. It can be discovered on the basis of the graph that the charge density of polymer

has a clear impact on the polymer adsorption onto fiber surface when the molecular weight is kept constant.

8.3 Drainage results

8.3.1 Single pass DDA test with polymer dosages

Figure 26 provides the results obtained from the drainage measurements of DDA analysis. The performance of the polyvinyl amines depicts the decreasing of dewatering times as a result of the polymer additions. The observations of the drainage time are the average values of the long and short fiber pulps. As can be interpreted from the graph below, the drainage of the liner and fluting OCC pulp advances as polyvinyl amine is used as an additive. However, clear deviances to the drainage within the properties of PVAms can be seen.

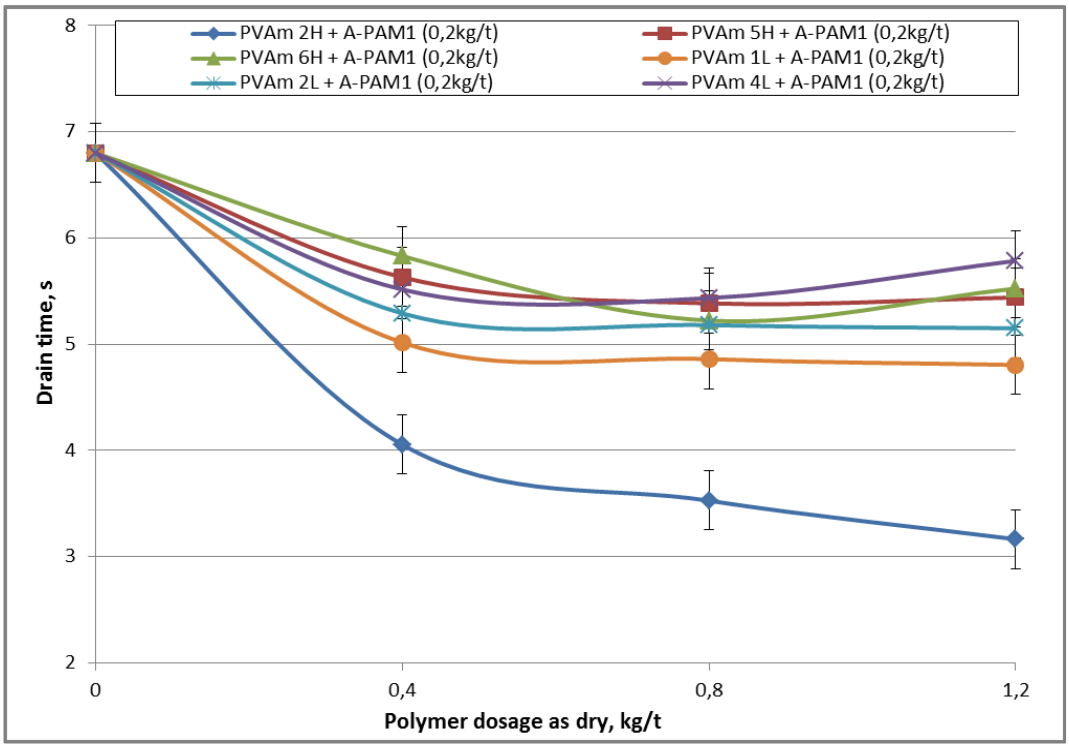

Figure 26. The drainage time of DDA as a function of polyvinyl amine dosages.

The drainage of the liner and fluting OCC pulp performs clearly faster with the combination of the high molecular weight PVAm 2H and A-PAM1. The improvement obtained with the two component system is over 50% faster than with the reference. It is apparent from the graph that the charge of PVAm contributes on the drainage behaviour. A clear benefit is achieved for both high and low molecular weight series with the low charge density. Interestingly, the continuous decreasing of the drainage time with increasing PVAm 2H dosages deviates from others that attain their maximum drain times at the lower dosages. Diminishing of the drainage with PVAm 6H and 4L at the high dosages may be a result of overflocculation. Denoting that high charge of the polymers may consume to the neutralization of anionic trash in aqueous pulp suspension.

Figure 27 indicates a similar drainage appearance, as shown in Figure 26, by using a multisystem of PVAm 2H, C-PAM and bentonite. Comparing the efficiency of the drainage with the difference systems can be stated that the lowest dosage of PVAm 2H achieves faster drainage by using the two component system of PVAm and A-PAM1. By contrast, the drainage becomes more efficient with the multisystem at the increasing polymer dosage. In case of the multisystem of PVAm 6H can be noted that the polymer does have any influence on the drainage, whereas in conjunction with the two component system the drainage is improved.

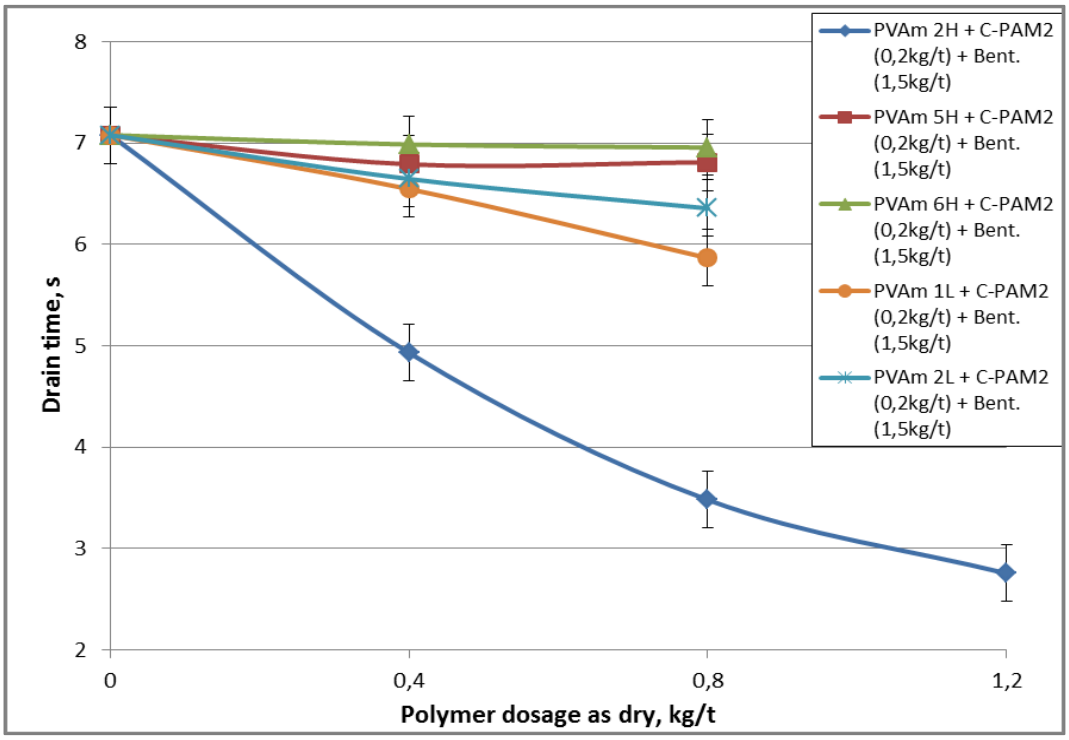

Figure 27. The drainage time of DDA with chemical dosages of PVAm+C-PAM+bentonite – multisystem.

The representation of Figure 28 shows the development of first-pass retention with the drainage time depending on the polymer dosage. The dosages of PVAm are highlighted in the graph. First-pass retention reveals how effectively materials of papermaking are retained in a paper web as it is being formed. High molecular weight PVAm 2H indicates a superior effect on first-pass retention. Such high first-pass retention means that the use of PVAm 2H cuts down solids losses into the circulation water by retaining fine material to fibers.

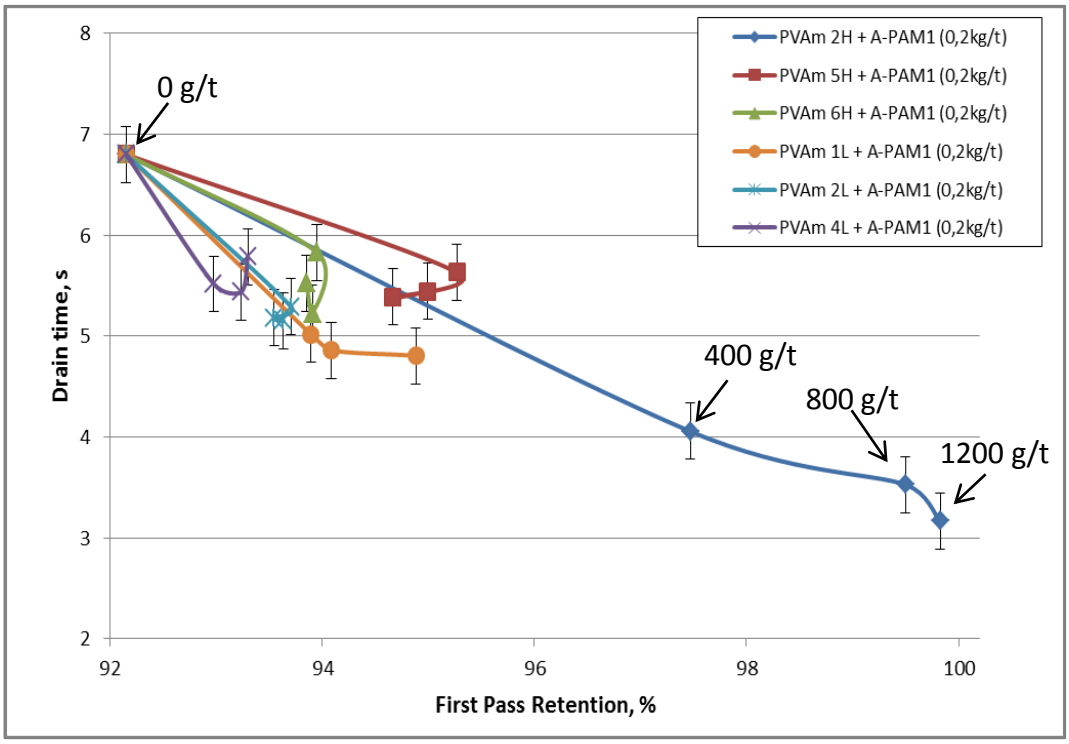

Figure 28. The drainage time as a function of first-pass retention.

The more surprising correlations are with PVAm 5H and 6H in conjunction with A-PAM1, which weaken first-pass retention with the higher PVAm dosage. Here, the issue may be that high charge operates better at lower dosage when the charge does not exceed the charge demand. Thus, the dosages of 800 and 1200 g/t are too large with such high charge density polymers. The result of PVAm 1L in conjunction with A-PAM1 supports that the low level of charge achieves a positive impact on first-pass retention. Nevertheless, the influence of the molecular weight can be seen as distinctive factor. The curves of low molecular weight series decline steeper affecting to a lesser extent first-pass retention.

8.3.2 Re-circulated filtrate DDA test

The target of DDA measurement by re-circulating the DDA filtrate was to simulate short circulation and to discover the adhering ability of polyvinyl amines on fiber surface by determining the charge of the filtrate.

Results of Figure 29 elucidate the charge development of the DDA filtrate with the drainage. The graph reveals that the charge performance of high molecular weight polyvinyl amines distinguishes obviously to three main trends of low, moderate and high charged. PVAm 1H and C-PAM2 achieve a rapid reduction in drainage, whereas the sequential higher charged PVAms reduce the drainage only with the higher number of the filtrate circulations. Thus, the graph indicates that PVAms require re-circulation of the filtrate (white water) to show their actual performance.

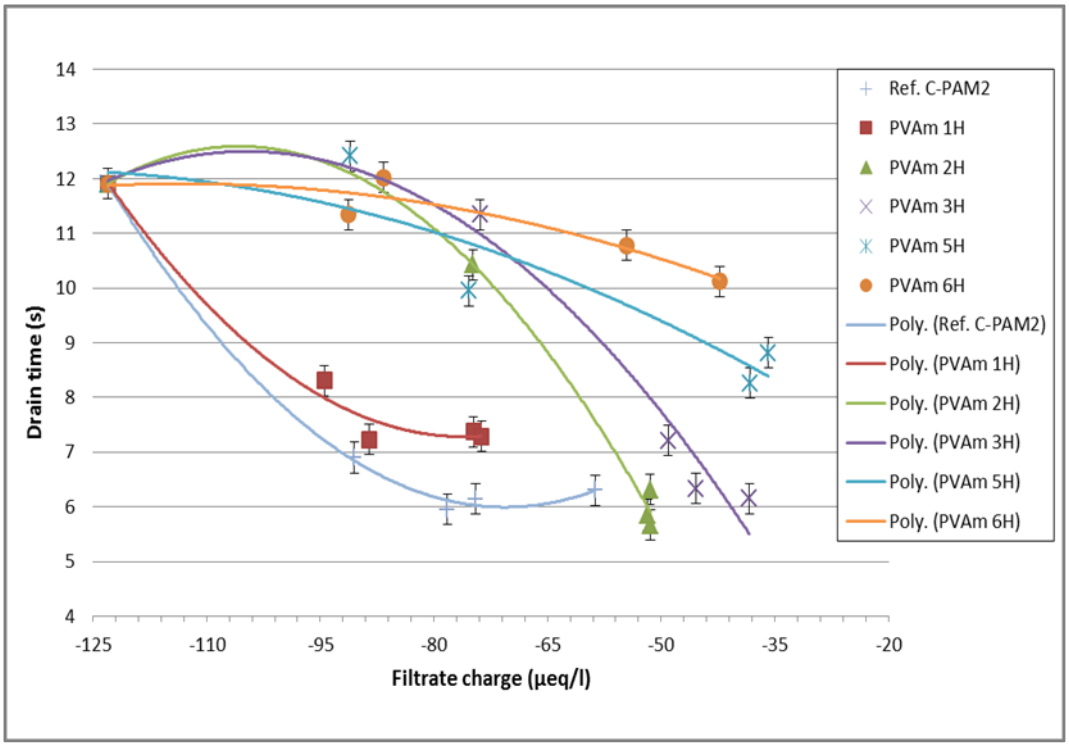

Figure 29. Drainage time as a result of DDA filtrate charge. Four charge measurements, i.e. every other DDA filtrate, were analyzed from each DDA measurements.

As can be seen from the graph, the filtrate charge stays anionic even though cationic polyvinyl amines are added. This may demonstrate that the rest of the charge of PVAm goes into the neutralization of the zeta potential. In other words, the additions of the polyvinyl amines are adsorbed onto fiber surfaces. Furthermore, Figure 29 reveals the difference in drainage mechanisms. Higher charged PVAms (above) will coagulate by charge neutralization mechanism,

whereas polymers (below) having lower charge density are based on flocculation due to high molecular weight.

Figure 30 provides the drainage curves of using re-circulated DDA filtrate. It is apparent to notice that the drainage of the high molecular weight polyvinyl amines performs depending on the charge. The most noteworthy observation to emerge from the graph is that the drainage of PVAm 1H does not improve after the second filtrate circulation, whereas the higher charged PVAm 2H and 3H have a long-standing enhancement to the drainage. Figure 30 indicates that 5 to 7 circulations are needed for the balance like in the short circulation of paper machine. It can be noted that PVAm 2H performs more effectively as compared to the reference C-PAM.

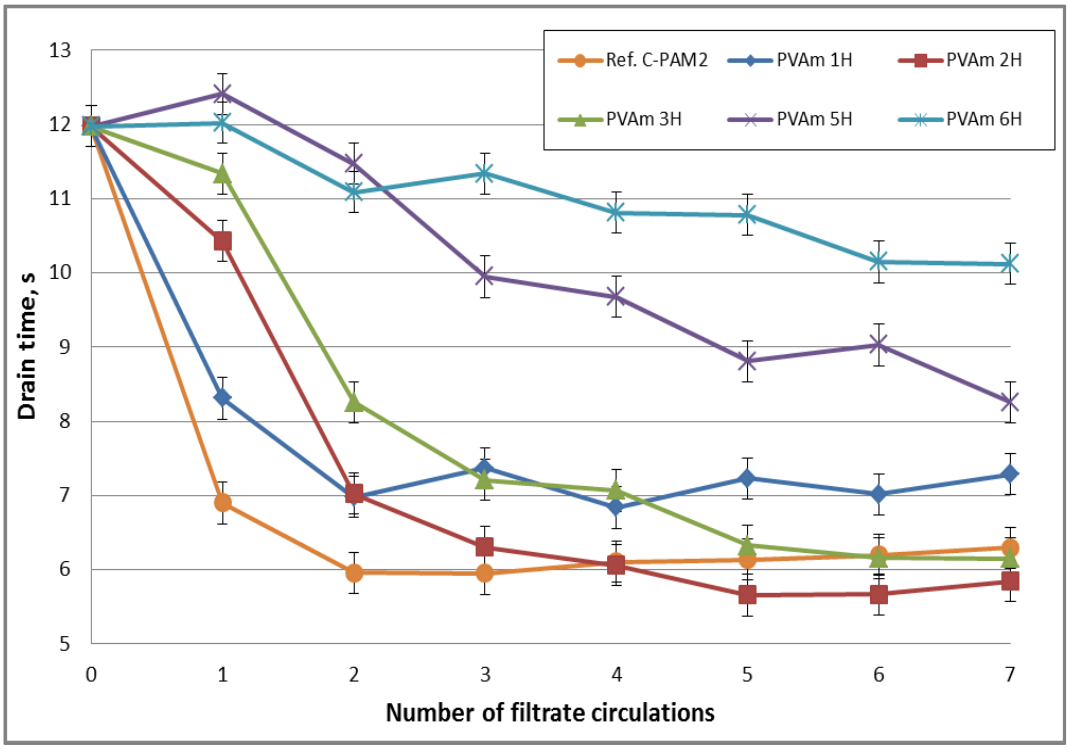

Figure 30. Result of drainage with PVAm additions of 0,8 kg/t as dry by re-circulating DDA filtrate.

On the basis of Figure 29, PVAm 5H and 6H appear as fixatives by treating DCS and reducing the cationic demand, whereas the filtrate charge remains more

negative with the low charged PVAms. This may indicate that the low charged PVAms adsorb more effectively onto fibers and improve drainage as shown in Figure 30.

8.4 Strength results of laboratory sheets

8.4.1 Burst strength

Burst strength of laboratory sheets was indexed in order to prevent the variations of the basis weight of the sheets. Moreover, the influence of filler content was leveled with the ash compensation. The overall results including error limits of the laboratory sheet measurements are presented in Appendices I and II. Figure 31 depicts the burst strength index of liner and fluting handsheets calculated as average values from separately measured long and short fiber pulps at 14% ash content.

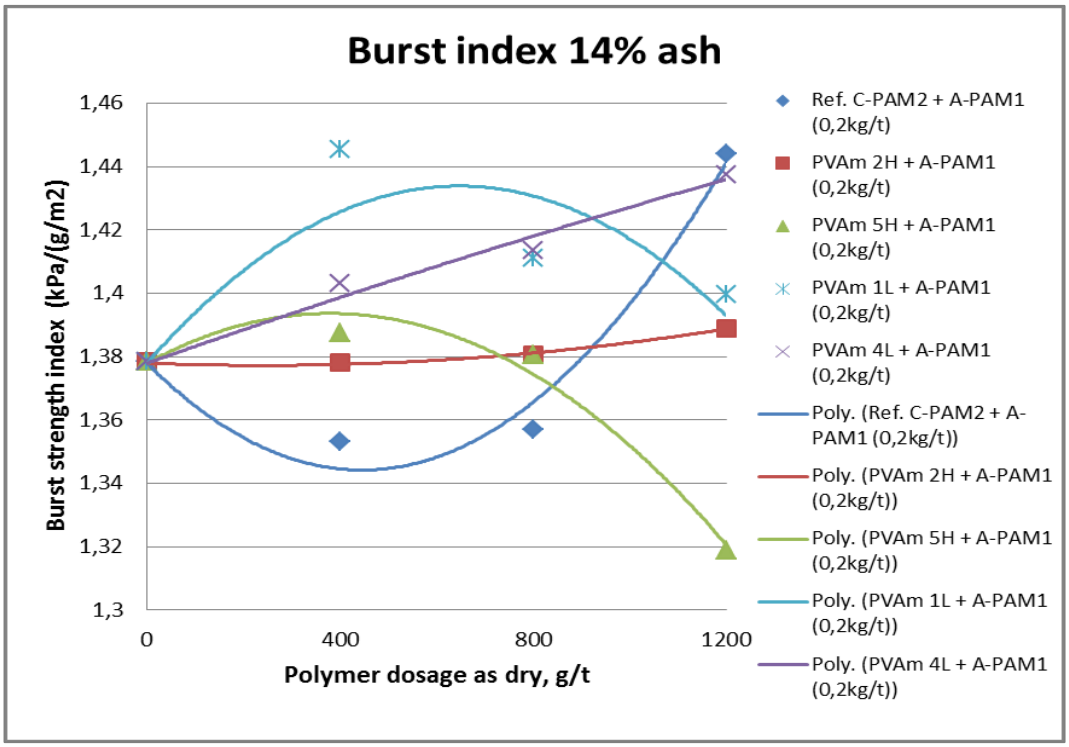

Figure 31. Burst index of liner and fluting handsheets at 14% ash content as a function of chemical dosages.

Cationic polyacrylamide was used as a reference in comparison with polyvinyl amine polymers. The burst index of the two component application of C-PAM2 with APAM1 decreases at lower C-PAM2 dosages but increases when the dosage rises above 900 g/t. The combination of PVAm 1L with A-PAM1 achieves the best improvement to the burst strength. Approximately 5% benefit can be gained with PVAm 1L at dosage of 400 g/t. Moreover, PVAm 4L in conjunction with A-PAM1 enhances burst strength with increasing polymer dosage. Alternatively, the additions of PVAm 2H and PVAm 5H gain only slight enhancement in the burst strength index of liner and fluting handsheets. The burst strength results of the handsheets reveal that the low molecular weight PVAms perform better than the high molecular weight in spite of the charge density difference.

8.4.2 SCT - Short span compression test

Figure 32 illustrates the compression index of liner and fluting handsheets with chemical additions at the ash content of 14%. The compression indexes of the SCT are calculated as average values from the separately measured long and short fiber pulps.

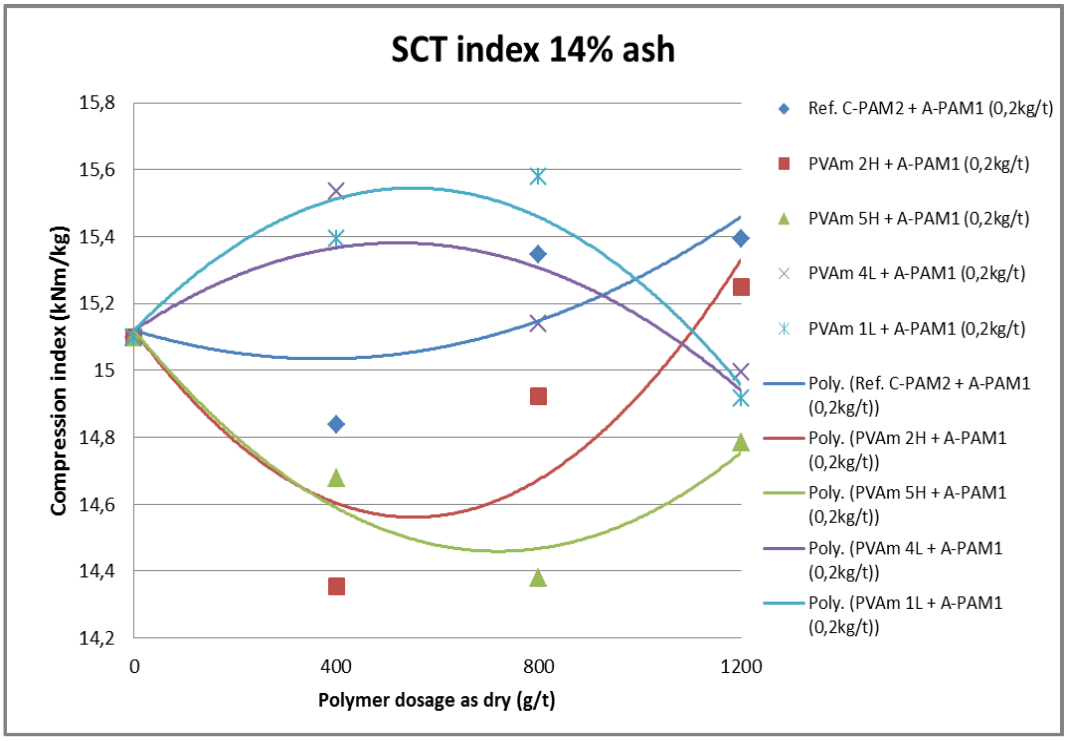

Figure 32. The performance of the SCT compression index with increasing polymer additions.

Figure 32 reveals that the polyvinyl amines of high molecular weight have merely a negative impact on the compression index, whereas low molecular weight PVAms contributes to the SCT of the liner and fluting handsheets. Low molecular weight PVAm 1L has a relative ~4% reinforcement to the compression index in comparison with the reference. Moreover, the result appears that the charge density of the polymer is associated with the compression strength of liner and fluting. Comparing the results of PVAm 4L and PVAm 1L, it can be seen that the lowest charged PVAm improves the SCT compression index the most effectively. The highest improvement to the compression strength is obtained at the PVAm

dosage of 600 g/t. In addition we can note that the compression index stabilizes at the dosage of 1200 g/t to the reference level.

8.4.3 Formation of laboratory sheets

The results obtained from the analysis of beta formation are presented in Figure 33. The single most striking observation to emerge from the data comparison is that every polyvinyl amine at the dosage of 1,2 kg/t achieves a deteriorated beta formation with relation to lower dosages. This denotes that 1,2 kg/t PVAm dosage may result in overdosing effect. Moreover, the poor development of beta formation at 1,2 kg/t dosage may be associated with the strength results of SCT and burst. As can be seen from Figures 31 and 32, the strength properties of the liner and fluting sheets become lowered or stabilized at the highest dosage. Particularly, observing the declining performances of PVAm 5H and 1L at 1,2 kg/t dosage is linked to the beta formation result. Poor formation may cause a negative impact on the strength performance of PVAm 5H and 1L at the higher dosages.

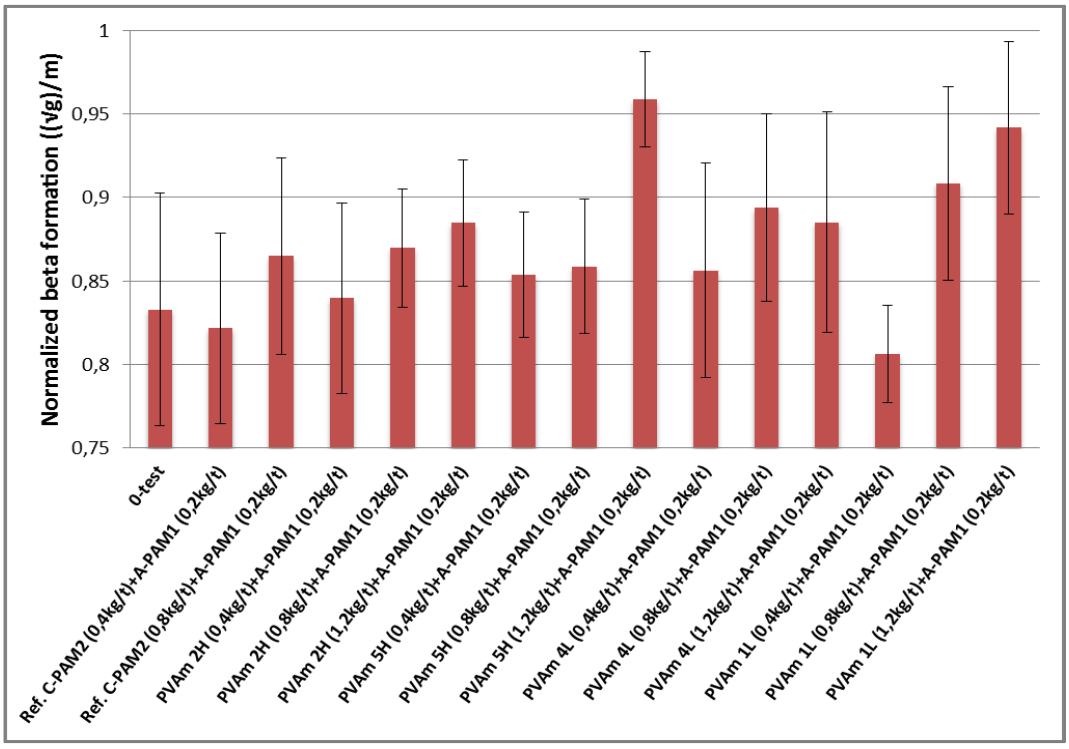

Figure 33. Normalized beta formation of the mean long and short fiber pulp handsheets with chemical additions.

8.5 Results from pilot paper machine trial

The present measurement was designed to determine the effect of paper machine conditions in the wet-end on the strength properties of liner and fluting. The aim of the test trial was to find out how a given strength additive affects and performs with OCC furnish in paper machine conditions improving dry-strength of the finished paper. In addition to the short span compression test (SCT) and burst strength -determinations, other typical strength measurements were made as shown in Appendix III. Figure 34 depicts the influence of the tested polymers either on the fixation of filtrate or on the adsorption onto fiber surface. The graph reveals that added polymers rather adsorbed onto the fibers than fixed anionic trash within the OCC pulp.

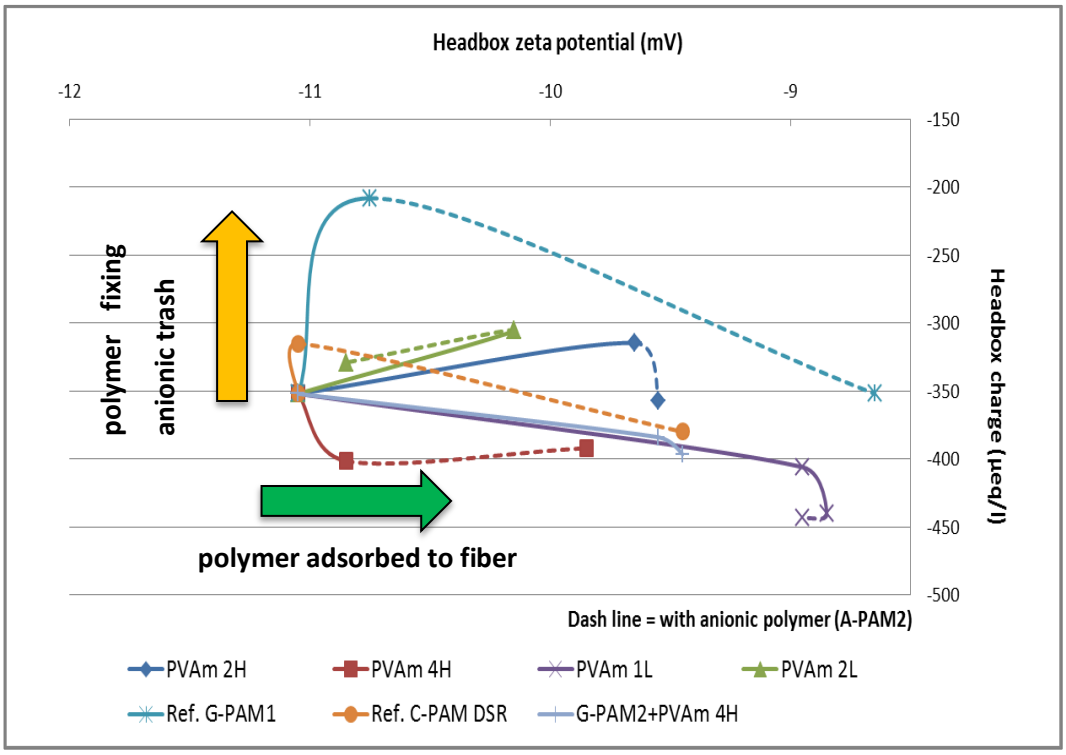

Figure 34. Indication of the polymer performance in the wet-end of the pilot PM.

The observations of the strength result diagrams were indexed and compensated to the same ash content in order to make comprehensive comparison between the tested polymers. Figure 35 provides the experimental data from SCT geometric indexes with different polymer additions. The most distinguishable result to appear from the diagram is the improvement (approx. 17 %) achieved with the addition of solely PVAm 2H. Moreover, the low molecular weight PVAm 1L in conjunction with A-PAM2 contribute to the compression strength of the SCT.

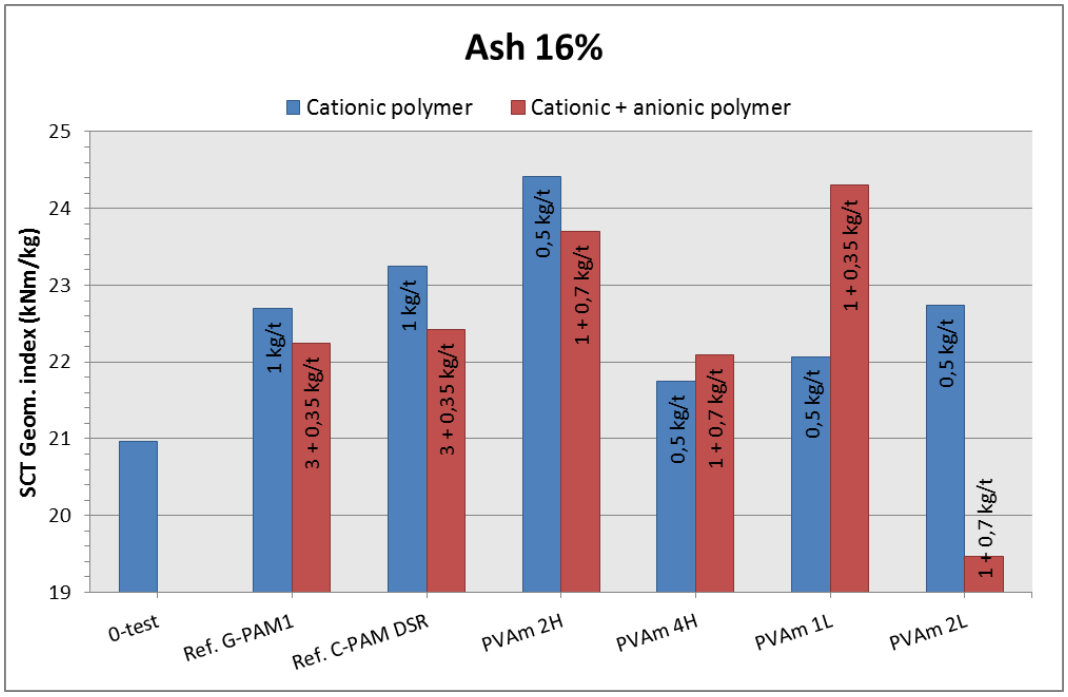

Figure 35. Results of SCT geometric indexes with polymer additions.

In contrast to the SCT results, the low charged and low molecular weight PVAm 2L promotes the most effectively the burst strength of liner and fluting, as shown in Figure 36. All PVAm additions improve burst strength in comparison with the 0-test.

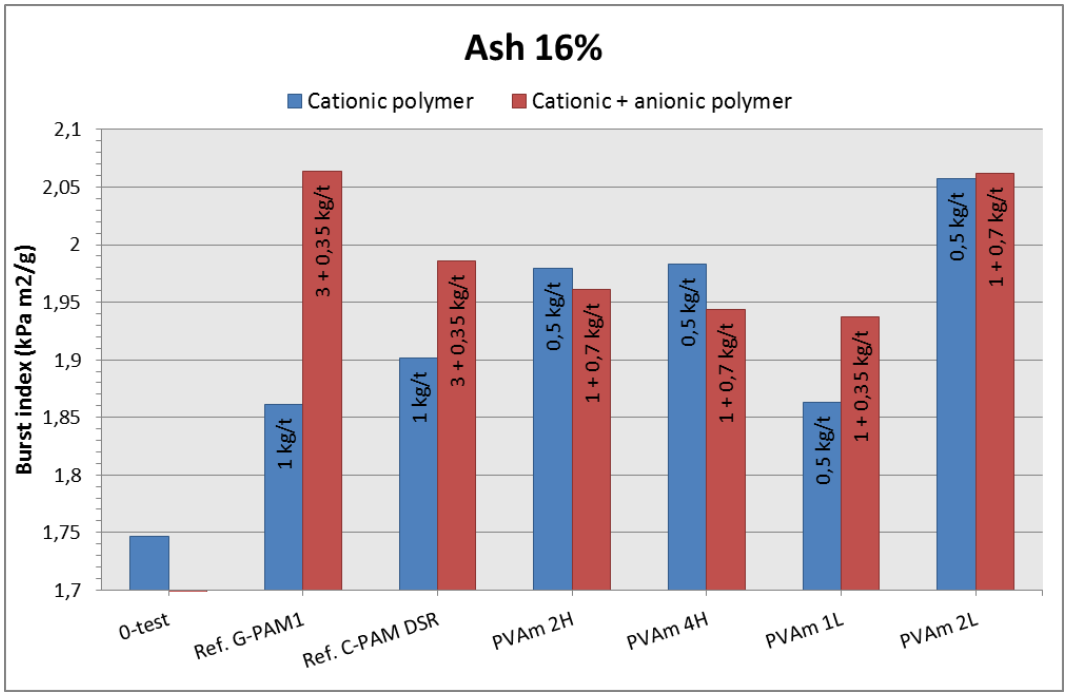

Figure 36. Results of burst strength indexes with polymer additions.

The effect of anionic polymer (A-PAM2) in conjunction with cationic PVAm do not appear significant improvement to the strength properties of liner and fluting in comparison with the solely added PVAms. Nevertheless, the anionic polymer with the reference strength polymers seems to contribute to the burst strength of liner and fluting.

8.6 Statistical analysis and error analysis

In this study, the correlation analysis is used to investigate statistical dependences between the wet-end measurements and the properties of sheets and to evaluate error sources in the experiments. Error analysis concerns the error limits related to the result graphs.

8.6.1 Correlation analysis

Correlation coefficient describes the intensity of this linear statistical relationship that assist understanding of dependences between variables. The numerical value of the correlation coefficient can vary between 0.0 and 1.0. The value closer to 1.0 refers to a strong relationship between the two variables, whereas the coefficient of 0.0 denotes the absence of the relationship. The sign of the correlation coefficient reveals a positive and negative correlation. The positive correlation occurs when the variables move in the same direction (variable 1 increases/decreases, variable 2 increases/decreases). By contrast, the negative correlation is achieved when the variables move opposite directions (variable 1 increases, variable 2 decreases and vice versa). To calculate correlation coefficients between two random variables, the following mathematical equations are defined:

$$\rho_{X,Y} = corr(X,Y) = \frac{cov(X,Y)}{\sigma_X \sigma_Y} = \frac{E[(x-\mu_X)(y-\mu_Y)]}{E[(x-\mu_X)^2][(y-\mu_Y)^2]} \qquad (17),$$

where

μ_X	is	expected value of X
μ_Y	¨	expected value of Y
σ_X	¨	standard deviation of X
σ_Y	¨	standard deviation of Y

The correlation analysis results of the handsheets made from the long and short fiber OCC furnish are presented in Tables 10 and 11. The correlation coefficients were calculated based on the measurement results listed in Appendices I, II and III. As it is generally known, it can be concluded from the chart that an increase of ash content decreases the strength properties of the sheets. Moreover, there is a significant negative correlation between the bulk and ash content of the

sheets denoting that the bulk of liner and fluting deteriorates with increasing filler loading.

Table 10. The correlation analysis results for the variables of the handsheets made from the long fiber OCC furnish.

	Grammage	*Bulk*	*Ash content*	*Burst strength index*	*SCT index*	*Norm. beta formation*
Grammage	1,00					
Bulk	-0,07	1,00				
Ash content	0,24	-0,63	1,00			
Burst strength index	-0,06	0,30	-0,48	1,00		
SCT index	0,34	0,19	-0,29	0,42	1,00	
Norm. beta formation	0,39	0,07	0,20	-0,13	-0,10	1,00

Table 11. The correlation analysis results for the variables of the short fiber OCC pulp made handsheets.

	Grammage	*Bulk*	*Ash content*	*Burst strength index*	*SCT index*	*Norm. beta formation*
Grammage	1,00					
Bulk	-0,08	1,00				
Ash content	0,11	-0,73	1,00			
Burst strength index	-0,16	0,33	-0,65	1,00		
SCT index	-0,03	0,26	-0,52	0,55	1,00	
Norm. beta formation	0,49	0,37	-0,35	-0,01	0,04	1,00

Respectively, Table 12 shows the correlation coefficients between the variables present in the pilot paper machine trial. To clarify an examination of the chart,

the consideration spots has numbered to the table and discussed below. In Appendix V, the corresponding chart has presented in more extensive form.

Table 12. The correlation analysis for the results of the pilot PM trial.

	Zeta-pot.	*Conductivity*	*Charge*	*Consistency (HB)*	*COD (HB)*	*Consistency (WW)*	*Turbidity*	*COD (WW)*	*Retention*	*Press solids*	*Basis weight*	*SCT Geom index*	*Burst index*	*Tensile Geom index*	*Scott bond*	*Bulk*	*Ash*
Zeta-pot.	1,00																
Conductivity	0,72	1,00															
Charge ave.	0,43	0,13	1,00														
Consistency (HB)	-0,17	-0,46	-0,17	1,00													
COD (HB)	-0,29	-0,37	-0,65	0,51	1,00												
Consistency (WW)	-0,68	-0,46	0,56	0,04	0,29	1,00											
Turbidity	0,67	0,60	0,42	0,46	-0,57	-0,44	1,00										
COD (WW)	0,32	-0,40	-0,67	0,49	0,96	0,27	-0,63	1,00									
Retention	0,67	0,30	0,52	0,07	-0,08	-0,91	0,27	-0,07	1,00								
Press solids	-0,26	-0,23	0,04	-0,11	-0,38	0,17	-0,07	-0,16	-0,23	1,00							
Basis weight	-0,18	-0,29	-0,12	0,44	0,42	0,15	-0,46	0,48	0,05	0,08	1,00						
SCT Geom index	0,50	0,51	0,27	-0,82	-0,50	-0,46	0,62	-0,49	0,13	0,03	-0,54	1,00					
Burst index	0,09	0,28	-0,11	-0,78	-0,39	-0,03	0,38	-0,35	-0,30	0,22	-0,46	0,80	1,00				
Tensile Geom index	0,47	0,49	0,31	-0,74	-0,59	-0,40	0,60	-0,56	0,10	0,09	-0,58	0,95	0,75	1,00			
Scott bond	0,38	0,35	0,24	-0,71	-0,48	-0,32	0,47	-0,44	0,03	0,16	-0,26	0,82	0,78	0,78	1,00		
Bulk	-0,08	-0,18	-0,04	0,77	0,29	0,17	-0,29	0,23	0,15	-0,15	0,25	-0,78	-0,79	-0,69	-0,64	1,00	
Ash	0,32	0,13	0,02	-0,27	0,24	-0,30	0,13	0,23	0,20	-0,26	0,11	0,45	0,25	0,28	0,28	-0,61	1,00

Strong evidence of functionality of polymers is found as shown in the spots 1. The strength properties of sheets improve when the zeta potential increases. In other words, the tested polymers adsorb onto the surface of recycled fibers. Likewise, a significant positive correlation between retention and zeta potential supports the deduction. The spot 2 reveals a fixing effect of the polymers. A reduction of turbidity correlates with decreasing zeta potential and conductivity. However, a positive correlation between turbidity and charge is unexpected and suggests that the fixation does not occur, while significant negative correlations of COD and charge (the spots 3) disclose opposite that the COD of process water reduces with increasing charge. The spot 4 observes a negative correlation of bulk and the strength properties. These contradictory findings could be explained by the fact that bonding brings fibers closer and decreases bulk. Thus, the tested polymers cannot increase both strength and bulk at the same time with the recycled OCC furnish.

8.6.2 Error analysis

The error limits of the drainage results have considered in the result graphs. Those were calculated based on the standard deviations of the DDA measurements. The error limits of the strength properties are rather presented in Appendices II-IV for the clarity of the figures. The statistical validity of SCT and burst strength was calculated based on a confidence level of 95%.

9. CONCLUSIONS

The present study was designed to examine the effect of the polyvinyl amine characteristics and the wet-end process conditions on the drainage and strength properties of liner and fluting OCC furnish. In addition, emphasizing on the challenges of recovered pulp to obtain the desired properties of the finished product was underlined. The empirical findings in this study confirm previous researches and suggest that molecular weight and charge density of a polymer have an impact on the polymer adsorption, and hence contribute to the end-uses.

The preliminary researches related to the polymer adsorption, fixation and flocculation brought comprehensive scientific knowledge on the functionality of the vinyl amine -containing polymers. The interpretation of turbidity, charge and zeta potential results verifies that the polymers are able to fixing the levels of high anionic loadings in the paper machine circuit or adsorbing to recycled fibers. Furthermore, the fixation effect achieved with polyvinyl amines may support the idea that the cationic polymer goes to anionic trash, impairing possibly the strength and drainage effects of the end product.

The applicability of the polymer concerning the molecular weight and charge density with OCC furnish was targeted in order to optimize suitable polymer nature to achieve additional strength and drainage improvements. The influences of OCC furnish characteristics such as charge, zeta potential, conductivity, pH, filler content on the bonding ability of the polymer were considered. This study has demonstrated that the nature of the polymer improving drainage in web formation is consistent with the strength enhancing properties of sheet.

One of the more significant findings to emerge from this study is the effect of the vinyl amine –containing polymer on the drainage property. Reviewing extensive comparison between the polymers adds substantially understanding of the

polymer nature. It is concluded that a high molecular weight polymer improves the drainage of liner and fluting furnish. The drainage performance of such polymer benefits by itself and in conjunction with A-PAM and with C-PAM and bentonite. Similarly first-pass retention improves as a result of the polymer. These findings provide additional evidences with respect to the cost efficiency of liner and fluting furnish.

Burst strength and a short compression strength test (SCT) were employed within study on the basis of the most commonly used strength parameters with the liner and fluting. The evidence from the results suggests that the successful development of burst and SCT strengths requires differing polymer attributes. The best burst strength improvement with a low molecular weight polymer is achieved, whereas the SCT enhances as results of high molecular weight. Herein, the relevance of formation is clearly supported by the current findings that the high dosages of the polymer cause poor formation, which presumably deteriorates the strength properties of hand sheets at those chemical dosages. However, this polymer allows still moderate burst strength improvement.

On the whole, the implications of this thesis demonstrate the molecular weight and the charge density effects of polyvinyl amine generating better drainage efficiency and strength improvements with liner and fluting. The applicability of the high molecular weight polymer is concluded to be suitable for achieving additional SCT strength and drainage improvements with liner and fluting OCC furnish.

10. RECOMMEDATIONS

Further investigation and experimentation into the characteristics of the polymer affecting the adsorption of recycled fiber is strongly recommended. The adsorption methods to find out polymer adsorption onto fiber surface have been developed. Studies using QCM –measurement could assess the ability of the polymer to adsorb to fibers or to fix anionic trash in filtrate. However, direct applications to research polymer adsorption on fiber level are challenging, for instance the model surface of the QCM employing recycled fibers has not introduced. More knowledge on the polymer affinity to fiber surface and to other types of material would be interesting in further research.

Challenges of varying process conditions and quality characteristics of recycled fiber are recommended to highlight. For instance the quality of mill water, the activity of the micro-organisms and the characteristic differences of recovered pulp are too difficult to control in papermaking. Considerably more tests will need to be done to determine the applicability of the polymer with other types of furnishes.

REFERENCES

1. Stenius, P. Macromolecular, surface, and colloid chemistry. Forest Products Chemistry. Ed. P. Stenius. Publ. Fapet Oy. Jyväskylä, Finland. 2000. pp. 170-276.
2. Barnes, G. T. & Gentle, I. R., Interfacial Science: Introduction. 2nd edition. Oxford University Press. New York, U.S. 2011. 319 p.
3. Adamson, A. W. & Gast, A. P., Electrical aspects of surface chemistry. Physical Chemistry of Surfaces. 6th edition. John Wiley & Sons. Canada. 1997. pp. 169-224.
4. Besra, L. & Liu, M. A review on fundamentals and applications of electrophoretic deposition (EPD). Prog. Mat. Sci. 2007:53. pp. 1-61.
5. Fleer, G. J. & van Male, J. Analytical Approximation to the Scheutjens-Fleer Theory for Polymer Adsorption from Dilute Solution. 1. Trains, Loops, and Tails of Terms of Two Parameters: The Proximal and Distal Lengths. Macromolecules. 1999:32. pp. 825-844.
6. Böhmer, M. R., Evers, O. A. & Scheutjens, J. M. Weak Polyelectrolytes between Two Surfaces: Adsorption and Stabilization. Macromolecules. 1990:23. pp. 2288-2301.
7. van de Steeg, H. G., Cohen Stuart, M. A., Keizer, A. & Bijsterbosch, B. H. Polyelectrolyte Adsorption: A Subtle Balance of Forces. Langmuir. 1992:8. pp. 2538-2546.
8. Fleer, G. J., Cohen Stuart, M. A., Scheutjens, J.M. et al. Polymers at interfaces. Publ. Chapman & Hall Inc. London, UK 1993. 496 p.
9. Wågberg, L. Polyelectrolyte adsorption onto cellulose fibres – A review. Nord. Pulp Pap. Res. J. 15(2000):5. pp. 586-597.
10. Tang, C. Y., Chong, T. H. & Fane, A. G. Colloidal interactions and fouling of NF and RO membranes: A review. Advances in Colloid and Interface Science. 164(2011). pp. 126-143.
11. Stenius, P. Paperikoneen märkäpään pinta- ja kolloidikemia. Pinta- ja kolloidikemian sovellutukset paperikoneella. Insinöörijärjestöjen Koulutuskeskus. Publ. 191-85. Helsinki 1985. 307 p.

12. Farinato, R. S., Huang, S.-Y. & Hawkins, P. Polyelectrolyte-Assisted Dewatering. Colloid-Polymer Interactions: From fundamentals to Practice. Ed. R. S. Farinato & P. L. Dubin. Publ. John Wiley & Sons Inc. Canada 1999. pp. 3-50.
13. van Duijneveldt, J. Effect of Polymers on Colloid Stability. Colloid Science: Principles, methods and applications. Ed. T. Cosgrove. Publ. Blackwell Publishing Ltd. Bristol, UK 2005. pp. 143-158.
14. Lafuma, F. Mechanisms of flocculation and stabilisation of suspensions by organic polymers. Paper Chemistry. Ed. J. C. Roberts. Publ. Blackie Academic & Professional 1996. pp. 44-63.
15. Ödberg, L., Tanaka, H. & Swerin, A. Kinetic aspects of the adsorption of polymers on cellulosic fibres. Nord. Pulp Pap. Res. J. 1993:11. pp. 6-10.
16. Adachi, Y., Kobayashi, A. & Kobayashi, M. Review Article: Structure of Colloidal Flocs in relation to the Dynamic Properties of Unstable Suspension. Intern. J. Polym. Sci. Volume 2012. 14 p.
17. Horvath, A. E. The Effects of Cellulosic Fiber Charges on Polyelectrolyte Adsorption and Fiber-Fiber Interactions. Doctoral Dissertation. Royal Institute of Technology. Department of Fibre and Polymer Technology. Stockholm 2006. 53 p.
18. Kislenko, V.N. Polymer adsorption at solid surfaces. Adsorption: theory, modeling, and analysis. Ed. J. Tóth. Publ. Marcel Dekker Inc. NY, USA 2002. 743-801 p.
19. Song, J., Liang, J., Liu, X., Krause, W.E. et al. Development and characterization of thin polymer films relevant to fiber processing. Thin Solid Films. 517(2009):15. pp. 4348-4354.
20. Schall, N., Krüger, E., Blum, R. et al. Polymers on a polyvinylamine basis improve dry strength of packaging papers. Technical Association of the Pulp and Paper Industry of Southern Africa. November 2008. Available: [http://www.tappsa.co.za/archive3/Journal_papers/Polymers_on_a_polyvinylamine/polymers_on_a_polyvinylamine.html]
21. Delgado, A. V., Gonzalez-Caballero, F., Hunter, R. J. et al. Measurement and interpretation of electrokinetic phenomena. J. Colloid Interface Sci. 309(2007). pp. 194-224.

22. Lindström, E. & Lindström, T. Polyelectrolyte charge titration of cellulosic fibres. 5th International Paper and Coating Symposium 2003. Montreal, Canada. June 16-19, 2003. Pulp and Paper Technical Association of Canada. pp. 175-177.
23. Saarinen, T., Österberg, M. & Laine, J. Properties of cationic polyelectrolyte layers adsorbed on silica and cellulose surfaces studied by QCM-D – Effect of polyelectrolyte charge density and molecular weight. J. Disp. Sci. Tech. 2009:30. pp. 969-979.
24. Notley, S.M. & Norgren, M. Adsorption of a strong polyelectrolyte to model lignin surfaces. Biomacromolecules. 2008:9. pp. 2081-2086.
25. Leino, T., Raulio, M., Salkinoja-Salonen, M., Stenius, P. et al. Adsorption of bacteria and polycations on model surfaces of cellulose, hemicellulose and wood extractives studied by QCM. Colloids and Surfaces B: Biointerfaces. 2011:86. pp. 131-139.
26. Österberg, M. On the interactions in cellulose systems: surface forces and adsorption. Doctoral Dissertation. Royal Institute of Technology and Helsinki University of Technology. Department of Chemistry and Forest Products Technology. Stockholm 2000. 63 p.
27. van der Heide, P. X-Ray Photoelectron Spectroscopy: An Introduction to Principles and Practices. Wiley. Hoboken, NJ, USA 2011. 261 p.
28. Holmbom, B & Stenius, P. Analytical methods. Forest Products Chemistry, Papermaking Science and Technology, Book 3. Ed. P. Stenius. Publ. Fapet Oy. Jyväskylä, Finland 2000. pp. 107-169.
29. Enarsson, L-E. Dynamic and Equilibrium Properties of Adsorbed Polyelectrolyte Layers. Doctoral Thesis. Royal Institute of Technology. Department of Fibre and Polymer Technology. Stockholm 2008. 66 p.
30. Dijt, J.C., Cohen Stuart, M.A. & Fleer, G.J. Reflectometry as a tool for adsorption studies. Adv. Coll. Int. Sci. 1994:50. pp. 79-101.
31. Hubbe, M.A. Bonding between cellulosic fibers in the absence and presence of dry-strength agents – a review. Bioresources. 1(2006):2. pp. 281-318.
32. Torgnysdotter, A. & Wågberg, L. Influence of electrostatic interactions on fibre/fibre joint and paper strength. Nord. Pulp Pap. Res. J. 19(2004):4. pp. 440-447.

33. Esser, A. Strength for the future – Modern concepts and mechanism. TAPPI PaperCon'09 Conference. St. Louis, MO, USA. May 31 – June 3, 2009. Available:[http://www.tappi.org/Downloads/Conference-Papers/2009/09PAPERCON/09pap127.aspx].
34. Kendall, K. Molecular adhesion and its applications: the sticky universe. Publ. Kluwer Academic/Plenum Publishers. New York 2001. 452 p.
35. Zhao, B. & Kwon, H.J. Adhesion of polymers in paper products from the macroscopic to molecular level – An overview. J. Adhes. Sci. Technol. 2011:25. pp. 557-579.
36. Lindström, T., Wågberg, L. & Larsson, T. On the nature of joint strength in paper – a review of dry and wet strength resins used in paper manufacturing. 13th Fundamental Research Symposium. Cambridge, UK. September, 2005. pp. 457-562.
37. Eriksson, M. The influence of molecular adhesion on paper strength. Doctoral Thesis. Royal Institute of Technology. Department of Fibre and Polymer Technology. Stockholm 2006. 72 p.
38. Torgnysdotter, A. & Wågberg, L. Study of the joint strength between regenerated cellulose fibres and its influence on the sheet strength. Nord. Pulp Pap. Res. J. 18(2003):4. pp. 455-459.
39. Batchelor, W. & Jihong, H. A new method for determining the relative bonded area. Tappi Journal. 6(2005):4. pp. 23-28.
40. McKenzie, A.W. The structure and properties of Paper. Part XXI: The diffusion theory of adhesion applied to interfibre bonding. Appita. 37(1984):7. pp. 580-583.
41. Frank, B. Revisiting paper strength measurements for estimating combined board strength. Tappi Journal. 9(2007):6. pp. 10-17.
42. Replogle, J.W. Ring Crush vs. STFI for testing compression. Corrugating International. 3(2001):3. pp. 15-18.
43. Paltakari, J. Kuitupohjaiset pakkausmateriaalit ja niiden keskeiset ominaisuudet. Toimiva pakkaus. Ed. T. Järvi-Kääriäinen & M. Ollila. Publ. Hakapaino Oy. Helsinki, Finland. 2007. pp. 128-137.

44. Dekker, A. Corrugated fibreboard packaging. Handbook of paper and paperboard packaging technology. Ed. M. J. Kirwan. Publ. John Wiley & Sons, Ltd. West Sussex, UK. 2013. pp. 313-339.
45. Pat. US. 0291971. Retention and drainage in the manufacture of paper. Hercules Inc. USA. F.J. Sutman, J.C. Harrington, R.A. Gelman. App. 551202, 2012-17.07. Publ. 2012-22-11. 9 p.
46. Pat. CA. 2087461. Fines retention in papermaking with amine functional polymers. Air Products and Chemicals Inc. USA. J.G. Smigo, T.L. Pickering, A.F. Nordquist & R.K. Pinschmidt. App 826330, 1992-24.01. Publ. 1993-25-11. 28 p.
47. Hubbe, M.A. & Heitmann, J.A. Review of factors affecting the release of water from cellulosic fibers during paper manufacture. BioResources. 2(2007):3. pp. 500-533.
48. Zhu, S., Pelton, R.H. & Collver, K. Mechanistic modelling of fluid permeation through compressible fiber beds. Chem. Eng. Sci. 50(1995):22. pp. 3557-3572.
49. Patel, M. & Trivedi, R. Variations in strength and bonding properties of fines from filler, fiber, and their aggregates. Tappi J. 77(1994):3. pp. 185-192.
50. Liu, X.A., Whiting, P., Pande, H. et al. The contribution of different fractions of fines to pulp drainage in mechanical pulps. J. Pulp Pap. Sci. 27(2001):4. pp. 139-143.
51. Hubbe, M.A., Heitmann, J.A. & Cole, C.A. Water release from fractionated stock suspensions. Part 2. Effects of consistency, flocculants, shear, and order of mixing. Tappi J. 7(2008):8. pp. 14-19.
52. Antunes, E., Garcia, F.A., Ferreira, P. et al. Use of new branched cationic polyacrylamides to improve retention and drainage in papermaking. Ind. Eng. Chem. Res. 47(2008):23. pp. 9370-9375.
53. Nasser, M.S. & James, A.E. The effect of polyacrylamide charge density of and molecular weight on the flocculation and sedimentation behaviour of kaolinite suspensions. Separation and Purification Technology. 52(2006):2. pp. 241-252.
54. Pinheiro, I., Ferreira, P., Garcia F. P. et al. Performance of cationic polyacrylamides in papermaking – Flocculation, drainage and retention. XXI

TECNICELPA. Lisbon, Portugal. 12-15 October 2010. [AVAILABLE: http://www.celso-foelkel.com.br/artigos/outros/14_Cationic%20polyacrylamides.pdf]

55. Scott, W.E. Principles of Wet End Chemistry. TAPPI PRESS. Atlanta, Ga. 1996. 185 p.
56. Wan, J., Yang, J., Ma, Y. & Wang, Y. Effects of pulp preparation and papermaking processes on the properties of OCC fibers. Bio Resources. 2:2011. pp. 1615-1630.
57. Howard, R.C. & Bichard, W. The basic effects of recycling on pulp properties. J. Pulp Pap. Sci. 18(1992):4. pp. 151-159.
58. Zhang, M., Hubbe, M.A., Venditti, R.A. & Heitmann, J.A. Effect of chemical pretreatments of never-dried pulp on the strength of recycled linerboard. Proc. TAPPI 2001 Papermakers Conf. 10 p. [Available: http://repository.lib.ncsu.edu/publications/bitstream/1840.2/47/1/Zhan]
59. Hamzeh, Y., Sabbaghi, S., Ashori, A. et al. Improving wet and dry strength properties of recycled old corrugated carton (OCC) pulp using various polymers. Carbohydrate Polymers. 2013:94. pp. 577-583.
60. Hubbe, M. A. Diffucult furnishes. Proc. TAPPI '99. 1999. pp. 1353-1367. [Available: http://etd.lib.ncsu.edu/publications/bitstream/1840.2/48/1/HubbeM_99_DifficultFurnishes_Tappi99.pdf]
61. Carty, B. Conditioning of secondary fibers. Secondary fiber recycling. Ed. R.J. Spangenberg. Publ. TAPPI PRESS. Atlanta, USA. 1993. pp. 185-195.
62. Schwarz, M. Design of recycled fiber processes for different paper and board grades. Recycled fiber and deinking. Ed. L. Göttsching & H. Pakarinen. Publ. Fapet Oy. Jyväskylä, Finland. 2000. pp. 210-239.
63. Hubbe, M.A., Sundberg, A., Mocchiutti, P. et al. Dissolved and colloidal substances (DCS) and the charge demand of papermaking process waters and suspensions: A review. BioResources. 7(2012):4. pp. 6109-6193.
64. Moore, G. & Blanco, M.A. The recycling paper industry. Paper recycling: An introduction to problems and their solutions. Ed. M.A. Blanco, C. Negro & J. Tijero. Publ. European Communities. Belgium. 1998. pp. 3-16.

65. Scott, G.M. & Abubakr, S. Fractionation of secondary fiber – A review. Progress in Paper recycling. 3(1994):3. pp. 50-59.
66. Bhardwaj, N.K., Kumar, S. & Bajpai, P.K. Effect of zeta-potential on retention and drainage of secondary fibres. Colloids and Surfaces A: Physicochem. Eng. Aspects. 2005:260. pp. 245-250.
67. Ellis, R.L. & Sedlachek, K.M. Recycled- versus virgin-fiber characteristics: a comparison. Secondary fiber recycling. Ed. R.J. Spangenberg. Publ. TAPPI PRESS. Atlanta, USA. 1993. pp. 7-19.
68. Foster, C. & Rende, D. How recycling, water reuse impact chemistry. PIMA's Papermaker. 1(79):1997. pp. 48-53.
69. Herrington, T.M. & Petzold, J.C. An investigation into the nature of charge on the surface of papermaking woodpulps 2. Analysis of potentiometric titration data. Colloids Surfaces. 1992:64. pp. 109-108.
70. Lindstrom, T. Chemical factors affecting the behaviour of fibres during papermaking. Nord. Pulp Pap. Res. J. 4(1992):1. pp. 181-192.
71. Pat. EP. 026578. Method for increasing the advantages of strength aids in the production of paper and paperboard. Ashland. US. (Krapsch, L., MC Gregor, C.J. & De la Varende, J.V.M.) App. 003582, 2012-24.08. Publ. 2013-02-28. 83 p.
72. Mayovsky, J. An evaluation of Asian OCC. Tappi Journal. 5(1995):78. pp.117-122.
73. Kast, T.R. Advancements in gap forming for lighter weight board and packaging papers. TAPPI PAPERCON 2010. May 2-5. Atlanta, USA. 10 p.
74. Meyer, T., Hellweg, T., Spange, S., Hesse, S. et al. Synthesis and Properties of Crosslinked Polyvinylformamide and Polyvinylamine Hydrogels in Conjuction with Silica Particles. J. Polym. Sci. 2002:40. pp. 3144-3152.
75. Pat. US. 7902312. Michael Addition adducts as additives for paper and papermaking. Hercules Inc. USA (Q-M. Gu & R.R. Staib). App. 804360, 2007-18.05. Publ. 2011-3-8. 9 p.
76. Pat. US. 5145559. Production of paper, board and cardboard. Basf Aktiengesellshaft, Germany (W. Auhorn, F. Linhart, P. Lorencak et al.). App. 641852, 1991-16.01. Publ. 1992-9-8. 5 p.

77. Pat. US. 6576086. Method for producing paper, paperboard and cardboard using an uncrosslinked fixing agent during paper stock draining. Basf Aktiengesellshaft, Germany (R. Ettl, H. Meixner, A. Esser et al.) App. 403769, 1998-24.4. Publ. 2003-6-10. 8 p.
78. Yamamoto, K., Imamura, Y. Nagatomo, E. et al. Synthesis and Synthesis and Functionalities of Poly(*N*-vinylalkylamide). XIV. Polyvinylamine Produced by Hydrolysis of Poly(*N*-vinylformamide) and Its Functionalization. J. Appl. Polym. Sci. 2003:89. pp. 1277-1283.
79. Gu, L., Zhu, S. & Hrymak, A. N. Acidic and Basic Hydrolysis of Poly(N-vinylformamide). J. Appl. Polym. Sci. 2002:86. pp. 3412-3419.
80. Witek, E., Pazdro, M. & Bortel, E. Mechanism for Base Hydrolysis of Poly(N-vinylformamide). J. Macrom. Sci. 2007:44. pp. 503-507.
81. Zhang, J., Pelton R., Wågberg, L.et al. The effect of molecular weight on the performance of paper strength-enhancing polymers. J. Pulp Pap. Sci. 27(2001):5. pp. 145-151.
82. Tiberg, F., Daicic, J. & Fröberg, J. Surface chemistry of paper. Handbook of Applied Surface and Colloid Chemistry. Ed. K. Holmberg. Publ. Wiley. New York, USA. 2001. pp. 123-173.
83. Wågberg, L., Ödberg, L., Lindström, T. et al. J. Colloid Interface Sci. 1988:1. Ref. Tappi J. 76(1993):12.
84. Pelton, R., Zhang, J., Chen, N. et al. The influence of dextran molecular weight on the dry strength of dextran-impregnated paper. Tappi J. 2(2003):4. pp. 15-18.
85. Linke, W.F. Polyacrylamide as a Stock Additive. Tappi. 1962:4. Ref. J. Pulp Pap. Sci. 27(2001):5.
86. Oulanti, O. Widmaier, J., Pefferkorn, E. et al. Relaxation Phenomena of Hydrolyzed Polyvinylamine Molecules Adsorbed at the Silica/Water Interface: I. Saturated Homogenous Polymer Layers. J. Colloid Interface Sci. 2005:291. pp. 98-104.
87. Pat. US. 0155339. Process for enhancing dry strength of paper by treatment with vinylamine-containing polymers and acrylamide-containing polymers. USA. (C.L. Brungardt, J.M. Mckay, R.J. Riehle) App. 975441, 2010-22.12. Publ. 2011-6-30. 12 p.

88. Pat. EP. 0331047. Papermaking process comprising the addition of high molecular weight poly(vinylamines) to the wet-end cellulose fiber slurry. Air Products and Chemicals Inc. USA (T-W. Lai & B.R. Vijayendran). App. 89103305, 1989-24.02. Publ. 1989-03-04. 10 p.
89. Hugel, T., Grosholz, M., Clausen-Schaumann, H. et al. Elasticity of single polyelectrolyte chains and their desorption from solid supports by AFM based single molecule spectroscopy. Macromolecules. 2001:34. pp. 1039-1047.
90. Voigt, I., Simon, F., Komber, H. et al. Controlled synthesis of stable poly(vinylformamide-co-vinyl amine)/silica hybrid particles by interfacial post-cross-linking reactions. Colloid Polym. Sci. 2000:278. pp. 48-56.
91. Eklund, D. & Lindström, T. Paper Chemistry: An Introduction. DT PAPER SCIENCE. Grankulla, Finland. 1991. 305 p.
92. Miao, Q., Huang, L. & Chen, L. Advances in the control of dissolved and colloidal substances present in papermaking processes: A brief review. Bioresources. 1(2013):8. pp. 1-25.

APPENDICES:

Appendix I: Paper measurement results of long fiber laboratory sheets

Appendix II: Paper measurement results of short fiber laboratory sheets

Appendix III: Paper measurement results of pilot paper machine trial

Appendix IV: Correlation analysis for the results of the pilot paper machine trial

APPENDIX I(1). Paper measurement results of long fiber laboratory sheets

Measurement	Sample	0-test	Ref. C-PAM2 (0,4kg/t) +A-PAM1 (0,2kg/t)	Ref. C-PAM2 (0,8kg/t) +A-PAM1 (0,2kg/t)	Ref. C-PAM2 (1,2kg/t) +A-PAM1 (0,2kg/t)	Ref. C-PAM2 (0,8kg/t) +A-PAM2 (0,35kg/t	PVAm 2H (0,4kg/t) +A-PAM1 (0,2kg/t)	PVAm 2H (0,8kg/t) +A-PAM1 (0,2kg/t	PVAm 2H (1,2kg/t) +A-PAM1 (0,2kg/t)	PVAm 2H (0,8kg/t) +A-PAM2 (0,5kg/t)
Grammage	g/m^2	124,9	123,53	126,75	124,39	122,62	121,0	123,0	123,74	120,91
St.dev.	g/m^2	1,09	2,58	0,75	0,47	0,76	0,37	1,10	3,51	0,97
Confidence 95%	g/m^2	1,1	2,5	0,7	0,5	0,7	0,4	1,1	3,4	1,0
Thickness	µm	215,7	210,8	215,4	209,9	210,6	210,1	213,1	212,5	200,0
St.dev.	µm	6,5	8,0	6,6	4,2	7,1	4,3	6,4	6,6	6,3
Confidence 95%	µm	5,7	7,0	5,8	3,7	6,3	3,7	5,6	5,7	5,5
Density	g/cm^3	0,58	0,59	0,59	0,59	0,58	0,58	0,58	0,58	0,60
Bulk	cm^3/g	1,73	1,71	1,70	1,69	1,72	1,74	1,73	1,72	1,65
Ash content	%	13,05	14,81	15,59	15,92	15,23	15,13	15,81	16,18	15,54
Burst strength	kPa	168,0	157,4	163,0	181,1	175,3	160,6	170,8	166,3	154,1
St.dev.	kPa	16,3	9,4	15,9	3,0	9,9	9,0	12,0	6,7	15,0
Confidence 95%	kPa	11,3	6,5	11,0	2,1	6,9	6,2	8,3	4,7	10,4
Burst strength index	kPa m²/g	1,344	1,273	1,286	1,456	1,429	1,327	1,388	1,341	1,348
St.dev.	kPa m²/g	0,130	0,076	0,126	0,024	0,081	0,074	0,098	0,054	0,124
Confidence 95%	kPa m²/g	0,090	0,053	0,087	0,017	0,056	0,052	0,068	0,038	0,086
SCT	kN/m	1,918	1,791	1,924	1,855	1,806	1,721	1,861	1,861	1,733
St.dev.	kN/m	0,148	0,210	0,157	0,282	0,146	0,210	0,151	0,157	0,151
Confidence 95%	kN/m	0,048	0,069	0,051	0,092	0,048	0,069	0,049	0,051	0,049
SCT index	kNm/kg	15,35	14,50	15,18	14,91	14,73	14,22	15,13	15,04	14,33
St.dev.	kNm/kg	1,18	1,70	1,24	2,26	1,19	1,73	1,23	1,27	1,25
Confidence 95%	kNm/kg	0,39	0,55	0,40	0,74	0,39	0,57	0,40	0,41	0,41
Formation	g/m^2	9,89	8,94	9,50	9,34	10,10	9,23	9,92	10,25	9,84
St.dev.	g/m^2	1,23	0,41	0,50	0,67	0,52	0,57	0,70	0,47	1,30
Confidence 95%	g/m2	1,21	0,40	0,49	0,66	0,51	0,55	0,68	0,46	1,28
Normalized beta formation	√g/m	0,885	0,804	0,844	0,837	0,912	0,839	0,894	0,921	0,895
St.dev.	√g/m	0,114	0,036	0,046	0,059	0,045	0,053	0,059	0,038	0,081
Confidence 95%	√g/m	0,111	0,036	0,045	0,058	0,045	0,052	0,058	0,037	0,080

APPENDIX I(2).

PVAm 5H (0,4kg/t)+A-PAM1 (0,2kg/t)	PVAm 5H (0,8kg/t)+A-PAM1 (0,2kg/t)	PVAm 5H (1,2kg/t)+A-PAM1 (0,2kg/t)	PVAm 5H (0,8kg/t)+A-PAM2 (1,14kg/t)	PVAm 4L (0,4kg/t)+A-PAM1 (0,2kg/t)	PVAm 4L (0,8kg/t)+A-PAM1 (0,2kg/t)	PVAm 4L (1,2kg/t)+A-PAM1 (0,2kg/t)	PVAm 4L (0,8kg/t)+A-PAM2 (1,67kg/t)	PVAm 1L (0,4kg/t)+A-PAM1 (0,2kg/t)	PVAm 1L (0,8kg/t)+A-PAM1 (0,2kg/t)	PVAm 1L (1,2kg/t)+A-PAM1 (0,2kg/t)	PVAm 1L (0,8kg/t)+A-PAM2 (1,67kg/t)
117,83	120,94	127,46	120,28	122,60	124,63	122,67	118,61	124,92	126,44	126,37	127,43
3,78	3,33	1,42	2,31	0,76	1,93	1,71	1,17	2,32	1,96	1,16	1,63
3,7	3,3	1,4	2,3	0,7	1,9	1,7	1,1	2,3	1,9	1,1	1,6
202,5	211,2	220,3	209,3	214,0	216,7	211,2	207,6	213,5	216,4	217,9	223,7
7,6	8,5	8,5	8,6	7,6	9,3	4,4	7,9	8,5	7,6	6,0	11,4
6,7	7,5	7,5	7,5	6,7	8,1	3,8	7,0	7,5	6,6	5,2	10,0
0,58	0,57	0,58	0,57	0,57	0,58	0,58	0,57	0,59	0,58	0,58	0,57
1,72	1,75	1,73	1,74	1,75	1,74	1,72	1,75	1,71	1,71	1,72	1,76
12,49	13,18	13,80	12,35	12,26	12,36	12,38	10,38	13,34	13,73	13,93	12,09
153,1	168,8	169,0	168,6	173,1	175,6	175,9	179,1	185,5	179,5	171,4	186,8
12,9	11,0	20,7	9,4	11,1	14,0	6,9	16,1	14,1	9,5	24,2	13,4
8,9	7,6	14,4	6,5	7,7	9,7	4,8	11,1	9,8	6,6	16,8	9,3
1,318	1,394	1,332	1,402	1,412	1,409	1,433	1,510	1,487	1,419	1,356	1,466
0,110	0,091	0,163	0,078	0,091	0,112	0,056	0,136	0,113	0,075	0,192	0,105
0,076	0,063	0,113	0,054	0,063	0,078	0,039	0,094	0,078	0,052	0,133	0,073
1,689	1,744	1,876	1,774	1,913	1,920	1,809	1,824	1,927	1,989	1,862	1,889
0,154	0,132	0,174	0,154	0,165	0,183	0,136	0,160	0,140	0,150	0,154	0,145
0,050	0,043	0,057	0,050	0,054	0,060	0,044	0,052	0,046	0,049	0,050	0,05
14,53	14,41	14,72	14,75	15,61	15,41	14,74	15,38	15,43	15,73	14,73	14,82
1,30	1,09	1,37	1,28	1,35	1,47	1,11	1,35	1,12	1,19	1,22	1,14
0,43	0,36	0,45	0,42	0,44	0,48	0,36	0,44	0,37	0,39	0,40	0,37
8,95	9,30	10,56	9,70	9,40	9,58	9,39	9,04	8,75	9,89	10,80	10,28
0,33	0,83	1,03	1,54	0,27	0,51	0,79	0,27	0,86	1,18	0,64	1,60
0,33	0,82	1,01	1,51	0,27	0,50	0,78	0,27	0,84	1,15	0,62	1,57
0,824	0,846	0,936	0,884	0,849	0,858	0,848	0,830	0,783	0,880	0,960	0,911
0,026	0,071	0,088	0,135	0,024	0,043	0,071	0,023	0,069	0,106	0,055	0,136
0,025	0,070	0,086	0,132	0,023	0,042	0,069	0,023	0,067	0,104	0,054	0,134

APPENDIX II(1). Paper measurement results of short fiber laboratory sheets

Measurement	Sample	0-test	Ref. C-PAM2 (0,4kg/t) +A-PAM1 (0,2kg/t)	Ref. C-PAM2 (0,8kg/t) +A-PAM1 (0,2kg/t)	Ref. C-PAM2 (1,2kg/t) +A-PAM1 (0,2kg/t)	Ref. C-PAM2 (0,8kg/t) +A-PAM2 (0,35kg/t)	PVAm 2H (0,4kg/t) +A-PAM1 (0,2kg/t)	PVAm 2H (0,8kg/t) +A-PAM1 (0,2kg/t)	PVAm 2H (1,2kg/t) +A-PAM1 (0,2kg/t)	PVAm 2H (0,8kg/t) +A-PAM2 (0,5kg/t)
Grammage	g/m^2	121,8	125,67	123,22	124,20	120,99	120,69	122,75	121,94	121,63
St.dev.	g/m^2	1,73	1,99	1,41	1,29	1,82	0,83	0,54	1,38	1,60
Confidence 95%	g/m^2	1,7	1,9	1,4	1,3	1,8	0,8	0,5	1,3	1,6
Thickness	µm	207,2	212,0	205,8	205,8	204,1	205,5	206,0	207,6	206,2
St.dev.	µm	4,8	6,8	5,1	5,1	4,7	6,1	3,8	9,0	7,8
Confidence 95%	µm	4,2	5,9	4,5	4,5	4,1	5,3	3,3	7,8	6,8
Density	g/cm^3	0,59	0,59	0,60	0,60	0,59	0,59	0,60	0,59	0,59
Bulk	cm^3/g	1,70	1,69	1,67	1,66	1,69	1,70	1,68	1,70	1,69
Ash content	%	13,97	16,43	16,75	17,15	16,39	15,79	16,06	16,16	16,00
Burst strength	kPa	174,5	175,3	170,5	171,5	164,8	169,0	164,5	171,0	167,8
St.dev.	kPa	6,0	12,0	10,6	12,4	20,2	7,8	12,4	11,3	12,4
Confidence 95%	kPa	4,2	8,3	7,3	8,6	14,0	5,4	8,6	7,8	8,6
Burst strength index	kPa m²/g	1,433	1,394	1,383	1,381	1,362	1,400	1,340	1,402	1,379
St.dev.	kPa m²/g	0,049	0,096	0,086	0,100	0,167	0,064	0,101	0,093	0,102
Confidence 95%	kPa m²/g	0,034	0,066	0,060	0,069	0,115	0,045	0,070	0,064	0,070
SCT	kN/m	1,817	1,859	1,852	1,904	1,822	1,710	1,756	1,830	1,873
St.dev.	kN/m	0,161	0,149	0,160	0,129	0,123	0,191	0,174	0,143	0,172
Confidence 95%	kN/m	0,052	0,049	0,052	0,042	0,040	0,062	0,057	0,047	0,056
SCT index	kNm/kg	14,93	14,79	15,03	15,32	15,06	14,17	14,30	15,01	15,33
St.dev.	kNm/kg	1,32	1,19	1,29	1,04	1,02	1,58	1,42	1,17	1,42
Confidence 95%	kNm/kg	0,43	0,39	0,42	0,34	0,33	0,52	0,46	0,38	0,46
Formation	g/m^2	8,62	9,41	9,83	8,73	8,57	9,24	9,37	9,37	9,30
St.dev.	g/m^2	0,65	1,34	1,26	0,81	0,44	0,65	0,50	0,47	0,38
Confidence 95%	g/m2	0,63	1,31	1,23	0,79	0,43	0,64	0,49	0,46	0,37
Normalized beta formation	√g/m	0,781	0,839	0,885	0,784	0,779	0,841	0,846	0,848	0,843
St.dev.	√g/m	0,057	0,117	0,116	0,074	0,043	0,057	0,044	0,043	0,031
Confidence 95%	√g/m	0,056	0,115	0,114	0,072	0,042	0,056	0,043	0,043	0,030

APPENDIX II(2).

PVAm 5H (0,4kg/t)+A-PAM1 (0,2kg/t)	PVAm 5H (0,8kg/t)+A-PAM1 (0,2kg/t)	PVAm 5H (1,2kg/t)+A-PAM1 (0,2kg/t)	PVAm 5H (0,8kg/t)+A-PAM2 (1,14kg/t)	PVAm 4L (0,4kg/t)+A-PAM1 (0,2kg/t)	PVAm 4L (0,8kg/t)+A-PAM1 (0,2kg/t)	PVAm 4L (1,2kg/t)+A-PAM1 (0,2kg/t)	PVAm 4L (0,8kg/t)+A-PAM2 (1,67kg/t)	PVAm 1L (0,4kg/t)+A-PAM1 (0,2kg/t)	PVAm 1L (0,8kg/t)+A-PAM1 (0,2kg/t)	PVAm 1L (1,2kg/t)+A-PAM1 (0,2kg/t)	PVAm 1L (0,8kg/t)+A-PAM2 (1,67kg/t)
121,65	123,87	125,30	122,68	125,51	126,49	125,97	123,23	121,69	122,07	126,44	120,87
1,70	1,12	0,89	0,90	1,79	1,28	0,87	1,02	1,73	1,74	1,69	1,54
1,7	1,1	0,9	0,9	1,8	1,3	0,9	1,0	1,7	1,7	1,7	1,5
209,2	214,2	215,4	211,4	215,8	215,2	212,5	212,9	211,5	211,1	215,9	205,0
6,8	8,0	8,1	8,0	9,9	8,5	7,6	6,1	6,8	7,5	9,3	6,4
6,0	7,0	7,1	7,0	8,7	7,5	6,7	5,3	6,0	6,5	8,1	5,6
0,58	0,58	0,58	0,58	0,58	0,59	0,59	0,58	0,58	0,58	0,59	0,59
1,72	1,73	1,72	1,72	1,72	1,70	1,69	1,73	1,74	1,73	1,71	1,70
12,84	13,53	14,27	12,35	14,13	14,51	14,84	12,94	12,33	12,45	12,97	10,62
179,6	170,4	163,0	181,8	174,8	178,5	179,9	177,5	174,1	174,3	184,6	177,4
8,7	8,3	12,7	16,3	7,4	7,1	5,1	7,4	16,1	11,0	4,8	8,3
6,0	5,8	8,8	11,3	5,1	4,9	3,6	5,1	11,1	7,6	3,3	5,8
1,477	1,375	1,301	1,481	1,392	1,411	1,428	1,440	1,431	1,428	1,460	1,467
0,071	0,067	0,102	0,133	0,059	0,056	0,041	0,060	0,132	0,090	0,038	0,069
0,049	0,046	0,070	0,092	0,041	0,039	0,028	0,042	0,092	0,062	0,026	0,048
1,836	1,792	1,859	1,952	1,955	1,889	1,923	1,884	1,901	1,910	1,927	1,897
0,154	0,116	0,196	0,176	0,170	0,171	0,143	0,170	0,137	0,131	0,185	0,176
0,050	0,038	0,064	0,057	0,056	0,056	0,047	0,056	0,045	0,043	0,060	0,06
15,10	14,47	14,83	15,91	15,58	14,93	15,26	15,29	15,62	15,65	15,24	15,69
1,27	0,93	1,56	1,43	1,36	1,35	1,14	1,38	1,13	1,07	1,46	1,46
0,41	0,31	0,51	0,47	0,44	0,44	0,37	0,45	0,37	0,35	0,48	0,48
9,67	9,71	10,99	9,24	9,68	10,46	10,35	10,54	9,10	10,36	10,37	9,57
0,41	1,35	0,89	0,41	0,68	1,16	0,72	0,70	0,46	1,02	1,12	0,76
0,41	1,33	0,87	0,40	0,67	1,14	0,70	0,69	0,45	1,00	1,09	0,74
0,877	0,872	0,982	0,834	0,864	0,930	0,922	0,949	0,824	0,937	0,922	0,870
0,043	0,120	0,078	0,034	0,058	0,105	0,065	0,061	0,041	0,087	0,105	0,071
0,042	0,117	0,076	0,034	0,057	0,103	0,063	0,060	0,040	0,085	0,103	0,069

APPENDIX III(1). Paper measurement results of pilot paper machine trial

Measurement	Sample	0-test	Ref. G-PAM1 (1kg/t)	Ref. G-PAM1 (3kg/t)+A-PAM2 (0,35kg/t)	Ref. C-PAM DSR (1kg/t)	Ref. C-PAM DSR (3kg/t) +A-PAM2 (0,35kg/t)	PVAm2H (0,5kg/t)	PVAm2H (1kg/t)+A-PAM2 (0,7kg/t)
Grammage	g/m^2	102,69	102,16	106,46	103,04	108	105,52	109,76
St.dev.	g/m^2	2,56	1,95	0,79	0,18	2,19	1,13	1,79
Confidence 95%	g/m^2	2,24	1,71	0,69	0,16	1,92	0,99	1,57
Thickness	µm	180,4	180,4	183,4	179,2	184,0	185,5	194,2
St.dev.	µm	7,6	7,0	6,4	8,7	7,6	7,0	7,0
Confidence 95%	µm	3,0	2,7	2,5	3,4	3,0	2,7	2,7
Density	g/cm^3	0,57	0,57	0,58	0,57	0,59	0,57	0,57
Bulk	cm^3/g	1,76	1,77	1,72	1,74	1,70	1,76	1,77
Ash content	%	15,64	15,65	16,28	16,39	16,03	16,69	17,86
Burst strength	kPa	179,4	190,1	217,5	193,4	213,1	181,7	183,0
St.dev.	kPa	18,5	13,7	10,7	14,3	17,6	17,9	15,9
Confidence 95%	kPa	11,5	8,5	6,6	8,9	10,9	11,1	9,9
Burst strength index	kPa m^2/g	1,747	1,861	2,043	1,877	1,973	1,722	1,667
St.dev.	kPa m^2/g	0,180	0,135	0,101	0,139	0,163	0,170	0,145
Confidence 95%	kPa m^2/g	0,125	0,093	0,070	0,096	0,113	0,118	0,100
SCT MD	kN/m	2,810	3,070	3,080	3,120	3,100	2,660	2,520
CoV	%	5,590	8,100	2,080	4,160	4,570	7,850	9,270
St.dev.	kN/m	0,396	0,499	0,253	0,360	0,376	0,457	0,483
Confidence 95%	kN/m	0,174	0,219	0,111	0,158	0,165	0,200	0,212
SCT CD	kN/m	1,65	1,75	1,78	1,81	1,86	1,65	1,72
CoV	%	10,98	3,93	5,88	6,12	9,43	8,03	4,71
St.dev.	kN/m	0,426	0,262	0,324	0,333	0,419	0,364	0,285
Confidence 95%	kN/m	0,19	0,11	0,14	0,15	0,18	0,16	0,12
SCT MD index	kNm/kg	27,36	30,05	28,93	30,28	28,70	25,21	22,96
St.dev.	kNm/kg	3,8593	4,8813	2,3776	3,4964	3,485	4,3305	4,4034
Confidence 95%	kNm/kg	1,6914	2,1393	1,0420	1,532	1,527	1,8979	1,9298
SCT CD index	kNm/kg	16,07	17,13	16,72	17,57	17,22	15,64	15,67
St.dev.	kNm/kg	4,1447	2,5671	3,0390	3,2301	3,877	3,4495	2,5931
Confidence 95%	kNm/kg	1,8165	1,1251	1,3319	1,4156	1,699	1,5118	1,1365
SCT Geom. Index	kNm/kg	20,97	22,69	21,99	23,06	22,23	19,85	18,97
St.dev.	kNm/kg	4,00	3,54	2,69	3,36	3,68	3,86	3,38
Confidence 95%	kNm/kg	1,75	1,55	1,18	1,47	1,61	1,69	1,48

Appendix III(2).

PVAm 4H (1kg/t)	PVAm4H (1kg/t)+ A-PAM2 (0,7kg/t)	PVAm 1L (0,5kg/t)	PVAm 1L (1kg/t)	PVAm 1L (1kg/t)+ A-PAM2 (0,35kg/t)	PVAm 2L (0,5kg/t)	PVAm 2L (0,5kg/t)+A-PAM2 (0,7kg/t)
103,49	106,81	107,74	110,70	107,89	99,83	103,58
1,57	2,02	1,09	0,37	1,04	2,33	1,48
1,37	1,77	0,96	0,32	0,91	2,04	1,29
178,0	180,3	196,1	200,2	191,1	170,0	188,4
7,2	8,3	6,3	7,6	10,3	5,5	5,3
2,8	3,2	2,5	3,0	4,0	2,2	2,1
0,58	0,59	0,55	0,55	0,56	0,59	0,55
1,72	1,69	1,82	1,81	1,77	1,70	1,82
16,37	17,78	15,53	16,75	16,68	15,89	15,12
202,7	200,1	178,5	192,5	181,8	204,6	191,3
21,7	21,8	15,9	10,4	13,5	11,4	19,5
13,5	13,5	9,9	6,4	8,4	7,1	12,1
1,959	1,873	1,657	1,739	1,685	2,049	1,847
0,210	0,204	0,148	0,094	0,125	0,114	0,188
0,145	0,141	0,102	0,065	0,087	0,079	0,130
2,840	2,970	2,290	2,640	2,770	2,990	2,560
4,710	5,200	12,580	10,620	5,780	4,640	5,310
0,366	0,393	0,537	0,529	0,400	0,372	0,369
0,160	0,172	0,235	0,232	0,175	0,163	0,162
1,74	1,77	1,68	1,71	1,64	1,70	1,61
8,26	6,49	6,71	7,78	6,66	5,86	6,17
0,379	0,339	0,336	0,365	0,330	0,316	0,315
0,17	0,15	0,15	0,16	0,14	0,14	0,14
27,44	27,81	21,26	23,85	25,67	29,95	24,71
3,5340	3,6793	4,9819	4,7833	3,7088	3,7310	3,5594
1,5488	1,6125	2,1834	2,0963	1,6254	1,6352	1,5599
16,81	16,57	15,59	15,45	15,20	17,03	15,54
3,6632	3,1732	3,1164	3,2950	3,0633	3,1616	3,0427
1,6054	1,3907	1,3658	1,4441	1,3425	1,3856	1,3335
21,48	21,47	18,21	19,19	19,76	22,58	19,60
3,60	3,42	3,94	3,97	3,37	3,43	3,29
1,58	1,50	1,73	1,74	1,48	1,51	1,44

APPENDIX IV. Correlation analysis for the results of the pilot paper machine trial

	Zeta-pot.	Conductivity	Charge ave.	Consistency (HB)	COD (HB)	Consistency (WW)	Turbidity	COD (WW)	Retention	Press solids	Basis weight	SCT Geom index	Burst index	Tensile Geom index	Scott bond	Bulk	Ash
Zeta-pot.	1,00																
Conductivity	0,72	1,00															
Charge ave.	0,43	0,13	1,00														
Consistency (HB)	-0,17	-0,46	-0,17	1,00													
COD (HB)	-0,29	-0,37	-0,65	0,51	1,00												
Consistency (WW)	-0,68	-0,46	-0,56	0,34	0,29	1,00											
Turbidity	0,67	0,60	0,42	-0,46	-0,57	-0,44	1,00										
COD (WW)	-0,32	-0,40	-0,67	0,49	0,96	0,27	-0,63	1,00									
Retention	0,67	0,30	0,52	0,07	-0,08	-0,91	0,27	-0,07	1,00								
Press solids	-0,26	-0,23	0,04	-0,11	-0,38	0,17	-0,07	-0,16	-0,23	1,00							
Basis weight	-0,18	-0,29	-0,12	0,44	0,42	0,15	-0,46	0,48	0,05	0,08	1,00						
SCT Geom index	0,50	0,51	0,27	-0,82	-0,50	-0,46	0,62	-0,49	0,13	0,03	-0,54	1,00					
Burst index	0,09	0,28	-0,11	-0,78	-0,39	-0,03	0,38	-0,35	-0,30	0,22	-0,46	0,80	1,00				
Tensile Geom index	0,47	0,49	0,31	-0,74	-0,59	-0,40	0,60	-0,56	0,10	0,09	-0,58	0,95	0,75	1,00			
Scott bond	0,38	0,35	0,24	-0,71	-0,48	-0,32	0,47	-0,44	0,03	0,16	-0,26	0,82	0,76	0,78	1,00		
Bulk	-0,08	-0,18	-0,04	0,77	0,29	0,17	-0,29	0,23	0,15	-0,15	0,25	-0,78	-0,79	-0,69	-0,64	1,00	
Ash	0,32	0,13	0,02	-0,27	0,24	-0,30	0,13	0,23	0,20	-0,26	0,11	0,45	0,25	0,28	0,28	-0,61	1,00